IJEST

ISSN: 0973-6255
Vol. 1 No. 2
July - December 2007

Indian Journal of Engineering, Science, and Technology

A Refereed Research Journal

BANNARI AMMAN
INSTITUTE OF TECHNOLOGY
Stay Ahead

BANNARI AMMAN INSTITUTE OF TECHNOLOGY
Sathyamangalam - 638 401 Erode District Tamil Nadu India

ABOUT BANNARI AMMAN INSTITUTE OF TECHNOLOGY

The Bannari Amman Institute of Technology (BIT) is a vibrant institute of higher education promoted by the Bannari Amman Group, a leading corporate house in the Southern part of India, under the aegis of the Bannariamman Educational Trust in 1996 in the town of Sathyamangalam in Erode District of Tamil Nadu.

It is an impressive campus situated in a serene surrounding at the foothills of the Nilgiris Mountains encompassing a sprawling area of 165 acres with a built-up area of more than 12 lakh square feet and presents an exemplary illustration of corporate contribution to society. BIT is a modern campus with up-to-date teaching facilities. It is an ideal, conducive, educational retreat where one can fully focus on studies and attain academic excellence.

With an overall strength of 3500 students on roll, the Institute offers 12 undergraduate programmes, and 12 postgraduate programmes in engineering, technology, & applied sciences, and 4 Ph.D./ M.S. (By Research) in engineering and technology under affiliation to Anna University, Coimbatore and approved by the All India Council for Technical Education, New Delhi. Six of the BE/BTech programmes have been accredited by NBA. The college is an ISO 9001:2000 certified institution. The zeal and dedication with which BIT pursues its motto 'Stay Ahead' makes it different from other institutions.

There are 30 doctorates among 235 members of faculty to provide personalised care for the students. The zeal and dedication with which BIT pursues its motto 'Stay Ahead' makes it different from other institutions.

Indian Journal of Engineering, Science, and Technology

IJEST is a refereed research journal published half-yearly by Bannari Amman Institute of Technology. Responsibility for the contents rests upon the authors and not upon the IJEST. For copying or reprint permission, write to Copyright Department, IJEST, Bannari Amman Institute of Technology, Sathyamanagalam, Erode District - 638 401, Tamil Nadu, India.

From the Editor's Desk

The Bannari Amman Institute of Technology started publishing the Indian Journal of Engineering, Science, and Technology as a part of celebration of its ten years of existence.

IJEST ia a half yearly publication. Its main objective is to disseminate knowledge on various research issues connected with Engineering, Science, and Technology, and to provide up-to-date information in these areas.

In order to motivate the research scholars and to enrich the knowledge of readers, the Indian Journal of Engineering, Science, and Technology has invited original research articles from members of faculty and persons connected with research activities in the industry as well. The journal has received an overwhelming response from the members of faculty and researchers of various institutions, who have contributed their research papers for publication.

This issue consists of 12 papers covering various disciplines of Engineering and Technology. We plan to reach this issue to various personalities, academicians and researchers connected with Engineering, Science, and Technology to make this a top-class refereed journal.

The Editorial Board is keen on receiving suggestions for further improvement of the journal and will appreciate any constructive suggestions from the readers.

(Dr.A.Shanmugam)
Editor in-Chief, IJEST

Indian Journal of Engineering, Science, and Technology

Volume 1 Number 2 **July - December 2007**

CONTENTS

EFFECT OF CHEMICAL ADMIXTURES ON CONCRETE - AN EXPERIMENTAL ANALYSIS

J. Megala[1] and S.S.Jayachandran[2]
[1]Vellore Institute of Technology, University, Vellore - 632 014,Tamil Nadu
[2]Vel SRS High Tech Engineering College, Chennai - 600 096,Tamil Nadu
E-mail: megala_jayaraman@yahoo.co.in; ssj1ht@gmail.com
(Received on 06 December 2006; revised received and accepted on 03 March 2007)

Abstract

In this paper, the results of experimental analysis on the use of two chemical admixtures to concrete are discussed. FOSROC chemicals, namely CONPLAST P 509 and CONPLAST RP 264 have been separately added to concrete to study their effects on compressive, tensile, and flexural strengths as well as workability of concrete. Adopting two different water / cement (w/c) ratios (0.45 and 0.50), strength tests have been carried out at the end of 3, 7 & 28 days on the specimens with and without the above two admixtures. Tests have also been conducted to study the workability of concrete with and without the above two admixtures. The results of using the above admixtures in concrete are presented.

Keywords: *Admixtures, Slump, Strength, Workability, W/C ratio*

1. INTRODUCTION

As a construction material, concrete has been widely used in the past, presently indispensable, and may be much more useful in future. It is highly resistant to fire, wind and water, and lends itself to almost any type of decorative or architectural expression. Limitations to its use are its relatively low tensile stress, its tendency to crack with temperature changes and deterioration due to permeability, and adsorption status under varying conditions. Improvements in these properties could significantly extend the usefulness of concrete.

An admixture is defined as a material other than cement, water and aggregate, that is added as an ingredient immediately before or during mixing to modify the properties of ordinary concrete, so as to make it more suitable for any situation [1, 2]. The concrete with admixture can attain maximum or required strength much earlier, thereby making it feasible to remove the shuttering early.

It is desirable to obtain lowest possible water/cement (w/c) ratio to achieve the required strength and workability. A typical curve showing variation of compressive strength with w/c ratio is shown in Figure 1. For any given mix proportion and method of compaction, w/c ratio cannot be reduced below a certain limit without affecting workability.

The concrete becomes unworkable when the w/c ratio is less than a particular value called the critical point. If w/c ratio is reduced to a value below the critical point by increasing the workability through suitable means, the strength can be increased. The use of suitable admixtures is one method of increasing the workability without affecting the strength. The critical point can be shifted to a new position by using admixtures.

2. MATERIALS AND METHODS

2.1 Materials

The following materials were used in the study:

(i) 43 grade ordinary Portland cement with initial setting time = 40 min; final setting time = 6hr; fineness of cement = 2%; consistency of cement = 31%,
(ii) Fine aggregate passing through 2.36-mm size sieve.
(iii) Coarse aggregate of 20 mm size,
(iv) CONPLAST – P 509, a formulated blend of polymeric materials based on hydrolyzed carbohydrate derivatives,
(v) CONPLAST – RP 264, a dark brown liquid based on selected lignosulphates. CONPLAST – P 509 &

CONPLAST – RP 264 are chosen for evaluation, and

(vi) Ordinary potable water.

2.2 Methods

The present work consists of evaluation of effects using CONPLAST – P 509 and CONPLAST – RP 264 admixtures by conducting:

- Tests to determine the cube compressive strength of concrete
- Tests to determine the cylinder split tensile strength of concrete
- Tests to determine the flexural strength of concrete
- Tests to determine the workability by slump on concrete

The above tests are carried out with and without CONPLAST – P 509 and CONPLAST – RP 264.

3. TESTING AND RESULTS

Concrete of mix 1:2:4 by weight is used throughout the work. The w/c ratios of 0.45 and 0.50 are adopted. For test specimen with admixtures, CONPLAST – P509 and CONPLAST – RP 264 are added according to the manufacturers recommendations as given below [3]:

CONPLAST – P509 at 100ml/50kg of cement and CONPLAST – RP264 at 150ml/50kg of cement.

The total quantity of water and chemical added has been kept equal to the total quantity of water required.

About 72 numbers in each of cube specimens of size 150mm x150mm x 150mm, 72 numbers in each of cylinder specimens of size 100mm diameter and 200mm height, and 72 numbers in each of beam specimens with admixtures and an equal number of companion specimens without admixtures have been cast. For beams, 400 mm span has been adopted. For testing under flexure, central concentrated load has been applied gradually.

Strength tests have been conducted at the end of 3, 7 & 28 days. Workability of concrete with and without the admixtures has been measured by slump test.

The results of the various tests carried out are given in Tables 1-5 and Figures 2-4.

Table 1 Compressive Strength of Concrete (in N/mm^2)

W/C Ratio	Age of Concrete (Days)	CONPLAST – P 509			CONPLAST – RP 264		
		Without Chemical	With Chemical	% Change	Without Chemical	With Chemical	% Change
0.45	3	28.97	22.83	-26.88	28.97	26.24	-10.40
	7	30.19	26.74	-12.90	30.19	28.26	-9.66
	28	40.87	48.69	19.13	40.87	42.24	3.35
0.5	3	24.11	19.65	-22.70	24.11	22.06	-9.29
	7	27.47	26.36	-4.21	27.47	26.47	-3.78
	28	36.33	41.2	13.40	36.33	38.06	4.76

Table 2 Tensile Strength of Concrete (in N/mm²)

W/C Ratio	Age of Concrete (Days)	CONPLAST –P 509			CONPLAST – RP 264		
		Without Chemical	With Chemical	% Change	Without Chemical	With Chemical	% Change
0.45	3	1.42	1.60	+12.68	1.42	1.14	-8.02
	7	1.88	2.60	+38.30	1.88	1.60	-17.50
	28	2.88	3.79	+31.60	2.88	3.65	+26.74
0.5	3	1.23	1.25	+1.63	1.23	1.23	00.00
	7	1.60	1.88	+17.50	1.60	1.88	+2.75
	28	1.96	2.57	+31.12	1.96	2.36	+20.41

Table 3 Flexural Strength of Concrete (in N/mm²)

W/C Ratio	Age of Concrete (Days)	CONPLAST – P 509			CONPLAST – RP 264		
		Without Chemical	With Chemical	% increase	Without Chemical	With Chemical	% increase
0.45	3	4.76	3.86	-23.33	4.76	4.04	-17.82
	7	5.31	5.26	-0.95	5.31	5.62	+5.84
	28	5.85	8.35	+42.74	5.85	8.44	+44.30
0.5	3	4.49	3.99	-12.53	4.49	3.86	-16.32
	7	4.90	5.17	-23.18	4.90	5.17	+23.98
	28	6.80	8.16	20.00	6.80	7.48	+10.00

Table 4 Details of Slump Cone Test on Concrete With and Without Conplast – P 509

Sl. No.	Mix	Water Content (ml)	W/C Ratio	Slump (mm)	
				With Chemical	Without Chemical
1	1:2:4	1019	0.45	0	0
2	1:2:4	1133	0.50	3	0
3	1:2:4	1247	0.55	4	0
4	1:2:4	1361	0.60	5	6
5	1:2:4	1475	0.65	7	8
6	1:2:4	1589	0.70	10	10
7	1:2:4	1703	0.75	60	15
8	1:2:4	1817	0.80	collapsed	20

Table 5 Details of Slump Cone Test on Concrete with and without Conplast RP - 264

Sl. No.	Mix	Water Content (ml)	W/C Ratio	Slump (mm)	
				With Chemical	Without Chemical
1	1:2:4	1017	0.45	0	0
2	1:2:4	1130	0.50	4	0
3	1:2:4	1243	0.55	5	0
4	1:2:4	1356	0.60	5	6
5	1:2:4	1469	0.65	7	8
6	1:2:4	1582	0.70	18	10
7	1:2:4	1695	0.75	45	15
8	1:2:4	1808	0.80	65	20
9	1:2:4	1931	0.85	collapsed	35

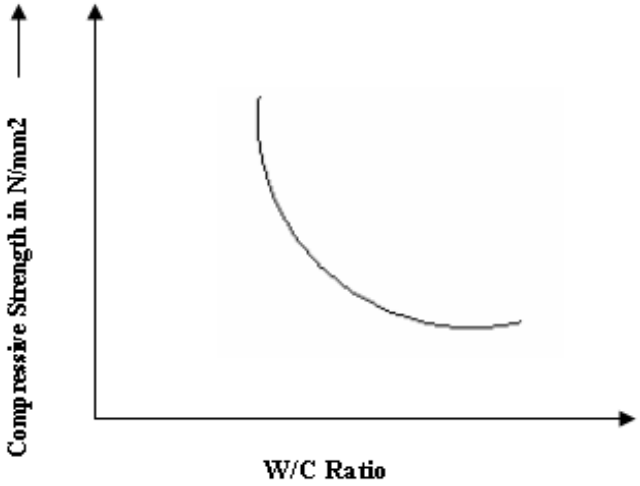

Fig.1 Variation of compressive strength with water cement ratio

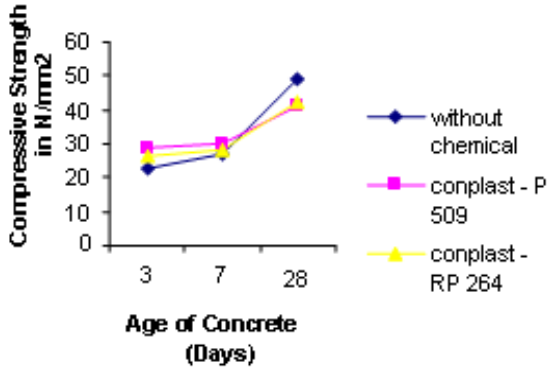

Fig.2a Compressive strength of concrete for w/c 0.45

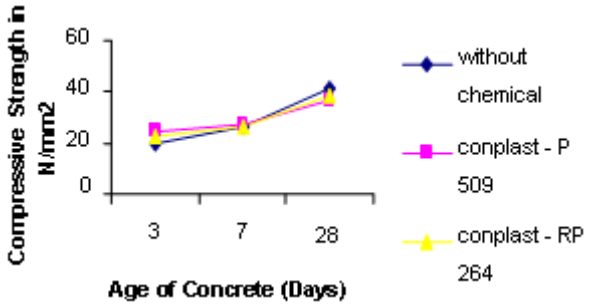

Fig.2b Compressive strength of concrete for w/c 0.50

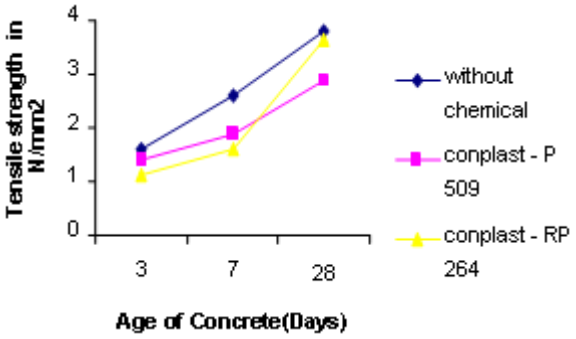

Fig.3a Tensile strength of concrete for w/c 0.45

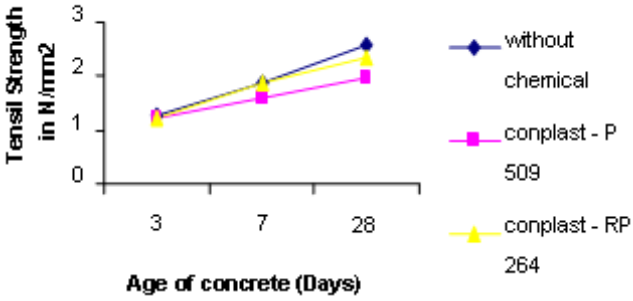

Fig.3b Tensile strength of concrete for w/c 0.50

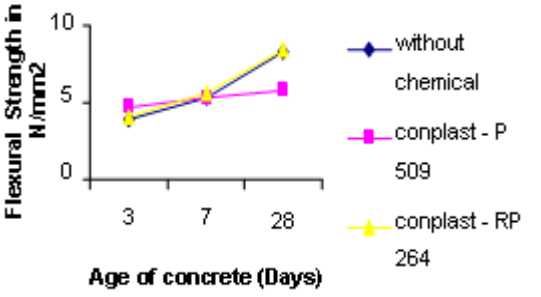

Fig.4a Flexural strength of concrete for w/c 0.45

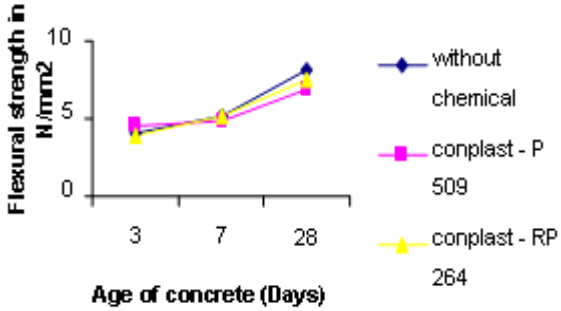

Fig.4b Flexural strength of concrete for w/c 0.50

4. CONCLUSIONS

From the experimental evaluation on the use of CONPLAST – P 509 and CONPLAST – RP 264 in concrete, the following points are noteworthy:

- For the same cement, the use of the above chemicals in concrete was found to change in 28 days, the compressive, tensile and flexural strengths at w/c ratios of 0.45 and 0.50.

- The use of CONPLAST P- 509 and CONPLAST RP-264 lead to change in slump of 3 mm and 4 mm for w/c ratios of 0.50 and 0.55. There is no change in slump due to the chemicals for a w/c ratio of 0.45. The slump has been almost equal for both the cases beyond w/c ratio of 0.60. However, it is significantly different for a w/c ratio of 0.75.

- The use of Conplast – RP 264 has led to change in slump of 4mm and 5mm for w/c ratios of 0.50 and 0.55 respectively. The slump was significantly high for w/c ratios beyond 0.65. The specimen collapsed at w/c ratio of 0.85.

- It is observed that up to w/c ratio of 0.7, concrete with chemical gives nearly the same workability as that of the ordinary concrete. Beyond a w/c ratio of 0.7, the concrete with chemical gives more workability. However, for w/c ratio of 0.50 both chemicals are found to give more workability compared to normal concrete.

- For concrete with CONPLAST-P509, the change in compressive strength is varying between -26.88% to +19.13% for a w/c ratio of 0.45 and between -22.7 % to +13.4% for a w/c ratio of 0.5.The change in tensile strength is varying between 12.68% to 38.30% for a w/c ratio of 0.45 and between 1.63% to 31.12% for a w/c ratio of 0.5. The change in flexural strength is varying between -23.33 % to 42.74 % for a w/c ratio of 0.45 and between -12.53% to 20 % for a w/c ratio of 0.5.

- For concrete with CONPLAST-RP264, the change in compressive strength is varying between -10.4 % to .3.35 % for a w/c ratio of 0.45 and between -9.29 % to 4.75 % for a w/c ratio of 0.5. The change in tensile strength is varying between -8.02 % to 26.74 % for a w/c ratio of 0.45 and between 0 to 20.41% for a w/c ratio of 0.5.The change in flexural strength is varying between -17.82 % to 44.30 % for a w/c ratio of 0.45 and between -16.32 to 10 % for a w/c ratio of 0.5.

- It is observed that CONPLAST – P509 is found to be better, revolutary in higher tensile strength compared to normal concrete, under both w/c ratios.

REFERENCES

[1] M.S.Shetty, “Concrete Technology”, S.Chand & Company Ltd, 1982.

[2] “Indian Standard Code of Practice for Plain and Reinforced Concrete”, I.S.456-1978.

[3] A.Vaidyanathan, R.Perumal and M.Antony Rajapazham, “Utilisation of Mineral Admixtures in Concrete”, National Seminar on Experimental Study on Evaluation of Concrete Admixtures, IIT Madras, 28-30 December, 1992.

A NOVEL METHOD FOR MULTI-AGENT COORDINATION IN TASK PROCESS MANAGEMENT

P. Sengottuvelan[1] and A. Shanmugam[2]
[1]Department of Information Technology; [2]Principal
Bannari Amman Institute of Technology, Sathyamangalam - 638 401, Tamil Nadu
E-mail: sengottuvelan@rediffmail.com; dras_bit@yahoo.com
(Received on 08 December 2006 and accepted on 06 March 2007)

Abstract

An agent works coordinately with the other agents in heterogeneous communication environments to solve intricate problems. An harmonious interaction in the local behaviour of individual agents is essential to provide an appropriate system-level behaviour. An agent-based system of activities in a product lifecycle has given a way to the utilization of concurrent engineering principles. An agent-based architecture is necessary for systems supporting strong collaboration. Improved communication and flow of task information between activities are necessary for process management. The main issue is to control task model processes effectively. This paper introduces a methodology for designing the necessity of Task Control Agent along with the issues in Multi-Agent Systems and aims to model a Communication Task Control Agent in the Concurrent Engineering environment.

Keywords: *Agent-based Systems, Concurrent Engineering, Multi-Agent, Task Controlling and Communication*

1. INTRODUCTION

Agent-based information systems have gained attention due to the proliferation and readily available information. Since the information required for solving a problem is continuously generated, processed and maintained within the distributed nodes, it should be recognized and integrated by a coordinator. In order for the coordination to be proper, the coordinator should be able to recognize the exceptions that are raised among different tasks and resolve them properly.

The coordination framework should be responsible for communicating the information and for ensuring progress towards the goal. The ability to capture and manage exceptions is essential for enhancing the effectiveness and efficiency of the coordination mechanism.

2. CONCURRENT ENGINEERING

Concurrent Engineering (CE) has been defined as a systematic approach to the integrated, concurrent design of products and their related processes, including manufacture and support. Concurrent engineering is intended to make the developers consider all elements of the product life cycle from conception through disposal, including quality, cost, schedule, and user requirements [1].

The techniques to share data and process information among teams form the area of active research. Developing techniques for effective collaboration is the key to cross-functional teams. Sharing information about local constraints, priorities and preferences early in the design process is a powerful conflict-management technique. Conflict avoidance is one of the founding principles of concurrent engineering. Since many processes are performed in parallel, incomplete or uncertain information can be used at an early stage. Sharing information or imperfect information may result in increasing the number of life-cycle areas and is described as concurrent chaos.

The researchers developed a tool that aims to construct concurrent engineering facilities to aid the cooperation / collaboration of people designing and producing products and services of any kind of industry [2].

3. MULTI-AGENT SYSTEMS

A process is carried out to solve a problem in order to attain a specified goal. The problem is usually

decomposed into smaller sub-problems [3]. Once the individual solutions of the lower most sub-problems are obtained, the sub-solutions at the lower levels can be aggregated to reach the solution of their parent problem. This process involves cooperative sharing of information among a group of agents.

A Multi-Agent System (MAS) is a coordinated execution of tasks to carry out a process. A process of equal level, need not be elucidated in detail before it is integrated [4]. The MAS require a coordination mechanism that facilitates dynamic collaboration of agents, with the goal of satisfying both local and global system objectives [5].

Agents have to decide not only which local action to perform, but also whether it is worthwhile to perform a communication action before deciding the local action [5]. It is suggested that this would provide a foundation for formal study of cooperative activities and may lead to some insight in the design of cooperative agent policies.

3.1 Multi-Agent Coordination

The primary phase of multi-agent coordination involves gathering the agents in to appropriate groups to carry out the process [6]. Each higher-level task (process) in the system is divided into partial sub-tasks and distributed to the relevant agents. The group generates in turn a set of collectively agreed objectives through an agent interaction model to attain a common goal. The processes are carried out by a group of agents. Each output of an agent is valuable in its own right and also helps to generate the next process.

Cooperative enquiry is a general method of organizing a group of agents to work out a collectively agreed understanding of a problem. The approach calls for a group of agents to afford equal results using the following phases [7]:

- Proposition: the agent proposes and aggress the next action it will take
- Active : the agent takes the agreed action
- Reaction : the agent looks at the action and gives its immediate reaction to it
- Reflection : the agent quietly reflects on what has been achieved by the action, and considers what else if everything needs to be done to complete the action, whether the result is correct and what action to take next.

3.2 Communication through Cooperative Agents

Coordination is the orderly arrangement of group efforts to provide units of action in pursuit of a common purpose. For example, agents must coordinate their activities during the design process to produce quality designs and to use resources effectively. Each task performed by a task agent (henceforth called coordinator) should accomplish a link with the agents that perform a subtask (henceforth called cooperative agent or cooperator). The primary purpose of cooperative agent is to retrieve relevant information by hiding the geographical distribution of data from the view of the coordinator.

Cooperation plays a vital role in the decision making process. A cooperating agent in multi-agent coordination can be developed through the following steps:

- Identify the agents,
- Fix the scope,
- Assess feasibility, and
- Evaluate the risk

The developed system concentrates only on simple (Data Manipulation) queries and it is cooperative up to some extent [6]. The limitation of this system is that the agents reside in the server only for a specific period of time. In case of any errors in cooperative agents, it was not properly intimated to the requesting coordinator. The coordinator unknowingly waits for the cooperative replies until the expiry time of the query, not being aware of the exceptions occurred in the cooperating agent. In order to rectify this problem the author proposes a model for exception handling services to guide the coordinator.

3.3 Team Work

This deals with what teams are, what makes teams work, and how to resolve teamwork problems.

A team consists of at least two people, who are working toward a common goal/objective, wheree a c h person has been assigned specific roles or functions to

perform, and where Completion of the mission requires some form of dependency among the group members[8].

The criteria for successful teams are that the team is clearly identified, its tasks are clear and distinct, the team members have control on their tasks, and there is a real need for the team. The team's success depends on all team members contributing their personal best efforts, supporting other team members, and working cooperatively to resolve issues and disagreements.

The first goal of all team members is to work cooperatively with the entire team to produce a high-quality product on time.

Effective Teamwork requires agreed team goals, established team-member roles, a supportive environment in which to work a common team work process a plan for the work a mutual team commitment to the goals, roles, and plan open and free communication among all the team members the mutual respect and support of all the team members.

4. COMMUNICATION AND COORDINATION IN CONCURRENT ENGINEERING

Coordination is the orderly arrangement of group efforts to provide units of communication action in pursuit of a common purpose. The agents must communicate their activities during the design process to produce quality designs and to use resources effectively (Figure 1).

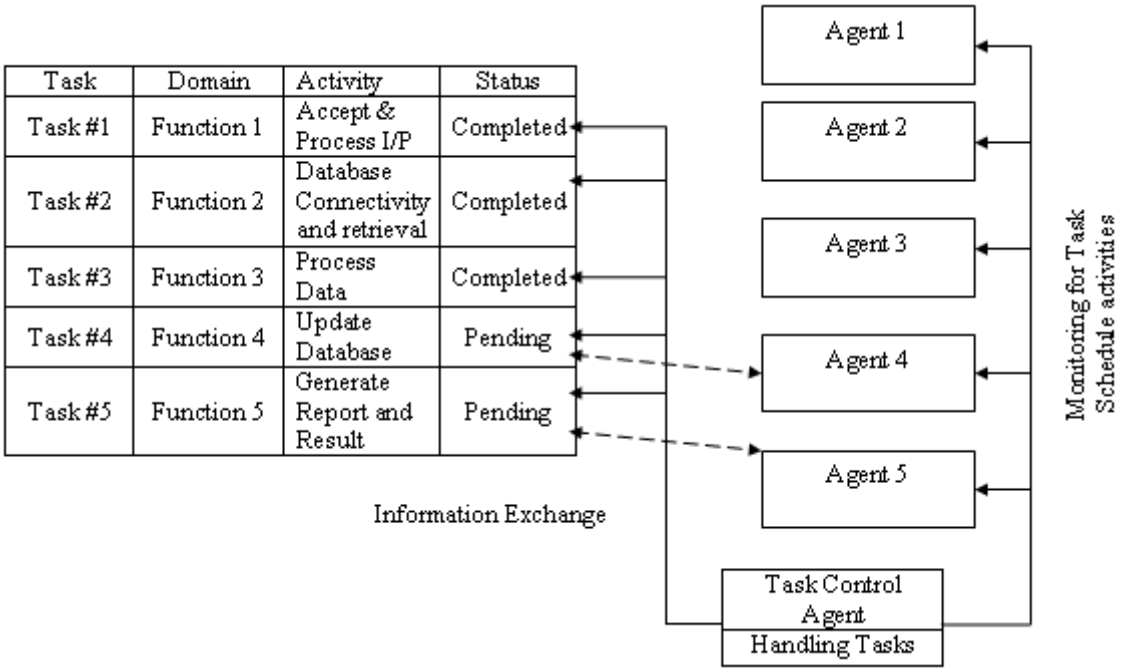

Fig. 1 Sample proposed system for task scheduling activities

Product development has increasingly become a cooperative endeavour that requires effective coordination in the face of complex dependencies over agents, time and functional perspectives. Distinct coordination support communication technologies have emerged for each of those kinds of distribution, but they face important limitations. A unified model of CE coordination was developed that synergistically combines existing approaches in a way that avoids many of their individual limitations and combines their communication strengths.

5. RESULTS AND DISCUSSION

MAS are concerned more with the design of the individual agent and how autonomous, self-motivated and even heterogeneous agents can function together. The agent invokes taking a large job that is divided into dependent tasks and finding a way to schedule the tasks among a group of networked agents with the goal of completing all of the tasks in the least amount of time.

Figures 2-4 depict the modeling of Task Control Agent and related aspects.

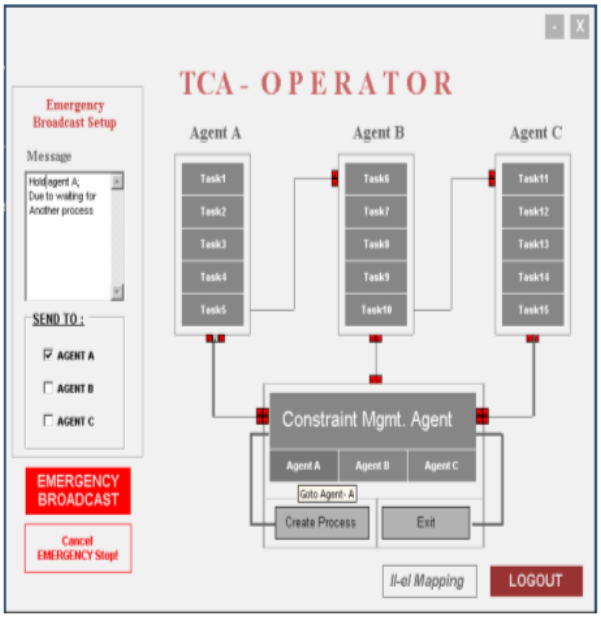

Fig. 2 Multi-agent system concepts using constraint management agent

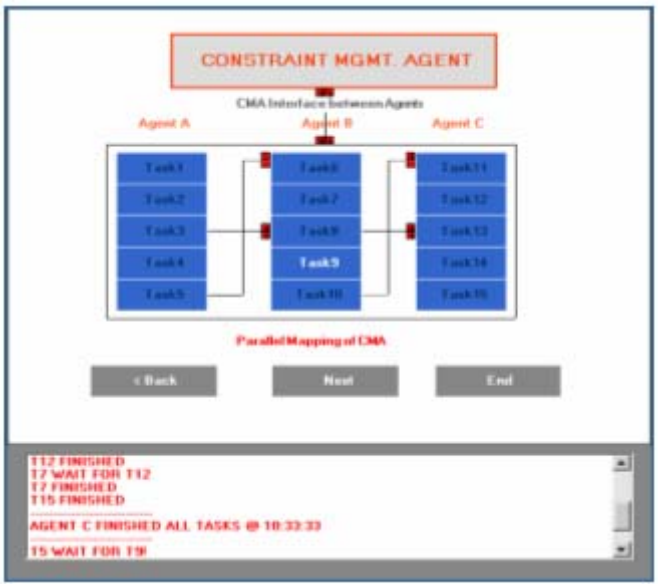

Fig. 3 Constraint management agent (CMA) interface between agent task coordination

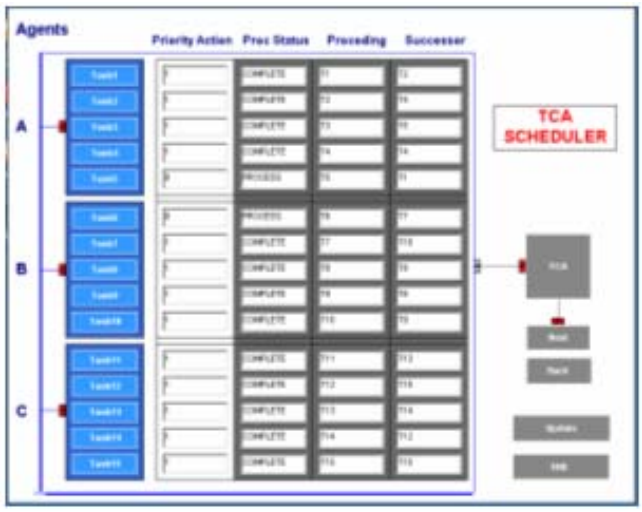

Fig.4 Sample task table for interaction to achieve the result

The result is a hierarchy of processes which are carried by agents. It is easier to establish roles and interactions between roles than processes and interactions between processes.

6. CONCLUSIONS

Agent-based working plays a key role in the design and implementation of distributed systems for cooperation purposes. Since the multifunctional teams have the same objectives, communication and information sharing among multiple teams tend to be more frequent. Hence, open

and free communication and information sharing plays a vital role in team working for Concurrent Engineering. This approach produces substantially superior performance without complicating agent development, since important failures are detected by handlers and not by coordinators.

The present study is focused exclusively on some exceptions occurring in the sub-task level at runtime and not on exceptions concerned with handling agents or information of alternative problem solving method.

The future work will focus on to implement task process enhancement. Efforts to improve efficiency by reducing the effects of interference by the sub-agents will also be dealt with.

REFERENCES

[1] K.J. Cleetus, "Definition of Concurrent Engineering", CERC-TR-RN-92-003,CERC Technical Report Series (Research Note), Vol.1, No.2, 1992, pp. 1-8.

[2] K.Kleinmann, R.Lazarus, and R.Tomlinson, "An Infrastructure for Adaptive Control in Multi-agent Systems", IEEE Conference on Knowledge-Intensive Multi-Agent Systems (KIMAS), Cambridge, Vol.6, No.5, 2003, pp. 714-723.

[3] N.G. Odrey and G.Mejía, "A Re-configurable Multiagent System Architecture for error Recovery in Production Systems", Robotics and Computer Integrated Manufacturing, Vol. 19, 2003, pp. 35-43.

[4] M.Fletcher and D.S. Misbah "Task Rescheduling in Multi-Agent Manufacturing,", Proceedings of the Tenth International Workshop on Database and Expert System Applications 99, 1999, pp 689-694.

[5] I.F. Alexander, "Supporting a Co-operative Requirements Engineering Process", Conference on European Industrial Requirements Engineering, London, 19-20 October 1998, pp. 453-461.

[6] M.Brinn and M.Greaves, "Leveraging Agent Properties to Assure Survivability of Distributed Multi-agent Systems," 2nd International Conference on Autonomous Agents and Multiagent Systems (AAMAS), Melbourne, 2003, pp. 226-232.

[7] Ping Xuan, Victor Lesser and Shlomo Zilberstain, "Communication in Multi-agent Marker Decision Process", Proceedings of the Fourth International Conference on Multi-Agent Systems, Vol.5, No.6, 2000, pp. 404-409.

[8] P. Davidsson and F. Wernstedt, "A Multi-Agent System Architecture for Coordination of Just-in-time Production and Distribution", Proceedings of SAC 2002, Spain, pp. 294-299.

[9] A.C.Dos Santos, S.V.Ribeiro,L.G.Fagundes, R.M.Kayo, T.I. Zanfolim and C.C. Brunetto, "A Synchronous Asynchronous Common Environment for Computer Supported Cooperative Work to Aid Concurrent Engineering Process (SACE-CSCW)", Proceeding of the 17th International Conference of the Chilean Computer Science Society (SCCC'97), Vol.8, 1997, pp. 695-703.

PARALLEL IMPLEMENTATION OF MULTIPLE ANT COLONIES USING MASTER-SLAVE APPROACH FOR STRUCTURAL OPTIMISATION

J. Raja Murugadoss[1], M. G. Rajendran[2] and R. Priya Vaijayanthi[3]
[1]Department of Civil Engineering, Bannari Amman Institute of Technology,
Sathyamangalam - 638 401, Tamil Nadu
[2]Department of Civil Engineering, Karunya Institute of Technology, Coimbatore - 641 114, Tamil Nadu
[3]Department of Computer Science and Engineering, Bannari Amman Institute of Technology,
Sathyamangalam - 638 401, Tamil Nadu
E-mail: rajamurugadoss@gmail.com
(Received on 08 January 2007; revised received and accepted on 08 March 2007)

Abstract

In the present work, an attempt has been made on the parallel implementation of Multiple Ant Colonies (MAC) using Master-Slave (MS) approach for structural optimisation. Results based on well known sizing optimisation of a 25-bar space truss reveal that the MS approach via MAC is a viable optimisation technique in generating safe and economical structural designs in a reasonable amount of computation time.

Keywords: *Parallelism, Master-slave Approach, Multiple Ant Colonies, Discrete Structural Optimisation*

1. INTRODUCTION

The design variables in all structural engineering problems are found to be discrete in nature due to practical time horizon. Therefore, the approach to optimal structural design becomes combinatorial [1] leading to certain difficulties in terms of solution procedure. Consequently, the computational time required to find an optimal solution grows exponentially with increase in number of possible combinations of the design variables. So it is essential to look for an alternative approach to find an optimal solution in a reasonable amount of computation time.

In today's fast computing environment the exploitation of ideal computer time is taking much interest among various researchers in the field of swarm intelligence. Parallel implementation or simply, parallelisation [2] is one such strategy that can be easily adopted in a distributed computing environment. In the first instance, parallelism has a clear adaptive advantage by allowing different ant colonies to build simultaneously at several locations. Secondly, parallel implementation allows huge exploration of possible combinations of design variables concurrently at different locations.

In the present work, parallel processing of MAC, a form of original Ant Colony Optimisation (ACO) algorithm has been attempted using MS approach for discrete structural optimisation. Ant colony optimisation [3] is a recently developed multi-agent, decentralised optimisation technique inspired from the foraging strategy [4] of real world ant species. Parallel implementation of ACO has produced promising solutions in the area of networking and it is further expected to reflect in the area of structural engineering. Surprisingly, it is also found that so far no work has been made using parallel implementation of ACO for structural optimisation problems.

Parallel implementation of MAC has been applied in the present work to find the minimum weight design of a standard 25-bar space truss [5]. The optimisation problem has been formulated as a constrained optimisation problem by treating the cross-sectional areas of the members of space truss as discrete design variables. The constraints are handled in a different approach by adopting negative pheromone deposition (section 3) instead of penalty function. The minimum weight obtained using the present approach has been compared with the earlier works [6 - 13].

2. FORMULATION OF OPTIMISATION PROBLEM

The optimal design of space truss can be considered as sizing optimisation or weight minimisation problem. The objective function f (x) can be defined as a vector for selecting the cross-sectional areas of members, which minimise the weight of the truss structure given by:

$$f(x) = \sum_{i=1}^{n_s} \rho A_i l_i \qquad (1)$$

where 'A_i' is the cross-sectional area of the structural member, 'l_i' is the length of the member, 'ρ' is the material density and 'n_s' is the total number of structural members. The objective function is subjected to displacement and stress constraints as follows:

$$u_{actual} < u_{allowable} \qquad (2)$$

$$\sigma_{actual} < \sigma_{allowable} \qquad (3)$$

where, $\mathbf{u}_{actual}$ and $\mathbf{u}_{allowable}$ are the actual and allowable joint displacements respectively. The $\boldsymbol{\sigma}_{actual}$ and $\boldsymbol{\sigma}_{allowable}$ are the actual and allowable stresses respectively. The constraints are handled by means of negative pheromone deposition, which is explained in the next section. The discrete areas are given by a finite set 'a_n' with their corresponding indices 'a'. The values for 'a_n', uallowable and σallowable have been taken similar to that of the ones taken by [7].

$$p_{ab}(t) = \frac{[\delta_{ab}(t)]^{\alpha}[\psi_{ab}(t)]^{\beta}}{\sum_{a=1}^{|a_n|}[\delta_{ab}(t)]^{\alpha}[\psi_{ab}(t)]^{\beta}}$$

3. IMPLEMENTATION OF MS APPROACH

There are several methods available for parallelising an ant based algorithm in a network of computers. The main categories [14] are Global Parallelism, Coarse-grained Parallelism, Fine-grained Parallelism and Hybrid Parallelism. In the present study an Island Model (IM), a kind of coarse-grained parallelism has been developed with MAC for minimising the weight of space truss. In this (IM) method, several slave processors (here it is taken as 3) are connected to a central processor, often called the master processor. IM has been implemented in a natural way by placing MAC in all the slave processors. These slave processors are centralised by one more MAC placed in the master processor.

The MAC algorithm consists of few sets of self-governing ant colonies. Each ant colony is populated by a group of artificial agents, the number of such agents remaining the same in all ant colonies. In the design of space truss, members with similar geometric properties are grouped together to form a member group. An individual ant colony is assigned to a member group which results in bringing out the optimal cross sectional area for those particular group members. As a whole, this results in a better quality solution.

The basis for choosing MAC instead of Single Ant Colony (SAC) is the actual behaviour observed in real ants. In SAC, an individual agent or an ant with the help of their communal behaviour is capable of performing only one task at a time. In other words, an agent can find only one optimal path from their nest to the food source which is at a distance. It cannot perform multiple tasks (finding more than one optimal path) simultaneously. Therefore, in the problem of weight minimisation of space truss, if more than one member group with different geometric properties is assigned to an individual ant colony, the area which is suitable for a particular set of members in a member group may not be sufficient for another set of members or it may be over-estimating the area for the other set of members. Eventually, it may vary the total weight of the truss leading to uneconomical or unsatisfactory solutions. In order to avoid this intricacy, an individual member group has been associated to an individual ant colony in such a way that it simulates the exact physical behaviour of real ants.

For the optimisation problem given herein we have various sets of ant colonies. Each set comprises of simulated ants that work together to obtain the total weight of the structure. The assignment of area to a particular member group is denoted by mapping (a, b) where 'a' is the area index and 'b' is the member group. Initially, areas are randomly assigned to the member groups and further assignment of areas to the member group is based on a probabilistic state transition rule given by:

(4)

where, δ_{ab} (t) is the trace intensity at time 't' on the mapping (a, b) and $\psi_{ab}(t)$ is the cross sectional area's desirability factor at time't' on the mapping (a, b). Parameters 'g' and 'h' represent the importance of trace intensity and the desirability, respectively, and both these values are user-defined positive quantities. $P^k_{ab}(t)$ represents the probability with which the area with index 'a' can be assigned to member group 'b' by ant 'k' at time 't'. The problem of early convergence to non-feasible solutions may be avoided by selecting the areas probabilistically using equation 4. At the end of iteration, we have a set of solutions equal to the number of ants in an individual colony. Using this set of solutions, which is equal to the number of ants in an ant colony, the trace intensity matrix as well as the desirability matrix is locally updated in the slave processor. The current best solution is also recorded. The trace intensity matrix is updated using the following equation.

$$\delta_{ab}(t+1) = \rho_p \, \delta_{ab}(t) + \sum_{k=1}^{m} \Delta\delta^k_{ab} + e.\delta^{best}_{ab} \qquad (5)$$

where, δ_{ab} (t+1) is the trace intensity in the next time step, ρ_p is the pheromone evaporation rate, δ_{ab} (t) is the trail intensity that already exists on the mapping (a, b). The $\ddot{A}\delta^k_{ab}$ is the amount of pheromone deposited on mapping (a, b) by an ant 'k' and 'm' is the number of ants in each colony. It is calculated as follows

$$\Delta\delta^k_{ab} = \frac{w_k}{W} \qquad (6)$$

where, $$W = \sum_{k=1}^{m} w_k$$

Here 'w_k' is the weight of space truss corresponding to the solution given by ant 'k' in each colony. If mapping (a, b) is a part of the solution given by ant 'k' then $\ddot{A}\delta^k_{ab} > 0$; otherwise it is zero, 'e' is the number of elitist ants [4]. The δ_{ab} best is the trace intensity that is contributed by elitist ants on the mappings of current best solution. This way of using elitist ants reinforces the best solution and thereby focuses future searches to be more effective around the best.

At the beginning of iteration, each mapping has equal probability of being selected by ants. In order to slowly remove the edges that are part of poor solutions, pheromone evaporation i.e. a negative feedback mechanism, takes place through a constant 'ρ_p'.

A significant contribution of this mechanism is that it avoids the algorithm termination at sub-optimal points. A negative feedback mechanism or negative pheromone deposition is also adopted in situations where a particular mapping (a, b) violates the objective function constraints. For example, in a particular solution vector (i.e. combination of design variables), if any of the design variable that corresponds to a particular member group for a particular ant, violates any of the design constraints [equations (2)-(3)], then that particular design variable for that member group in that combination is suppressed by a pheromone quantity of -1. By suppressing this particular violated design variable, the whole combination of design variables is suppressed. Consequently the possibility of choosing this violated design variable associated with a particular member group for a particular combination of design variables becomes void; thereby we can forbid ants from moving to these unfeasible solutions again. The duration of pheromone trail intensity should not be long for avoiding non-feasible solutions to stay in memory for a long time leading to deviation of the algorithm. The desirability factor is updated based on the number of occurrences (i.e. in mathematical terms, the actual frequency or relative occurrence) of a particular area index (a) that has been selected by all ants for a particular member group (b) using the following equation

$$\Psi_{ab}(t+1) = \begin{cases} \Psi_{ab}(t)+1 & \text{if } a \in a_n \\ \Psi_{ab}(t) & \text{otherwise} \end{cases} \qquad (7)$$

In the present algorithm, each ant colony is not allowed to act independently i.e. the ant colonies communicate by sharing the best design values with the inmates of other colonies of the same slave processor for constructing a complete solution and hence inter-colony interaction is permitted. The number of predefined iteration (here it is 1000) has been taken as the termination criteria for the algorithm. In the IM, each processor evaluates the islands separately and independently from other islands, except for periodical migrations of good solutions from the islands (or) slave processors to the master processor. In this model, the exchange of information from the master to the slave is restricted as in a one-way communication. At an interval of every 5 iterations, the best solutions (current best weight with the corresponding areas) evaluated in an island is automatically communicated to the master processor for updating the global pheromone trails. In

the master processor two different types of trail update schemes have been adopted. In the first method, the best solutions that come from the slave processors are compared with the current best solution available in the master processor. If the solutions contributed by the slave processors are superior to the one available in the master processor, then some amount of pheromone is additionally reinforced in the respective cross-sectional areas of the member group proportional to the quality of solution. In the second method, the pheromone is regularly updated for every 5 iterations for all the best solutions contributed by the slave processors are superior to the one available in the master processor, then some amount of pheromone is additionally reinforced in the respective cross-sectional areas of the member group proportional to the quality of solution.

In the second method, the pheromone is regularly updated for every 5 iterations for all the best solutions contributed by the slave processors. The programmes needed for the analysis and optimisation are written in an object oriented design approach using Java and Java Swing and a sample GUI is shown in Figure 1.

4. NUMERICAL INVESTIGATION AND DISCUSSIONS

The 25-bar space truss as shown in Figure 2 is taken as a bench mark problem to demonstrate the effectiveness of the proposed algorithm in two different modes namely stand-alone mode and parallel mode. The material properties (given Table 1), loading conditions (given in Table 2), boundary conditions, member groupings (given in Table 3) and the range of cross sectional areas (0.064516, 0.64516, 1.29032… 25.8064 cm^2) of members of the space truss have been taken similar to those of the values adopted in studies [7, 12].

Initially, the algorithm has been investigated under various parameter settings to find the most encouraging values for the parameters, like the number of ants (m), importance of trail intensity or pheromone deposition (g), importance of desirability (h) and finally, the pheromone evaporation rate (ρ_p). Based on this preliminary investigation, the most promising values are found to be 6, 1, 5 and 0.45 respectively, and these values are adopted for further investigation.

Then the investigation is extended by conducting ten different trials using MAC in the master processor in stand-alone mode. Accordingly, the results are presented in Table 4. It is found that the MAC algorithm yields a minimum weight of 202.798 kg by consuming an average execution time of 1366 seconds by attempting 12059 functional evaluations. Then the minimum weight of 202.798 kg obtained using MAC is compared with the minimum weight of 209.3 kg obtained by using ACOTS (ACO and Tabu Search) which is claimed to be the optimal weight as on-date for this particular problem [7]. It is clear that with MAC a substantial weight reduction of 3.12 % is obtained when compared to ACOTS. Though the percentage of saving in material seems to be less, it accounts more in mass fabrication involved in actual construction practices. The reduction in weight is mainly due to the assignment of an individual ant colony to a single member group instead of all others in the 25-bar space truss.

The optimisation is further continued by parallelising MAC using MS approach via IM. For each trail update scheme as discussed earlier, five numerical experiments were separately carried out and the results, in terms of weight, computation time and functional evaluations are furnished in Table 5. It is evident that the parallel implementation of MAC using MS approach via IM always yields better quality solutions as compared to stand-alone mode by consuming same range of computation time with increased number of functional evaluations. As shown in Table 5 the overall lowest values obtained by the present distributed algorithm are 183.043 kg & 195.55 kg for the method 1 and method 2 respectively.

On the other hand, the solutions attained using methods 1 and 2 are exclusively compared with each other (Table 5), the expected performance of parallelism is not that much pronounced with the second scheme. With the second method, it is observed from the numerical investigation that the algorithm performs comparatively similar to stand-alone mode and only a petite improvement is observed. Another major disadvantage observed with method 2 is that the algorithm attempts more number of functional evaluations by selecting the recently visited solutions. Also, the solution quality is not found to be improved after a certain number of iterations. In contrast, the solutions given in Table 5 for the first method are found to be very much comparable and the effect of

parallelism is well reflected in the lightest truss design having a minimum weight (to-date) of 183.043 kg. A reduction in weight by 12.54 % is observed with the minimum weight of 183.043 kg (Table 5), when it is compared with the optimal weight of 209.3 kg obtained using ACOTS [7]. Also, a comparative study (Table 6) provides evidence that the percentage of saving in material is found to be significant as compared to other approaches, like genetic algorithm, standard ant colony optimisation algorithm and so on. The results showed that it is better to exchange the best solutions found so-far for every fixed number of iterations and to use them in the pheromone update rather than for all the best solutions coming from the slave processors. The main observation was that the best results can be obtained by limiting the information exchange to the master processor in order to achieve a near optimal solution in a reasonable amount of computation time.

5. CONCLUSIONS

The IM of MAC in a distributed computing environment is an effective tool for solving discrete structural optimisation problems. The lightest 25-bar space truss designed by the proposed algorithm weighs 183.043kg, which is lower than the one traced by other recent heuristics approaches. Though the present example provides strong evidence that parallelism using MAC is a useful and viable optimisation technique, the algorithm can be further enhanced by increasing the number of slave processors and adopting two-way communication between the master and slave processors for achieving very high promising solutions.

REFERENCES

[1] C.H. Papaddimitriou and K.Steiglitz, "Combinatorial Optimisation: Algorithms and Complexity", Dover Publications, INC, Minelo, New York, 1998.

[2] R. Michel and M. Middendorf, "An Island Model Based ant System with Lookahead for the Shortest Supersequence Problem", Proc. of PPSNV-Fifth Int. Conf. on Parallel Problem Solving from Nature, Springer Verlag 1998, pp.692-701.

[3] M. Dorigo and L. M. Gambardella, "Ant Colony System: A Cooperative Learning to the Traveling Salesman Problem", IEEE Trans. Evol. Comp., Vol. 1, 1997, pp. 53-66.

[4] E. Bonabeau, M. Dorigo and G. Theraulaz, "Swarm Intelligence from Nature to Artificial System", Oxford University Press, New York, 1999.

[5] V. B. Venkayya, N. S. Khot and V. S. Reddy, "Energy Distribution in an Optimal Structural Design", AFFDL-TR-68-156, Flight Dynamics Laboratory, Wright Patterson AFB, Ohio 2, 1969.

[6] H. Adeli and O. Kamal, "Efficient Optimisation of Space Trusses", Computers and Structures, Comput. Struct., Vol. 24, No.3, 1984, pp. 501-511.

[7] J. A. Bland, "Optimal Structural Design by Ant Colony Optimisation", Engineering Optimisation, 33, 2001, pp. 425-443.

[8] N. H. Chao, S. J. Fenves and A. W. Westerberg, "Application of Reduced Quadratic Programming Techniques to Optimal Structural Design", New Directions in Optimum Structural Design, John Wiley, New York, 1984.

[9] C. V. Camp, S. Pezeshk and G. Cao, "Optimized Design of Two Dimensional Structures Using Genetic Algorithm", Journal of Structural Engineering, Vol.124, No.3, 1998, pp. 551- 559.

[10] C. V. Camp and Bichon, "Design of Space Trusses Using Ant Colony Optimisation", Journal of Structural Engineering, Vol.130, No.5, 2004, pp. 741-751.

[11] D. M. Zhu, "An Improved Templeman's Algorithm for Optimum Design of Trusses with Discrete Member Sizes", Engineering Optimisation, Vol.9, 1986, pp.303-312.

[12] S. Rajeev and C. S. Krishnamoorthy, "Discrete Optimisation of Structures using Genetic Algorithms", J. Structural Engineering , Vol.118, No.5, 1992, pp. 1233 – 1250.

[13] M. P. Saka, "Optimum Design of Pin-Jointed Steel Structures with Practical Applications", Journal of Structural Division, ASCE, Vol. 116, No.10, 1990, pp. 2599-2620.

[14] M. Dorigo, and T. Stutzle, "Ant Colony Optimisation", MIT Press, Cambridge, MA, USA, 2004.

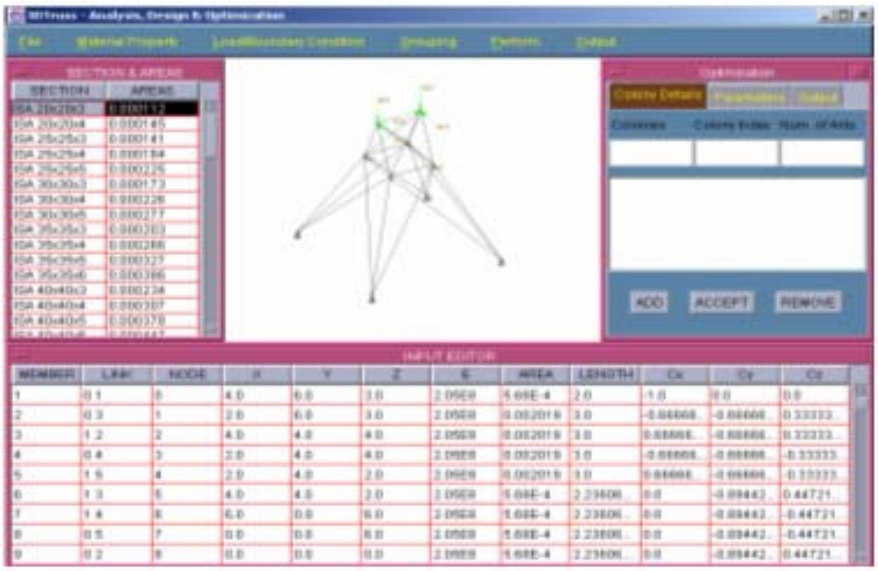

Fig. 1 Software for analysis and optimisation of space trusses

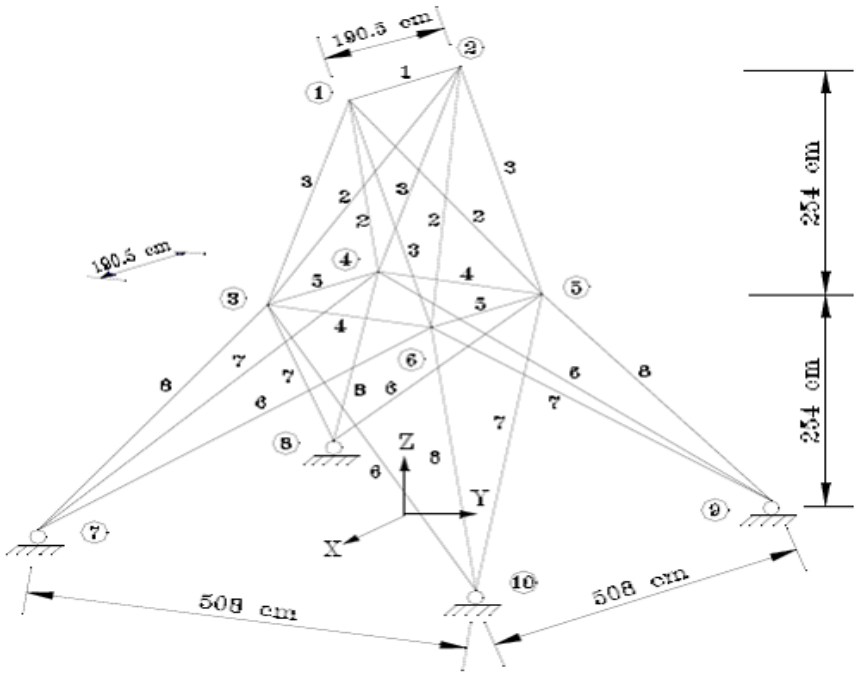

Fig.2 Representation of 25-bar space truss

Table 1 Material Properties

Material	Aluminium
Young's Modulus (E)	6.895×10^7 kN/m^2
Density (ρ)	2767.042 kg/m^3

Table 2 Loding Condition

Joint Number	Joint Load (kN)		
	x	y	z
1	4.4482	44.482	-22.241
2	0.0	44.482	-22.241
3	2.2241	0.0	0.0
4	2.2241	0.0	0.0

Table 3 Member Groupings

Group Number	Member Numbers
1	1
2	2, 3, 4, 5
3	6, 7, 8, 9
4	10, 11
5	12, 13
6	14, 15, 16, 17
7	18, 19. 20, 21
8	22, 23, 24, 25

Table 4 Minimum Weights for the 25-bar Space Truss (stand-alone mode)

Trial No.	Minimum Weight (kg)	Maximum Execution Time (sec)	Time Required to Reach the Minimum Weight (sec)	Functional Evaluations*	Total Number of Possible Combinations of Design Variables
1	225.020	1449	1340	6498	1.06338×10^{37}
2	224.175	1561	1461	4931	1.06338×10^{37}
3	202.798	1411	1311	10857	1.06338×10^{37}
4	234.575	1465	1399	5535	1.06338×10^{37}
5	216.195	1414	1410	7560	1.06338×10^{37}
6	227.336	1460	1385	9849	1.06338×10^{37}
7	212.846	1395	1325	13171	1.06338×10^{37}
8	202.798	1423	1420	13260	1.06338×10^{37}
9	229.749	1421	1389	3982	1.06338×10^{37}
10	212.846	1458	1426	13309	1.06338×10^{37}
Average	218.833	1446	1387	8932	1.06338×10^{37}
Minimum	202.798	1417**	1366***	12059****	1.06338×10^{37}

* Number of functional evaluations attempted by the algorithm to reach the optimal solution

** Average maximum execution time required to reach a minimum weight of 202.798 kg which corresponds to trials 3 and 8

*** Average minimum time required to reach a minimum weight of 202.798 kg which corresponds to trials 3 and 8

**** Average number of functional trials required to reach a minimum weight of 202.798 kg which corresponds to trials 3 and 8

Table 5 Minimum Weights for the 25-bar Space Truss (MS approach)

Trial No.	Method 1				Method 2			
	Minimum Weight (kg)	Maximum Execution Time (s)*	Time Required to Reach Minimum Weight**	Functional Evaluations***	Minimum Weight (kg)	Maximum Execution Time (s)	Time Required to Reach Minimum Weight	Functional Evaluations
1	186.441	1498	1347	23842	218.621	1458	1021	19724
2	183.043	1521	1486	20432	209.327	1376	1126	46896
3	188.855	1492	1382	25146	202.798	1420	1389	36936
4	183.355	1518	1510	22147	195.553	1412	1231	25992
5	186.441	1487	1423	18728	195.553	1422	1198	25964

* Maximum time required to complete 1000 iterations

** Minimum time required to reach the lowest weight

*** Number of functional evaluations attempted by all the processors

Table 6 Designs for 25-bar Truss using Various Approaches

	(1)	(2)	(3)	(4)	(5)	(6)	(7)	(8)	Weight (kg)	Saving in Material (%)
Adeli and Kamal, 1984	0.0645	12.8097	19.100	0.0645	0.0645	5.2013	10.8355	16.3213	247.522	26.049
Chao et al., 1984	0.0645	13.1709	19.3619	0.0645	0.0645	4.4103	10.4825	17.2361	247.236	25.964
Zhu, 1986	0.6451	12.2580	16.7741	0.64516	0.64516	5.16128	13.5483	16.7741	255.262	28.292
Saka, 1990	0.06451	13.2770	19.2770	0.064516	0.06452	4.49	10.774	16.723	247.226	25.961
Bland, 2001	0.0645	0.64516	21.93544	0.064516	16.1290	5.16128	0.64516	25.1612	209.300	12.545
Camp and Bichon, 2004	0.0645	12.9032	19.1354	0.0445	0.0774	4.4451	10.8373	17.2129	247.463	26.032
MAC (stand-alone mode)	13.5483	5.806439	13.54836	0.064516	0.06452	3.87096	13.54836	13.5484	202.798	9.741
MAC (parallel mode)	0.06451	5.161280	13.54836	0.064516	0.06452	3.87096	10.32256	13.5484	183.043	

VIENNA RECTIFIER FOR CRITICAL CIRCUIT TOPOLOGY AND CONTROL METHOD

V. Ramkumar, V. Gopalakrishnan and S. Palaniswami
Department of Electrical and Electrnoics Engineering, GCT, Coimbatore - 641 013, Tamil Nadu
E-mail: ramkumarenigma@gmail.com
(Received on 10 January 2007 and accepted on 12 April 2007)

Abstract

The Vienna Rectifier topology is proposed to achieve 3-phase power factor correction, and maintaining constant output voltage. The Vienna Rectifier approach is highly efficient when compared to the conventional two-level, six-switch boost PWM Rectifier. Its embodiment with reduction of plant size needs only three active switches,and there is no need for a neutral wire, reduction in voltage stress and switching losses of power semi conductors. The topology of Vienna Rectifier comprises a semiconductor switch, a MOSFET in each Phase leg of a 3-Phase diode bridge. By adjusting the width of the pulse, that turns ON the MOSFET, corresponding line current is forced to be sinusoidal and inphase with the voltage. For a short switching period, the capacitors charge linearly. This offsets -Vdc and +Vdc.The offset depends on the corresponding phase voltage and the switch "ON" time duration. In the control scheme, two control loops were adopted, to achieve reference current tracking and DC-link regulation. The functions of the control scheme are to obtain unity power factor at the AC-side, and to balance the neutral-point voltage.

Keywords: *AC-DC Power Conversion,Unity Power Factor, Vienna Rectifier*

1. INTRODUCTION

Among the conventional rectifiers the Vienna Rectifier is highly efficient in its performance, which has only three power switches, the selection of the Pulse Width Modulation (PWM) carrier signals for three-phase, three-wire PWM converter systems, which if not considered, would result in higher phase current ripple and reduced efficiency [1]. Vienna rectifier discusses the final topology of the power circuit but it introduces all important issues required for understanding the system concept. The paper investigates the stability of the output voltage neutral point in detail. It shows that the control of the neutral point potential can be incorporated into the phase current control with low additional effort. Furthermore, it is verified that in case the neutral point potential control is provided, even large amounts of current drawn from the neutral point or fed into the neutral point do not cause an asymmetry of the output voltage partitioning. The paper is of theoretical appearance but in summary does show clearly that there is no reason to be concerned about the neutral point potential stability and/or control [2]. The classical proportional-integral voltage controller and carrier-based current controller are adopted in the outer loop and inner loop to implement DC-bus voltage.

Three level rectifiers with reduced number of switches (such as the Vienna Rectifier) have been receiving wide interest in the past years to improve the input power quality of rectifier systems. In this paper, a new carrier-based PWM control algorithm is proposed for such converters to eliminate the low frequency harmonics in the line current while achieving unity power factor at the rectifier input terminals. A promising cost reduction opportunity can be seen with elimination of input current sensing to operate the Vienna Rectifier [3].

The DC-bus voltage controller in the outer loop obtains the amplitude of line-current command. A carrier-based current controller in the inner loop tracks line-current command. Here are good line current waveforms with almost unity power factor and low current harmonics [4].

2. PRINCIPLE AND OPERATION

It is a highly efficient method of high current, 3-phase AC to DC conversion and is particularly attractive for achieving unity power factor operation.

2.1 Topology

Figure1 shows 440V, 50Hz, 3-phase sinusoidal line Voltages. -Vdc and +Vdc are the DC outputs connected to load.

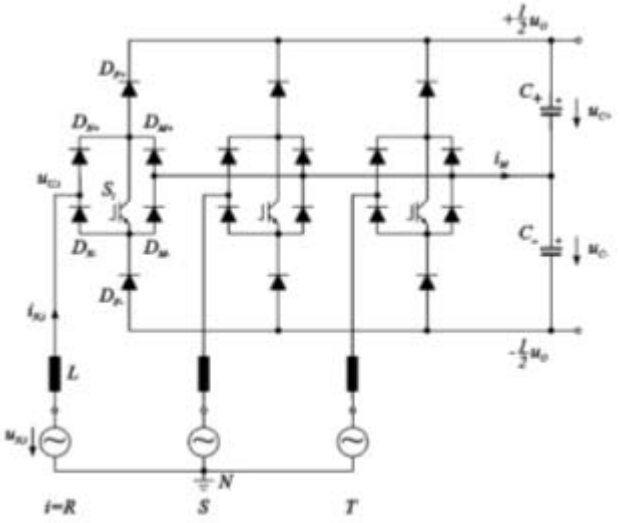

Fig. 1 Power circuit of Vienna rectifier

There are three semiconductor switches, corresponding to each phase T_1, T_2, T_3. These are switched continuously at around 25 KHz. The duty cycle of the PWM switching is so designed that the current drawn from each phase is sinusoidal and in phase with the corresponding line voltage, thus ensuring near unity power factor and minimum total harmonic distortion.

2.2 Operation

In Vienna rectifier configuration, as shown in Fig.1, the output capacitor is split in two equal parts as two equal value capacitors, C_1, C_2, connected in series. Across the output capacitors the -Vdc and +Vdc are developed as 3-phase peak detected outputs.

A switch for each phase is connected, such that when "ON", it connects the line phase to the center node of C_1, C_2 through a series inductance. For a short switching period, assuming 10 microseconds, the capacitors charge linearly. This offsets - Vdc and +Vdc. This offset depends on the corresponding phase voltage and the switch "ON" time duration. The common node of C_1,C_2 will have voltage with triangular wave shape, having three times the main frequency and its amplitude will be one quarter of the phase voltage.

3. SWITCHING REALIZATION CONSTRAINTS

The ideal switch can be realized using different combinations of controlled switches and diodes. One of the realizations is the unidirectional topology with reduced count of controlled switches is the Vienna Rectifier as shown in Figure 2. In each phase-leg, only one controlled switch is used.

With assumption of continuous conduction mode (CCM), the Rectifier pole voltages (V_{AN}, V_{BN}, V_{CN}) have a definite state determined by on/off states of controlled switches and the polarity of line currents at any instant of operation. For instance, if the line current *ia* is positive and the controlled switch *Qa* is off, the voltage between the converter pole A and dc bus midpoint N, i.e., V_{AN} is Vdc/2. The conduction path for this case is illustrated in Figure 2 (a).

If the line current *ia* is positive and the controlled switch *Qa* is on, the voltage V_{AN} is 0, in which case the conduction path is illustrated in Figure 2 (b). Similarly, if the line current *ia* is negative, the voltage V_{AN} can be either - Vdc/2 if the switch *qa* is off or 0 if the switch *Qa* is on as illustrated in Figures 2(c) and (d) respectively. This operating principle also applies to phase legs B and C. To avoid low frequency (lower than the switching frequency) harmonics in line currents, the rectifier phase voltages must be free of low frequency harmonics except for triplen harmonics, which may present on the modulation signals to increase the fundamental component without invoking over-modulation.

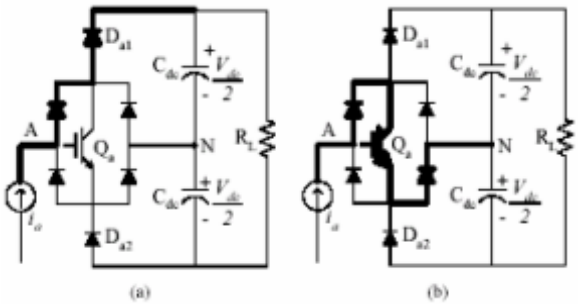

Fig. 2 Illustrations of conduction paths

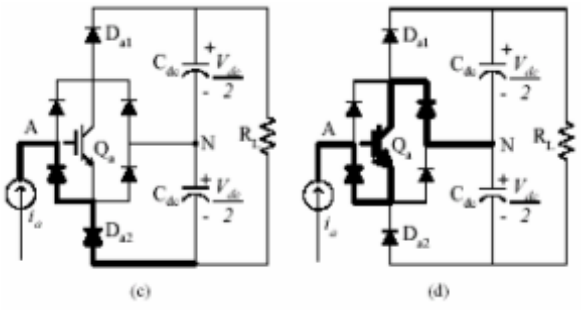

Fig. 2 Illustrations of conduction paths

Under CCM an important operating constraint can be recognized. If continuous sinusoidal PWM is used, the polarity of the line currents and the polarity of the imposed line to neutral voltage from the switching devices have to be identical. In the past this has been referred to as the pulse polarity consistency rule (PPCR). Thus on an average basis, the line currents have to be in phase with corresponding pole to neutral voltages. Otherwise, low frequency harmonic distortion will occur in both line currents and pole voltages. This requirement is equivalent to the unity power factor at the rectifier poles (not at the source voltages). On the other hand, under space vector modulation mode the input power factor angle at the rectifier input terminals may lie between (-Đ/6, Đ/6) . Although this appears to be a drawback, realistic value of input inductors lead to a power factor at the line terminals to be greater than 0.98 for typical cases.

4. CONTROL SCHEME

The proposed converter is operated as a power factor corrector to reduce the current harmonics, increase input power factor, draw sinusoidal line currents from the AC source, and maintain DC-bus voltage constant.

Two control loops were adopted in the control scheme to achieve reference current tracking and DC-link regulation. In the outer loop control a classical proportional-integral controller was used to balance the AC-side input power and DC-side output power so that the DC-side capacitor voltage can be a constant value. If the DC-side voltage is lower than the reference voltage, the output value of the PI controller will increase the amplitude of the line current command to increase the input AC power for compensation of DC-bus voltage drop. If the DC-bus voltage is higher than the reference voltage, the output value of PI controller will decrease the input AC power for compensating the DC-side voltage. The line current amplitude from the output of PI controller is expressed as

$$I_s = K_p(v^*_{dc} - v_{dc}) + Ki\int (v^*_{dc} - v_{dc})dt \qquad (1)$$

where Kp and Ki are proportional and integral gains respectively, Vdc* is the DC-bus voltage command, and Vdc is the measured DC-side voltage. One of the main functions of the control scheme is to obtain unity power factor at the AC-side. Therefore, a phase-locked loop circuit is adopted to generate three unit sinusoidal waves with 120° phase shift. These three balanced sinusoidal waves are synchronized to three-phase source voltages and expressed as

$$u_a(t) = \sin \omega t \qquad (2)$$

$$u_b(t) = \sin(\omega t - 2\pi/3) \qquad (3)$$

$$u_c(t) = \sin(\omega t + 2\pi/3) \qquad (4)$$

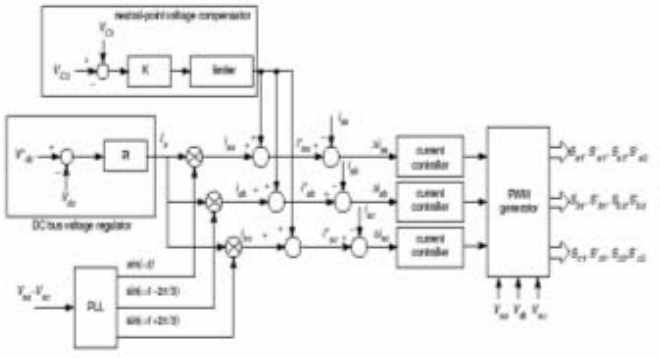

Fig.3 Block diagram of the control scheme

The output value of the PI voltage controller is multiplied by three balanced sinusoidal waveforms to obtain the line currents:

$$i_{sa}(t) = I_s u_a(t) = I_s \sin \omega t \qquad (5)$$

$$i_{sb}(t) = I_s u_b(t) = I_s \sin(\omega t - 2\pi/3) \qquad (6)$$

$$i_{sc}(t) = I_s u_c(t) = I_s \sin(\omega t + 2\pi/3) \qquad (7)$$

The second function of the proposed control scheme is to balance the neutral-point voltage. The neutral-point voltage on the DC-side may be unbalanced under load variation. To reduce the neutral-point voltage unbalance problem, a voltage compensator was used to add a small

DC in the line-current command to compensate the neutral-point voltage. This small direct compensated current for neutral-point voltage balance is given as

$$I_{npc}=K[V_{c1}-V_{c2}] \tag{8}$$

where Vc_1 and Vc_2 are average voltages across capacitors C1, C2 respectively, and K is a small gain of the neutral-point voltage compensator. To avoid a large DC-term in the line current due to unbalance neutral-point voltage, a limiter can be placed after the neutral-point compensator. If the DC capacitor voltage Vc_2 is greater than Vc_1, then a small positive direct current is added to the line current-command. Capacitor voltage Vc_1 will be increased in the following line period. Therefore, the capacitor Voltage Vc_1 is compensated. The resultant line-current commands are given as:

$$i^*_{sa}(t) = I_s \sin(\omega t) + I_{npc} \tag{9}$$

$$i^*_{sb}(t) = I_s \sin(\omega t - 2\pi/3) + I_{npc} \tag{10}$$

$$i^*_{sc}(t) = I_s \sin(\omega t + 2\pi/3) + I_{npc} \tag{11}$$

The carrier-based current controller is used to track the reference line current. The sine-triangular PWM scheme is adopted to generate proper signals for the switches. An average model of the proposed converter is adopted to find the state variable in the steady state

$$I_n = -D_a[1-\sin(D_a)]I_{sa} - D_b[1-\sin(D_b)]I_{sb} - D_c[1-\sin(D_c)]I_{sc}$$

$$X = \frac{1}{T}\int_t^{t+1} x(\tau)d\tau \tag{12}$$

where x is a voltage or current variable, and X is an average value of state variable x in a switching period. The instantaneous AC-terminal voltages and DC-side currents can be expressed as the average values using the PWM control. The average models of the AC-side voltages and DC-side currents are given as

$$V_{a0} = D_a\frac{V_{dc}}{2}\quad , V_{b0} = D_b\frac{V_{dc}}{2}\quad , V_{c0} = D_c\frac{V_{dc}}{2} \tag{13}$$

$$I_p = D_a\sin(D_a)I_{sa} + D_b\sin(D_b)I_{sb} + D_c\sin(D_c)I_{sc} \tag{14}$$

(15)

where D_a, D_b and D_c are duty ratios of AC-terminal voltages Va_o ,Vb_o and Vc_o, respectively ; sin(y) = 1, if y>0, or 0, if y<0; y = D_a, D_b, D_c and -1<y<1. The system behaviour of the converter on the AC-side is expressed as:

$$V_{x0} = V_{sx} - rI_{sx} - L\frac{dI_{sx}}{dt} \tag{16}$$

where x = a, b, c. If the voltage drop across the resistor r can be neglected one can obtain the duty ratio for each converter leg based on (13) and (16) as:

$$D_x \approx \frac{2}{V_{dc}}(V_{sx} - L\frac{dI_{sx}}{dt}) \tag{17}$$

Based on the analysis of three operating states, one high voltage level and one low voltage level can be generated on the AC-side during the positive and negative phase voltage to track line-current commands. At the positive phase voltage, high voltage level Vdc/2 (state 1) and low voltage level 0 (state 2) are generated on the AC terminal to neutral-point voltage. At the negative phase voltage, high voltage level 0 (state 2) and low voltage level -Vdc/2 (state 3) are generated on the AC-side. The high voltage level is generated to decrease the line current and low voltage level is generated to increase the line current. Based on this analysis and the measured voltage and current error, the PWM signals for each switch are expressed as

$$D_{sa1} = \begin{cases} 1, & if \quad V_{sa} > 0 \\ 1+\frac{2}{V_{dc}}(V_{sa} - L\frac{dI_{sa}}{dt}). & if \quad V_{sa} < 0 \end{cases} \tag{18}$$

$$D_{sa2} = \begin{cases} \frac{2}{V_{dc}}(V_{sa} - L\frac{dI_{sa}}{dt}), \\ 0, \end{cases} \tag{19}$$

$$D_{sb1} = \begin{cases} 1, & if \quad V_{sb} > 0 \\ 1+\frac{2}{V_{dc}}(V_{sb} - L\frac{dI_{sb}}{dt}), & if \quad V_{sb} < 0 \end{cases} \tag{20}$$

$$D_{sb2} = \begin{cases} \frac{2}{V_{dc}}(V_{sb} - L\frac{dI_{sb}}{dt}), & if \quad V_{sb} > 0 \\ 0, & if \quad V_{sb} < 0 \end{cases} \tag{21}$$

$$D_{sc1} = \begin{cases} 1, & if \quad V_{sc} > 0 \\ 1+\frac{2}{V_{dc}}(V_{sc} - L\frac{dI_{sc}}{dt}). & if \quad V_{sc} < 0 \end{cases} \tag{22}$$

$$D_{sc2} = \begin{cases} \frac{2}{V_{dc}}(V_{sc} - L\frac{dI_{sc}}{dt}), & if \quad V_{sc} > 0 \\ 0, & if \quad V_{sc} < 0 \end{cases} \tag{23}$$

From the derived PWM signals the switch S_{x1} is turned on at the positive mains voltage. Therefore, the operating states 1 and 2 are selected to generate AC terminal voltage $Vx_o = Vd_c/2$ and 0 respectively. On the other hand, switch S_{x2} is turned off at the negative phase voltage. The operating states 2 and 3 are selected to generate AC terminal voltage Vxo = 0 and $Vd_c/2$ respectively. The block diagram of the proposed control scheme is given in Fig.3. The outer loop controller is implemented by the PI voltage controller to maintain the DC-bus voltage constant and to output the amplitude of line current command. Because the unity power factor is one of the control functions, the output of the PI voltage controller is multiplied with three unit sinusoidal waves in phase with mains voltages to generate the line-current commands. A neutral-point voltage compensator is used to compensate the capacitor voltage unbalance on the DC-side due to load changed. The carrier-based current controller is used in the inner loop to track the line-current commands.

For the proposed Vienna rectifier of fewer semiconductors, a simple control scheme was established. The propor-tional-integral (PI) voltage controller is used in the outer loop to regulate the DC-link voltage. In the inner loop, the carrier-based current controller is used to track line-current commands. A voltage compensator is adopted to balance the neutral-point voltage due to the load variation.

5. SIMULATION RESULTS

In order to validate the concept, a simulation model of a three phase Vienna rectifier prototype has been created in the simulation software package MATLAB® 7.0. Here the simulation has been performed for three phase Vienna rectifier of three phase system, in open loop and closed loop. The parameters of the simulated system can be found below. The parameters have been chosen such that it will be possible to build the prototype using MOSFET modules.

Input voltage=3Ø, 50Hz, 440V (p-p), Rated power=1KW, Source Inductor=10e-6H, Source Resistor=5Ù, DClink capacitor=2,200Ìf, Resistive Load=100Ù, Switching Frequency=18 KHz.

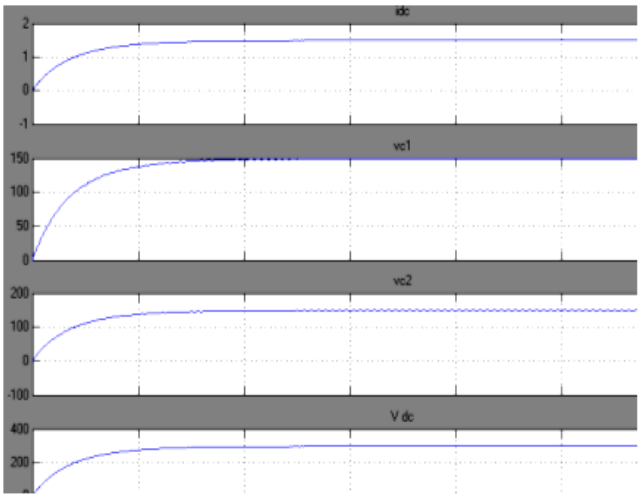

Fig.4 Simulation waveform of constant

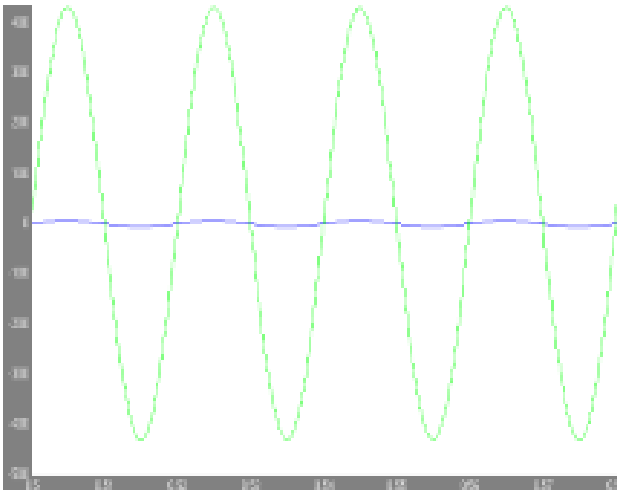

Fig.5 Simulation waveform of inphase of line voltage and current

6. CONCLUSIONS

The Vienna rectifier holds only three switches to improve the current drawn from each phase.This is to be sinusoidal and in phase with the corresponding line voltage, thus ensuring near unity power factor. It maintains the DC-bus voltage constant, and balance the neutral-point voltage due to the load variation.

For the proposed Vienna rectifier of fewer semiconductors, a simple control scheme was established. The proportional-integral (PI) voltage controller is used in the outer loop to regulate the DC-

link voltage. In the inner loop, the carrier-based current controller is used to track line-current commands. A voltage compensator is adopted to balance the neutral-point voltage due to the load variation. The control scheme here established provides support to attain unity power factor. The Vienna rectifier is simulated and its waveforms for open-loop and closed-loop are presented, which shows the unity power factor, and maintaining constant dc output voltage.

REFERENCES

[1] U.Drofenik and J.W. Kolar "Comparison of Not Synchronized Saw Tooth Carrier and Synchronized Triangular Carrier Phase Current Control for the Vienna Rectifier 1", Proceedings of the IEEE International Symposium on Industrial Electronics, Bled, Slovenia, Vol.1, 12-19 July 1999, pp.13-19.

[2] J.W.Kolar, U.Drofenik and F.C. Zach, "Current Handling Capability of the Neutral Point to a Three-Phase/Switch/Level Boost-Type PWM (Vienna) Rectifier", Proceedings of the 27th IEEE Power Electronics Specialists Conference, Baveno, Italy, Vol.2, 24-27 June 1996, pp.1329-1336.

[3] Giri Venkataraman and Ashish Bendre, "Unity Power Factor Control for Three Phase Three Level Rectifiers Without Current Sensors", IEEE Proceeding, Electronics, Power Application, Vol.152, No.3, 2005.

[4] B.R.Lin and T.Y.Yang, "Experimental Verification of Three-Phase Four-Wire Current Regulated PWM Converter", IEEE Proceeding Electronics, Power Application, Vol.152, No.3, May 2005.

DESIGN OF ARTIFICIAL INTELLIGENCE BASED TEMPERATURE CONTROLLER FOR WATER BATH PROCESS

P. Melba Mary [1] and N.S.Marimuthu [2]
[1]National College of Engineering, Tirunelvelli - 627 007, Tamil Nadu
[2]Government College of Engineering,Tirunelvelli - 627 007, Tamil Nadu
E-mail: melbance_2k4@yahoo.co.in ; drnsmphd@yahoo.co.in
(Received on 12 March 2007 and accepted on 05 May 2007)

Abstract

This paper proposes a novel approach based on fuzzy logic and neural network for design of a temperature control process, capable of providing optimal performance over an entire operating range of the process. In recent years, fuzzy logic control has emerged as one of the practical solutions when the process is too complex and non-linear for analysis by conventional quantitative techniques. However, the development of a fuzzy controller has to rely on the experience of the experts for deriving effective fuzzy control rules. Recently, there has been an increasing use of artificial neural networks (ANNs) for various applications particularly because of their capability for learning from examples and adaptation. In order to evaluate the performance of the proposed control system methods, comparative results from simulation of the process are presented.

Keywords: *Artificial Intelligence (AI), Artificial Neural Network (ANN), Back Propagation, Fuzzy Logic Control (FLC), Optimal control*

1. INTRODUCTION

Fuzzy logic control systems, which have the capability of transforming linguistic information and expert knowledge into control signals [1, 2] are currently being used in a wide variety of engineering applications. The simplicity of designing these fuzzy logic systems has been the main advantage of their successful implementation over traditional approaches such as optimal and adaptive control techniques. Despite the advantages of the conventional fuzzy logic controller (FLC) over traditional approaches, there remain a number of drawbacks in the design stages. Even though rules can be developed for many control applications, they need to be set up through expert observation of the process. The complexity in developing these rules increases with the complexity of the process. The FLC also consists of a number of parameters that need to be selected and configured in prior, such as selection of scaling factors, configuration of the center and width of the membership functions, and selection of the appropriate fuzzy control rules.

Due to their learning capability, artificial neural networks are being sought in the development of neuro-fuzzy controllers or adaptive FLCs. Berenji [3] developed a FLC that is capable of learning as well as tuning of its parameters by using neural length strings. In another development, Shimojima *et al*. [4] used Genetic Algorithem to tune a type of RBF based fuzzy model, with only three fuzzy memberships for each fuzzy variable. Lee *et al*. [5] proposed a self-organizing fuzzified basis function based on the competitive learning scheme. Jang [6] developed a self-learning FLC based on a neural network trained by temporal back-propagation. This paper presents the design of a self-learning fuzzy logic controller based on neural networks for controlling the water-bath temperature process.

2. PROBLEM FORMULATION

The continuous time Temperature control system is described as [7]:

$$\frac{dy(t)}{dt} = \frac{f(t)}{C} + \frac{Y_o - y(t)}{RC} \qquad \text{.....(1)}$$

where t denotes time, y(t) is the output temperature in °C, f (t) is the heat flowing inward the system, Yo, is the room temperature (constant, for simplicity), C denotes the system thermal capacity, and R is the thermal resistance between the system borders and surroundings.

Assuming that R and C are essentially constant, obtaining the pulse transfer function for the system in equation (1) by the step response criterion results in the discrete-time system given by:

$$y(k+1) = a(T_s)y(k) + b(T_s)u(k) \qquad \ldots\ldots(2)$$

where k is the discrete-time index, u(k) and y(k) denote the system input and output respectively, and Ts is the sampling period. Denoting by α and β some constant values depending on R and C, the remaining parameters can be expressed as:

$$a(T_s) = e^{-\alpha T_s} \quad \text{and}$$

$$b(Ts) = \frac{\beta}{\alpha}(1 - e^{-\alpha(Ts)}) \qquad \ldots\ldots(3)$$

The system described in equations (1)-(3) was modified to include a saturating non-linearity so that the output temperature cannot exceed some limitation.

The simulated control plant is described as:

$$y(k+1) = a(T_s)y(k) + \frac{b(T_s)}{1+e^{0.5y(k)-\gamma}}u(k) + [1-a(T_s)]Y_o \quad \ldots.(4)$$

Where a(Ts) and b(Ts) are given by equation (3). The parameters for simulation are α = 1.00151E-4, β = 8.67973E-3, y =40.0, and Yo = 25 °C, which were obtained from a real water bath plant. The plant input u(k) was limited between 0 and 5, and it is also assumed that the sampling period is limited by:

$$T_s \geq 10s \qquad \ldots\ldots.(5)$$

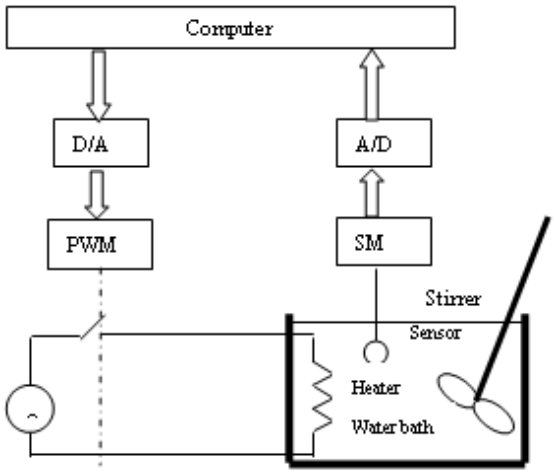

Fig.1 Water bath control system

With the chosen parameters, the simulated system is equivalent to a SISO temperature control system of a water bath that exhibits linear behaviour up to about 70°C and then becomes nonlinear and saturates at about 80°C. The schematic diagram of the water bath process is shown in Fig.1.

3. DESIGN PROCEDURE

3.1 Design of FLC

This section presents main ideas underlying the FLC. Figure 2 shows basic configuration of an FLC applied to the water bath process, which comprises of four principal components: a fuzzification interface, a knowledge base, decision making logic, and a defuzification interface.

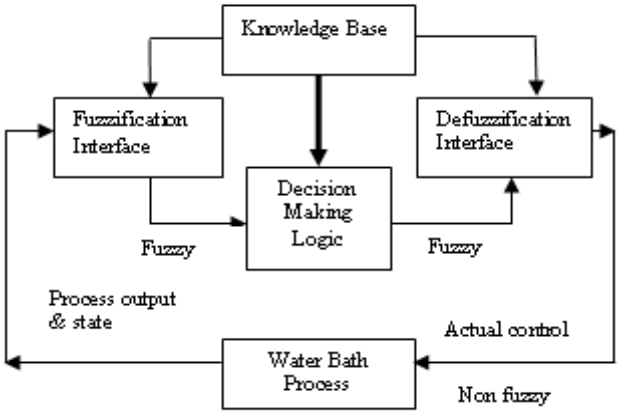

Fig. 2 Configuration of FLC

The fuzzification interface involves the following functions:

(a) measures the values of input variable.
(b) performs a scale mapping that transfers the range of values of input variable into corresponding universe of discourse.
(c) performs the function of fuzzification that converts input data into suitable linguistic values.

The knowledge base consists of database and a linguistic control rule base as described below:

(a) The database provides necessary definitions, which are used to define linguistic control rules.
(b) The rule base characterizes the control goals and control policy of the domain experts by means of a set of linguistic control rules.

The decision-making logic is the kernel of an FLC. It has the capability of simulating human decision-making based on fuzzy concepts and of inferring fuzzy control actions employing fuzzy implication and the rules of inference in fuzzy logic.

The defuzzification interface performs the following functions:

(a) A scale mapping, which converts the range of values of output variables into corresponding universe of discourse.
(b) Defuzzification, which yields a non-fuzzy control action from an inferred fuzzy control action.

Thus the idea behind the FLC is to fuzzify the controller inputs, and then infer the proper fuzzy control decision based on defined rules. The output is then produced by defuzzifying this inferred control decision.

3.1.1 *Membership Functions*

All membership functions (MF's) for: (i) controller inputs, i.e., error and change of error and (ii) incremental change in controller output for PI-type FLC or controller output for PD-type FLC, are defined on the common interval [-1, 1]; whereas the MF's for the gain updating factor is defined on [0, 1]. Gaussian MF's with equal base and 50% overlap with neighbouring MF's are used for all the variables as shown in Fig. 3. This is the most natural and unbiased choice for MF's.

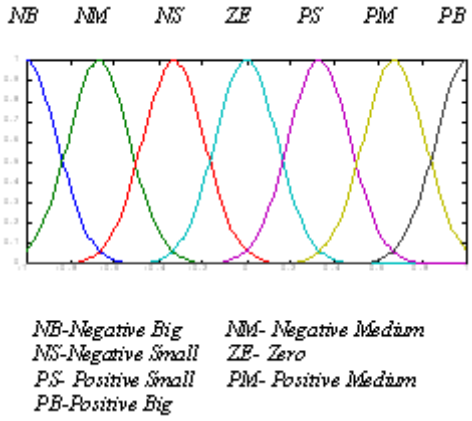

Fig. 3 Gaussian membership function

The fuzzy control rules have the form:

R_1: if x is A_1 and y is B_1 then z is C_1
R_2: if x is A_2 and y is B_2 then z is C_2
Rn: if x is A_n and y is B_n then z is C_n

where x, y and z are linguistic variables representing two process state variables and one control variable; Ai , Bi and Ci are linguistic values of x , y and z in the universes of discourse U , V and W respectively, with i = 1,2,…7; and an implicit sentence connective also link the rules into a rule set or, equivalently a rule base. For converting the inferred fuzzy control action to real value centroid method is used.

3.2 Design of ANN

Artificial Neural Networks (ANNs) are systems that are deliberately constructed to make use of some organizational principles resembling those of biological neuron. ANNs are weighted directed graphs in which neurons are nodes and directed edges (with weights) are connected between neuron inputs and neuron outputs.

3.2.1 *Back Propagation Learning Algorithm*

Based on this algorithm, the networks learn a distributed associative map between the input and output layers. What makes this algorithm different than the others is the process by which the weights are calculated during the learning phase of the network. In general, difficulty with multilayer perceptrons in calculating the weights of the hidden layers in an efficient way that results in the least (or zero) output error; the more hidden layers there are; the more difficult it becomes. To update the weights, one must calculate an error. At the output layer this error is easily measured; which is the difference between actual and desired (target) outputs. At the hidden layers however, there is no direct observation of the error, hence some other technique must be used to calculate error, as this is the ultimate goal [7].

During the training session of the network, a pair of patterns is presented (xk, dk), where xk is the input pattern and dk is the target or desired pattern. The xk pattern causes output responses at each neuron in each layer and, hence actual output Ok at the output layer. At the output layer, the difference between the actual and target outputs yields an error signal. This error signal depends on the values of the weights of the neurons in each layer. This error is minimized, and during this process new values for the weights are obtained. The

speed and accuracy of the learning process i.e., the process of updating weights also depends on the factor known as learning rate. The basis for this weight update algorithm is simply the gradient descent method as used for simple perceptrons with differentiable units. The neural controller is designed with the temperature error and the change in error as inputs, one hidden layer and output is the control voltage for the temperature process [8]. A total of 100 input - output data pairs are created for the training of neural based water bath controller. This is shown in Figure 4.

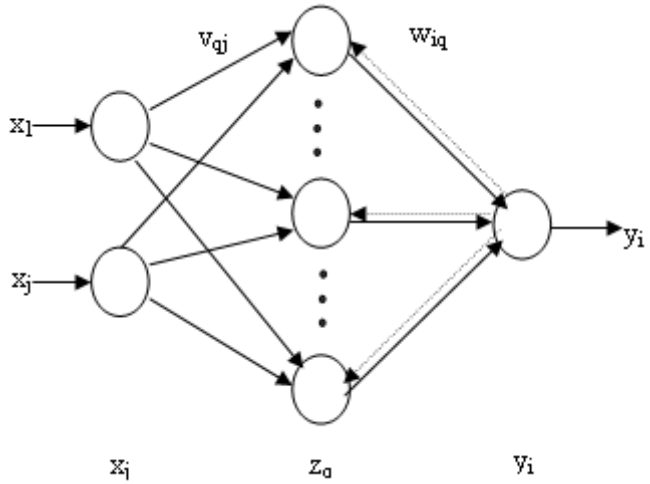

Fig. 4 Architecture of Neural Network

The error back propagation algorithm can be outlined as below:

Step 1: Initialize all weights to small random values.

Step 2: Choose an input-output training pair.

Step 3: Calculate the actual output from each neuron in a layer by propagating the signal forward through the network layer - by - layer (forward propagation).

Step 4: Compute the error value and error signals for output layer.

Step 5: Propagate the errors backward to update the weights and compute the error signals for the preceeding layers.

Step 6: Check whether the whole set of training data has been cycled once; if yes go to step 7, otherwise go to step 2.

Step 7: Check whether the current total error is acceptable; if yes terminate the training process and output the field weights, otherwise initiate a new training epoch by going to step 2.

4. SIMULATION STUDY

Using the mathematical model of the real water bath plant, the proposed approaches have been tested. From the initial condition y(0) = Yo = 25°C, the target is to follow a control reference set to 35°C for 0 <=t <=30 min, 45°C for 30 < t <=60 min, 55°C for 60 < t <=90 min, 65°C for 90 < t <=120 min, 75°C for 120 < t <=150 min ,and 80°C for 150 < t <=180 min with sampling time Ts = 25s.

The performances of the simulated water bath temperature process using the proposed approaches are shown in Figures 5-6.

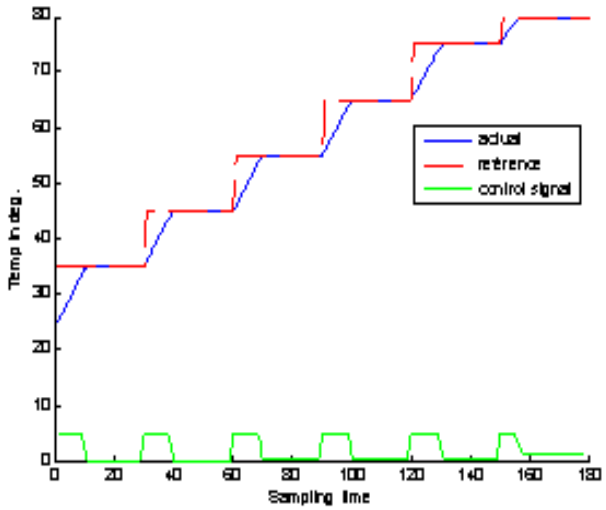

Fig. 5 Performance of the simulated system Using FLC

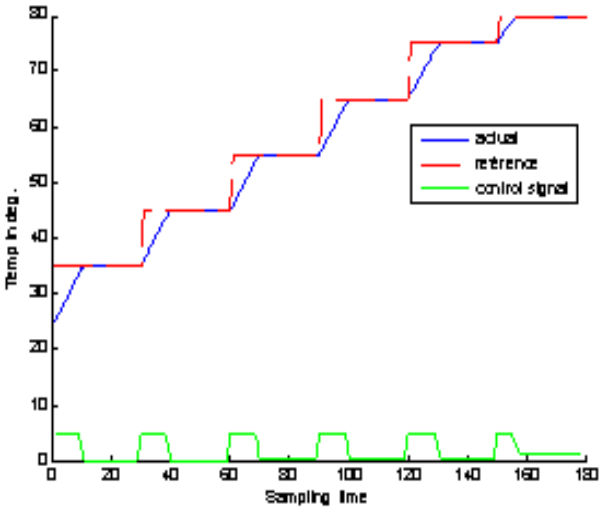

Fig. 6 Performance of the simulated system using Neural Network controller

The comparison of the proposed approaches is made by calculating the performance index absolute error over the entire simulation period and is shown in Table 1. Results show that the absolute error is minimized in the design using neural network controller as compared to fuzzy approach.

Table 1 Comparison of Absolute Error

Methodology	Absolute error
Fuzzy	306.22
Neural Network	247.1

The other performance indices such as peak overshoot (Table 2) and steady state error (Table 3) are also found out and compared using the proposed methodologies.

Table 2 Comparison of Peak Overshoot for Different Temperature Range (Ts =25sec)

PERCENT PEAK OVERSHOOT		
TEMP IN ^{0} C	Fuzzy control	Neural control
0-20	1.9739	0.0025
20-40	-0.8387	0.0021
40 -60	1.3515	0.0021
60-80	0.5205	5.378e-04
80-100	-1.4079	-0.422
100-120	0.6715	-6.3634e-04
120-140	0.6199	-0.0219
140-160	-0.1141	-0.1854

Table 3 Comparison of Steady State Error for Different Temperature Range (Ts =25sec)

TEMP IN ^{0} C	STEADY STATE ERROR	
	Fuzzy control	Neural control
0-20	-0.4789	-8.5897e-04
20-40	0.3774	-9.5411e-04
40 -60	0.0261	-5.5476e-04
60-80	-0.0494	-2.9578e-04
80-100	0.9152	0.0275
100-120	-0.0518	4.1362e-04
120-140	-0.1932	0.0164
140-160	0.2286	0.1483

5. CONCLUSION

The major contribution of this work has been the application of fuzzy and neural network logic in the design of a controller for a water bath temperature process. The neural network controller is designed from the training examples and the designed controller is adaptive. By appropriate coding of the FLC parameters, the controller can achieve self-tuning properties from an initial random state. Simulation result shows that the designed neural-network based controller is more efficient in reducing the absolute error, steady state error, peak overshoot and is more stable as compared to fuzzy logic controller.

REFERENCES

[1] C. C. Lee, "Fuzzy Logic in Control Systems: Fuzzy Logic Controller-Part I," IEEE Trans. Syst., Man, Cybern., Vol.20, 1990, pp. 404-418.

[2] C .C .Lee , "Fuzzy Logic in Control Systems: Fuzzy Logic Controller-Part II," IEEE Trans. Syst., Man, Cybern., Vol.20, 1990, pp. 419-435.

[3] H. R. Berenji, "Learning and Tuning Fuzzy Logic Controllers Through Reinforcements," IEEE Trans. Neural Networks, Vol.3, September 1992, pp.724–740.

[4] K. Shimojima, T. Fukuda and Y. Hasegawa, "Self-Tuning Fuzzy Modeling with Adaptive Membership Function, Rules and Hierarchical Structure Based on Genetic Algorithm," Fuzzy Sets Syst., Vol.71, 1995, pp. 295–309.

[5] T. H. Lee, J. H. Nie and W. K. Tan, "A self-Organizing Fuzzified Basis Function Network Control System Applicable to Nonlinear Servo Mechanisms," Mechatronics, Vol.5, No. 6, 1995, pp. 695–713.

[6] Jyh-Shing and R.Jang,"Self – Organizing Fuzzy Controlles Based on Temporal Back Propogation", IEEE Trans on Neural Networks,Vol.3, N o.5, September 1992, pp.714-723.

[7] J.S.R. Jang, C.T. Sun, and E. Mizutani, "N euro-Fuzzy and Soft Computing – A Computational Approach to Learning and Machine Intelligence – Prentice –Hall International, 2002.

[8] C.T.Lin and C.S.George Lee, "Neural-Network Based Fuzzy Logic Control and Decision system". IEEE Trans.on Computers, Vol.40, 1991, pp.1320-1336.

MOBILE PHONE LOCATION DETERMINATION AND ITS ACCURACY IMPROVEMENT

K. Ramesh and M. Nareshkumar
Department of Electronics and Communication Engineering
Jayam College of Engineering and Technology, Dharmapuri - 636 813, Tamil Nadu
E-mail: ramesh_k@gmail.com
(Received on 18 April 2007 and accepted on 13 June 2007)

Abstract

Location technologies are gaining prominence in the wireless market for several reasons, primarily the FCC mandate require all wireless cellular carriers to be able to provide the location of emergency 911 callers to a public safety answering point. However, geolocation technology has proved to be significant for both military and commercial applications in general beyond emergency location. Improvement in the accuracy location estimate will help to enhance quality of the location based services.

The main aim of this paper is to design and implement the mobile positioning system using GSM mobile station simulator V0.01b and to evaluate the accuracy of Timing Advance/Network Measurement location method, which will produce an accuracy of 0 to 360m and to further improve the accuracy to 0 to 250m by implementing the Enhanced Observation Time Difference location method. The location methods used in this paper produce greater accuracy as compared to the accuracy produced by BSNL service provider, which is of 0 to 570m. The paper finally visualizes the subscriber location with improved accuracy on the map using Geographical Information System.

Keywords: *Enhanced Observed Time Difference (E-OTD), Geographical Information System(GIS), Timing Advance Network Measurement (TA/NMR).*

1. INTRODUCTION

Wireless location is used to determine the position of a mobile station (MS) in a wireless cellular communications system. It has received considerable attention over the past few years. Emergency services, besides commercial applications such as vehicle fleet management, intelligent transport system, and location-based billing, have recently driven the research and standardization activities in the field of mobile station positioning. In 1996, the Federal Communications (FCC) mandated U.S. cellular operators to locate mobile phones originating calls to the emergency number 911.

The initial studies on positioning of mobile phones date back to 1970s. Since that time, several techniques to locate the MS by measuring attenuation, direction of arrival, and delay of the radio signals exchanged between the MS and multiple base transceiver stations (BTSs) have been proposed.

The methods to locate mobiles by processing attenuation measurements are found after 1984. Positioning of global system for mobile communications (GSM) phones through angle of arrival (AOA) method was analyzed during the period of 1990s.

FCC requires manufacturers to begin selling and activating location-capable handsets no later than 2003. Although certain companies are still petitioning the FCC to relax this new edict, FCC's action could facilitate the development of many vehicle location and navigation applications that use communications infrastructure similar to those used for wireless E911. Besides emergency assistance, it will certainly trigger many location-based services with the mobile phone or wireless network. In this paper, the simulation model of GSM network architecture was designed and the mobile station location center which is an entity in the GSM system for locating the mobile subscriber was developed using the GSM mobile station simulator V0.01b.

2. LOCATION TECHNOLOGIES

A great variety of location technologies have been proposed and developed, and some are mature enough to be standardized as a part of current cellular and PCS networks, as well as the future, third-generation wireless systems. Commonly studied technologies are angle-of-arrival (AOA) positioning, time-of-arrival(TOA) positioning, and time-difference-of-arrival (TDOA).Timing advance and network measurement report(TA/NMR) and enhanced observed time difference method.

The AOA system determines the mobile phone position based triangulation. It is also called direction of arrival. The intersection of two directional lines of bearing defines a unique position, each formed by a radial from a base station to the mobile phone in a two dimensional space. This technique requires a minimum of two stations (or one pair) to determine a position. Because directional antennas or antenna arrays are required, it is difficult to realize AOA at the mobile station.

The TOA method works by having all BTSs within range listening to a burst from the MS. When a base station receives this burst, it records the time when it was received and sends it to a server. The server gathers the information from multiple BTSs and by comparing the time of arrivals and the BTSs positions, the server can by triangulation calculate the position of the MS. The accuracy of this method varies according to the knowledge of surrounding BTSs, propagation of the received signals and synchronization of the clocks in the network. Since this solution is entirely network based, the investment cost for the operator is high.

The TDOA system determines the mobile phone position based on triangulation. This system uses time difference measurements rather than absolute time measurements as TOA does. It is often referred to as the hyperbolic system because the time difference is converted to a constant distance difference to two base stations. The accuracy of the system is the function of the relative base station geometric locations.

In the Cell Global Identity (CGI) and Timing Advance (TA) methods, all the required parameters are implemented in the network today. The only update needed is a mobile positioning centre that calculates the position estimate. The single-cell timing advance (TA) positioning method uses the CGI and the TA parameters to determine the location of the MS. The CGI identifies the cell the MS is located in. A cell can be a circular (omni) or a triangular sector. The TA parameter is an estimate of the distance from the MS to the serving BTS. TA values are divided into 64 slots (0-63), each with a radius of 550 m.

The TA/NMR method is an enhancement of timing advance method. The usage of received signal levels (RXLEV in NMR) refines and adds reliability to position. This method produces the accuracy from 0 to 360 m, which is an improved accuracy as compared with the location technologies.

The Enhanced Observed Time Difference (E-OTD) method is based on the measured Observed Time Difference (OTD) between arrivals of bursts from serving and other BTSs. The E-OTD method requires network update in the form of Location Measurement Units (LMUs) to compensate for the GSM network not being synchronized. This method produces the accuracy of 0 to 250 meters.

3. GSM NETWORK ARCHITECTURE AND MOBILE STATION LOCATION CENTRE

GSM mobile station V0.01b simulates the behaviour of MS location centre to track the mobile subscriber for both idle modes as conversation mode. When a user dials the emergency number the call setup will be established. During the call setup remote switch detects the call. Location request with international ISDN - number MSISDN to the MSLC for the location calculation. MSLC calculates the subscriber location and transfers the position reference to the emergency call centre.

The GSM system consists of a number of separate entities. These are shown in Figure 1. The entities are connected through interfaces with their own names.

According to the specifications, these names are shown on the Figure. Each of the different entities are described below.

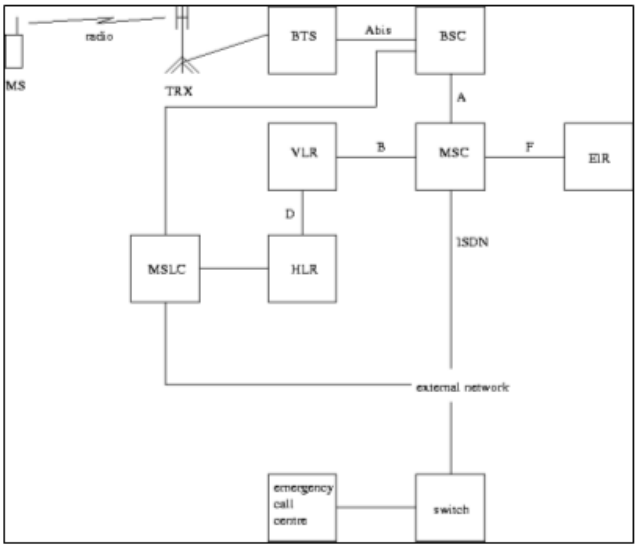

Fig. 1 Entities of GSM system

3.1 Mobile Station

The Mobile Station (MS) is the user equipment in GSM. The MS is what the user can see of the GSM system, the cellular phone itself. Production of MS is done by many different manufacturers, and there will almost always be a wide range of different MSs in a mobile network. The MSs in GSM are independent from network - providers. The identity of the subscriber is obtained from a SIM (Subscriber Identity Module) that has to be inserted into the MS to make it work.

The SIM contains the IMSI (International Mobile Subscriber Identity) which uniquely identifies the subscriber to the network. It also contains information necessary to encrypt the connections on the radio interface. The MS itself is identified by an IMEI (International Mobile Equipment Identity), which can be obtained by the network upon request. Without the SIM, calls to and from the mobile station are not allowed.

3.2 Base Transceiver Station

The Base Transceiver Station (BTS) is the entity corresponding to one site communicating with the mobile stations. Usually, the BTS will have an antenna with several TRXs (radio transceivers) that each communicate on one radio frequency.

The link-level signaling on the radio-channels is interpreted in the BTS, whereas most of the higher-level signaling is forwarded to the BSC and MSC. Speech and data-transmissions from the MS is recoded in the BTS from the special encoding used on the radio interface to the standard 64 kbit/sec encoding used in telecommunication networks. Like the radio-interface, the Abis interface between the BTS and the BSC is highly standardized allowing BTSs and BSCs from different manufacturers in one network.

3.3 Base Station Controller

Each Base Station Controller (BSC) controls the magnitude of several hundred BTSs. The BSC takes care of a number of different procedures regarding call setup, location update and handover for each MS. The handover control procedures will come especially into focus in this thesis. It is the BSC that decides when handover is necessary. This is accomplished by analyzing the measurement results that are sent from the MS during a call and ordering the MS to perform handover if this is necessary. The continuous analyzing of measurements from many MSs requires considerable computational power. This puts strong constraints on the design of the BSC.

3.4 Mobile Switching Centre (MSC)

The Mobile Switching Centre is a normal ISDN-switch with extended functionality to handle mobile subscribers. The basic function of the MSC is to switch speech and data connections between BSCs, other MSCs, other GSM-networks and external non-mobile-networks. The MSC also handles a number of functions associated with mobile subscribers, among others registration, location updating and handover. There will normally exist only a few BSCs per MSC, due to the large number of BTSs connected to the BSC. The MSCs and BSCs are connected via the highly standardized A-interface. However, due to the lack of standardization on operation and management protocols, network providers usually choose BSCs, MSCs and location registers from one manufacturer.

3.5 Location Registers

With each MSC, there is associated a Visitor Location Register (VLR). The VLR can be associated with one or several MSCs. The VLR stores data about all customers who are roaming within the location area of that MSC.

This data is updated with the location update procedure initiated from the MS through the MSC, or directly from the subscriber Home Location Register (HLR). The HLR is the home register of the subscriber. Subscription information, allowed services, authentication information and localization of the subscriber are at all times stored in the HLR. This information may be obtained by the VLR/MSC when necessary.

3.6 Signaling MS-BSS-MSC

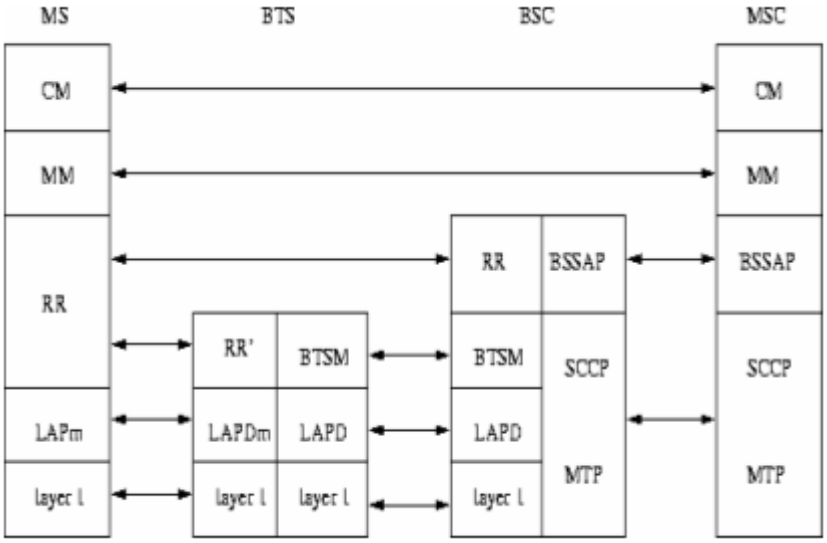

Fig. 2 Signaling protocols from MS via BTS and BSC to MSC

Figure 2 shows an overview of the signaling protocols in the GSM network between the entities MS and MSC. Above the lower layers in the BSS, is the Radio Resources protocol (RR). This protocol deals with the allocation, location and parameters of the radio-channel and is crucial in the setup of all communication with the MS. Above this layer is the Mobility Management (MM) and Circuit Mode Connection Call Protocol (CM or CC). The MM deals with administration of localization and handover. The CM administrates the setup and termination of calls. There also exist protocols between the different entities in the network intended for network internal messages. These are BTS Management protocol (BTSM) across the Abis interface and the BSSAP (BSS Application Part) across the A interface. The BSSAP is divided into BSSMAP (BSS Management Application Part) and DTAP (Direct Transfer Application Part). The lower layers of the A interface are the transport layers of the ITU-T signaling system 7, SCCP and MTP.

In order to be able to implement Mobile Station Location (MSL) in a GSM network, it is very important to understand the signaling protocols and procedures used in GSM. In this section, an overview of the signaling protocols and some important signaling sequences will be given.

3.7 Mobile Application Part

All functional signaling between the MSCs, the VLRs, the HLR and the EIR uses the Mobile Application Part protocol (MAP). MAP includes all signaling procedures required for location updates, localization of customers and many other functions that are special for mobile networks.

3.8 Operations and Management System in GSM

Operations and management systems are extremely important in GSM networks. When an operator extends its network in order to establish coverage over large areas, the network can quickly grow to contain tens or even hundreds of thousands of entities. An operations and management system ties the management of all these entities together into one or several Operations and Management Centres.

A trace is activated by sending the TRACE_ACTIVATION message from the OMC in question to the HLR or a VLR. In this message the subscriber to be traced is identified by the IMSI, and a number of parameters to identify the trace type, the OMC id and others is given. If the trace activation is sent to the HLR, the HLR will send a MAP_ACTIVATE _TRACE_MODE to the VLR the subscriber is registered with, if any. The VLR will in turn inform the MSC using MAP_TRACE _SUBSCRIBER_ ACTIVITY which in turn will inform the BSC using the BSSMAP MSC_INVOKE_TRACE message [Figure 3].

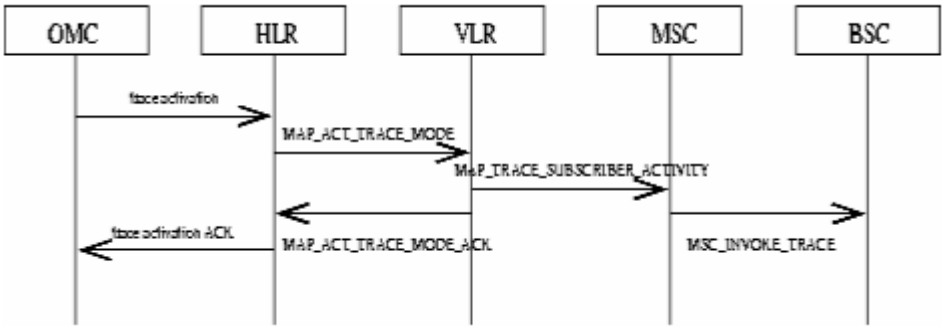

Fig. 3 Signaling on trace activation

After the trace activation, the entities of the GSM system will report all data relevant to the traced subscriber to the OMC. The contents of the reports are

- IDs for MSC, BSC, BTS and TRX
- Cell and location IDs
- All radio measurements received from the MS
- Actual TA used on the link
- All parameters leading to handover

It can be specified in the trace invocation, that the trace shall continue on handover. In this case, the BSC will inform the new base station that trace is invoked when handover is performed. The OMC will then receive trace reports from the new BSC after the handover.

The subscriber tracing is activated by sending the HLR and the activation of all tracing activities in the O&M section. The data about the mobile station that are sufficient for locating the mobile station are retrieved by receiving the trace report. Computation of the position now continues by finding the serving cell in the cell database by using the BTS id received in the trace data. The BSICs of the surrounding cells identify adjacent cells in the cell database, and the position of the serving and adjacent base stations. The received signal level of the adjacent stations, and the signal level and timing advance of the serving station reveal the distance between the MS and each of the stations. With these data, the approximate position of the MS can be computed.

4. LOCATION CALCULATION

4.1 Timing Advance

TA gives a distance estimate between the BTS and the MS. Measurements of TA can be used to calculate distance directly. Since 1 bit of the TA represents a difference of 3 -70 µs of the signal BTS - MS - BTS, and the refraction index of air is approximately 1 the distance per bit of TA is

$$3.70\mu s.c.\tfrac{1}{2} = 3.70.3.10^{8}.\ \tfrac{1}{2} = 550m \quad (1)$$

$$dTA = \tfrac{1}{2} \bullet 3.69\mu s \text{ symbol period} \bullet 3e8 \text{ m/s} = 550m \quad (2)$$

Since TA is rounded to the nearest bit period, the actual BTS-MS distance is

$$550 \times (TA-1/2)d'' \ dTA < 550 \times (TA+1/2) \text{ for } TA>0 \quad (3)$$

4.2 Network Measurement Report

The measurement report consists of signal strength for the six neighbour stations, timing advance value. The reports are sent over SACCH at least every second. Along with the report each received level follows the BSIC (Base Station Identity Code) to identify that BTS. The received level to maximum probability distance is calculated using the most popularly used propagation model called HATA and Okumara model.

"P (dB) = 69.55+26.19 $\log_{10} f_c$ -13.82 $\log_{10}$hBTS a(h_{MS})+(44.9-6.55 $\log_{10}$hBTS) $\log_{10}$d (4)

The correction factor a(h_{MS}) compensates the antenna variations of the Mobile Stations, and is given as:

In small or medium cities:

$a(h_{MS}) = (1.1 log_{10} f_c - 0.7) h_{MS} - (1.56 log_{10} f_c - 0,8)$ (5)

For larger cities:

$a(h_{MS}) = 3.2(\log_{10}(11.75 h_{MS}))^2 - 4.97$ (6)

$f_{c\text{- carrier}}$ frequency ranging from 150MHz to 1500MHz.

h_{BTS}- effective transmitter antenna(base station) height ranging from 30m TO 200m.

h_{MS}- effective receiver antenna height ranging from 1m to 10m.

d- Base station to Mobile station separation distance.

Distance d to BTSs based on measured path loss L;given by:

$$\frac{d_{+x\,dB}}{d} = 10^{\frac{x}{44,9-6,55 log 50}} \quad (7)$$

4.3 Calculating Intersection Using Triangulation

The coordinates (x_1 ,y_1) and (x_2 ,y_2) for each of theBTSs is known. In addition, the mean distances d_1 and d_2 are known from the calculated RX level to distance table.

$$d_{bts} = \sqrt{(x_2 - x_1)^2 + (y_2 - y_1)^2} \quad (8)$$

$$l_1 = d_1 + d_2 - d_{bts} \quad (9)$$

$$l_2 = \sqrt{d_2^2 - l_1^2} \quad (10)$$

$$sin(a) = \frac{y_2 - y_1}{d_{bts}} \quad (11)$$

$$cos(a) = \frac{x_2 - x_1}{d_{bts}} \quad (12)$$

Now the point p where l_1 and l_2 meets is obtained as follows

$$x_p = x_2 - l_1 \cdot cos(a) \quad (13)$$

$$y_p = y_2 - l_1 \cdot sin(a) \quad (14)$$

The point of intersection of two circles is

$$x = x_p + l_2 \cdot sin(a) = x_2 - l_1 \cdot cos(a) + l_2 \cdot sin(a) \quad (15)$$

$$y = y_p - l_2 \cdot cos(a) = y_2 - l_1 \cdot sin(a) - l_2 \cdot cos(a) \quad (16)$$

4.4 Enhanced Observed Time Difference Method

The Enhanced Observed Time Difference (E-OTD) method is based on the measured, Observed Time Difference (OTD) between arrivals of bursts from serving and other BTSs. The positioning of E-OTD is shown in Figure 4.

The three basic timing quantities associated with E-OTD location are: Observed Time Difference (OTD), is the time interval that is observed by a MS between the receptions of signals (bursts) from two different BTSs in the cellular network. Real Time Difference (RTD), is the relative synchronization difference in the network between two BTSs. Geometric Time Difference (GTD), is the time difference between the receptions (by a MS) of bursts from two different base stations due to geometry.

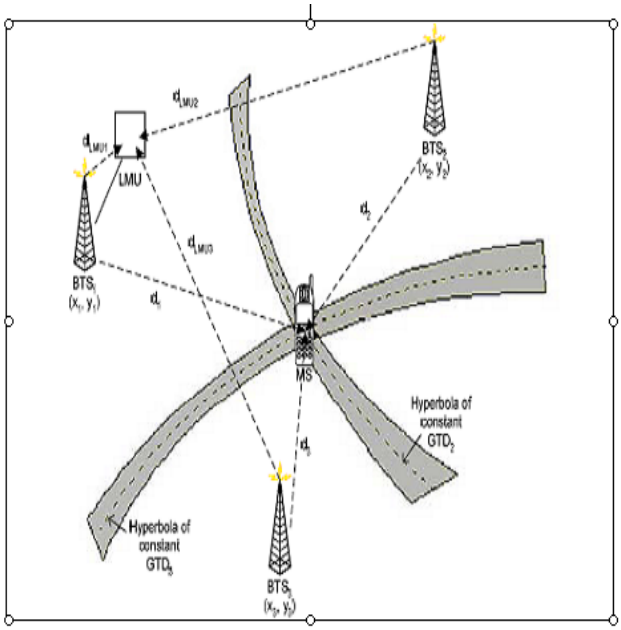

Fig 4. E-OTD positioning

4.5 MS Location Calculation

The positioning problem in absence of measurement errors can be formulated with a set of N-1 equations describing hyperbolas having their foci at the BTSs coordinates (x_1, y_1) and (xi, yi). The hyperbolic equation is written as x_1, y_1

$$c * GTD_i = \sqrt{(x_1 - x)^2 + (y_1 - y)^2} - \sqrt{(x_i - x)^2 + (y_i - y)^2}$$

In an error free case, a unique and exact solution can be found at the intersection of the hyperbolas at P=[x,y]. In a real case, however, errors will be present and a statistical solution must be sought. In the simulation model, an optimization routine was used, to produce a location estimate. From the above moving the square root terms to the other side, we obtain

$$F_i = c * GTD_i - \sqrt{(x_1 - x)^2 + (y_1 - y)^2} + \sqrt{(x_i - x)^2 + (y_i - y)^2}$$

In the error free case, all Fi are identically equal to zero at the solution where the hyperbolas intersect. In the simulations, a least square optimization was used, to minimize the sum of the Fi squared. The position estimate for each measurement point was then found, as from equation where M is the number of BTS-pairs available. A plot of the calculated Hyperbolas, BTSs and MS pointer is given in Figure 5.

5. Location Presentation

In order to show how the results of a MSL implementation with TA/NMR technique can be visualized, some mapping screenshots have been produced. The maps have been produced by geo referencing the IKONOS satellite image and by digitizing the Geographic features using ArcGIS 9.1mapping application. The maps show the street, building, shoreline, and height layers of a map database of central Bergen. Figure 6 shows the probable MS Location to Anna University Chennai.

6. CONCLUSIONS

It is proposed to place the Mobile Station Location procedure in a separate entity in the GSM network. This separate entity, called MSLC (Mobile Station Location Centre), can perform mobile station location upon request from external phone-network entities, such as an emergency call centre. The data necessary for performing the location can be obtained from the GSM network by using a combination of GSM application protocols (MAP) and GSM Operations & Maintenance protocols (O&M). The procedures for the linkage of the MSLC to the GSM-network, and the procedures for gathering the necessary data has been specified in SDL, and tested in a simulating implementation.

This study provides procedures that are TA/NMR and E-OTD for calculating the position from the obtained data's. The two different methods differ in complexity and in accuracy. From the above implementation it is concluded that Enhanced Observed Time Difference Method (E-OTD) is producing subscriber location with an accuracy of 0 to 260 meters from the serving base transceiver station. A system for geographical location information has been chosen, and a way of storing and communicating location probability areas using this system has been identified.

REFERENCES

[1] Christopher Drane and Malcom Macnaughtan, "Positioning GSM Telephones",IEEE Communications Magazine, 1998.

[2] G. Djuknic and S. Wilkus, "Geolocation And Wireless Multimedia", IEEE International Conference on Multimedia and Expo, 2000.

[3] K.C. Ho and Y.T. Chan , "Solution And Performance Analysis of Geolocation By TDOA ", IEEE Transaction on Aerospace and Electronic Systems, Vol.29 No.4, 1993.

[4] James M. Zagami and Steen A. Parl, "Providing Universal Location Services Using a Wireless E911 Location Network", IEEE Communications Magazines,1998.

[5] Jeffrey H. Reed, Kevin J. Krizman, Brian D. Woerner and Teodore S. Rappaport , "An Overview of the Challenges and Progress in Meeting the E-911 Requirement for Location Services", IEEE Communications Magazines,1998.

[6] Li Cong and Weihua Zhuang , "Hybrid TDOA/AOA Mobile User Location for Wideband CDMA Cellular Systems", IEEE Transactions on Wireless Communications, Vol.1 No.3, 2002, pp.439.

[7] Martin Hellebrant and Rudolf Mathar, "Location Tracking of Mobile in Cellular Radio Networks", IEEE Transcations on Vehicular Technology, Vol.48, No.5, 1999, pp.1558-1562.

[8] Maurizio A. Spirito, "On the Accuracy of Cellular Mobile Station Location Estimation", IEEE Transactions on Vehicular Technology, Vol.50, No.3, 2001, pp.674-685.

[9] S.C. Swales, J.E.Maloney and J.O.Stevensen, "Locating Mobile Phones and the US Wireless E-911 Mandate", IEEE Conference, 1999.

[10] Theoder S.Rappaport "Wireless Communications Principles and Practice", Pearson Education (Singapore) Pvt. Ltd.

[11] Yillin Zhao and Senior Member, "Mobile Phone Location Determination and Impact on Intelligent Transportation Systems", IEEE Transaction on Intelligent Transportation System, Vol.1, 2000, pp. 55-64.

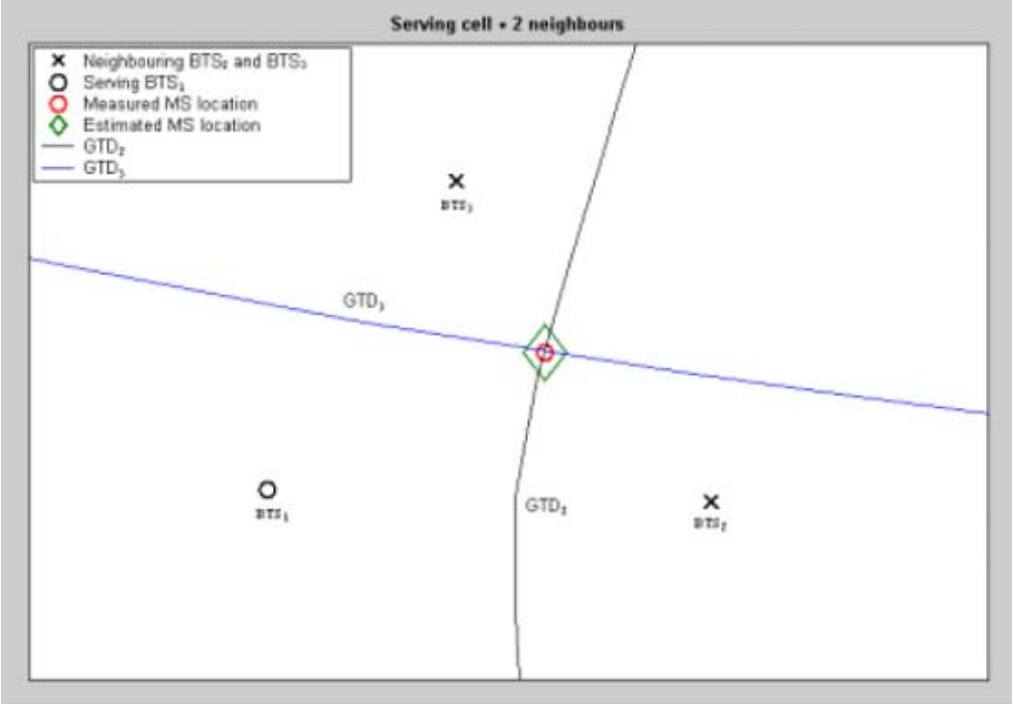

Fig. 5 Plot of the calculated hyperbolas, BTS s, calculated and measured MS position

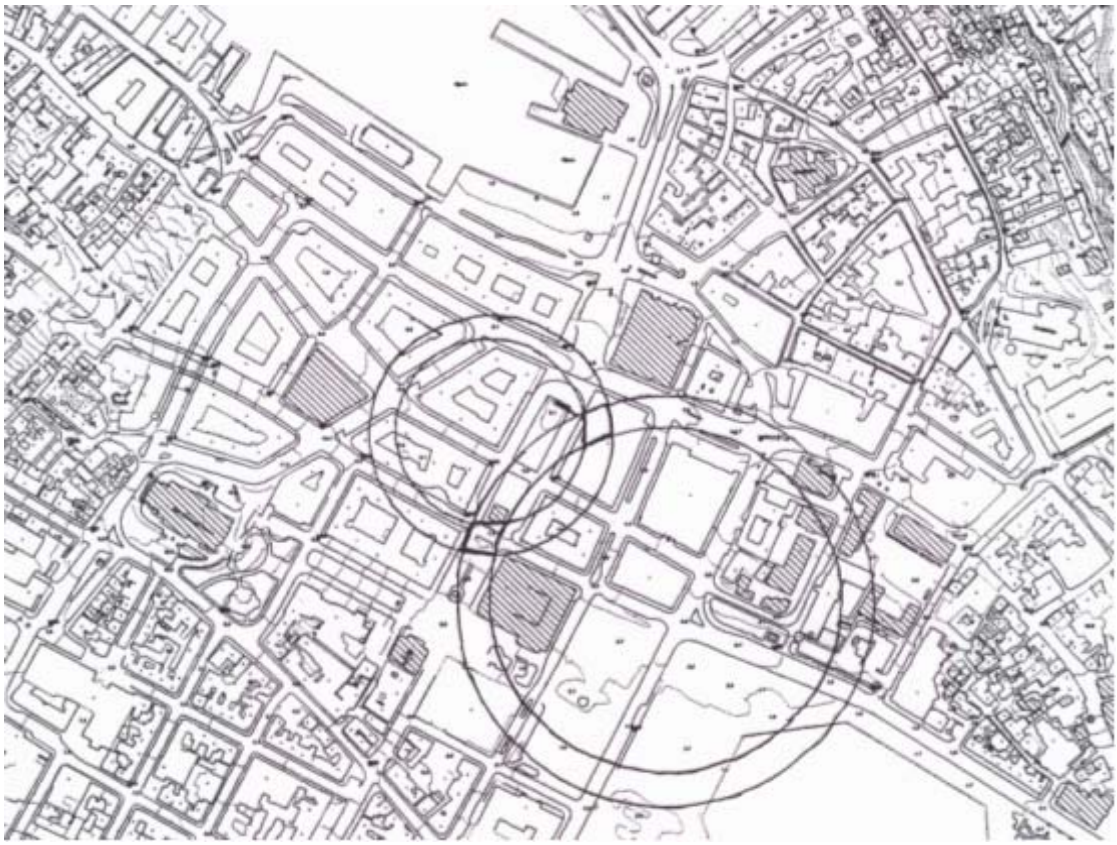

Fig. 6 The probable MS location in the Anna University, Chennai using TA/NMR

TOUGHNESS EVALUATION OF POLYPROPYLENE FIBRE REINFORCED CONCRETE BEAMS UNDER BENDING

D. Suji[1], S.C. Natesan[2] and R. Murugesan[3]

[1]Department of Civil Engineering, Sathyabama University, Chennai - 600 029, Tamil Nadu

[2]Principal, VLBJ College of Engineering and Technology, Coimbatore - 641 042, Tamil Nadu

[3]Principal, Gojan School of Business and Technology, Red Hills, Chennai - 600 052, Tamil Nadu

E-mail: suji_mohan2002@yahoo.com

(Received on 22 April 2007 and accepted on 08 July 2007)

Abstract

Generally, the performance of most materials is characterized by parameters based on the mechanical properties such as strength, strain, stiffness, etc. However, in fibre reinforced concrete (FRC), unlike other materials, strength or stiffness alone is not sufficient to characterize its behaviour, and the value of toughness is often used instead. In this study, two different methods (ASTM C1018 and JSCE SF-4) are used to measure the toughness of polypropylene fibre reinforced concrete subjected to bending. Results indicate that in the JSCE method, the information obtained by only one specified deflection toughness seemed to be insufficient in reflecting the characteristics of the load-deflection curves of FRC. On the other hand, in the ASTM method, the obtained information using the four toughness values at different deflections appeared to better clarify the characteristics of FRC.

Keywords: *Fibre Reinforced Concrete, Polypropylene Fibre, Toughness*

1. INTRODUCTION

Short fibres have been known and used for centuries to reinforce brittle materials like cement or masonry bricks. At that time, natural fibres, such as horse hair, straw, etc., were used. Now, there are numerous fibre types available for commercial use, the basic types being steel, glass, synthetic materials (polypropylene, carbon, nylon, etc.) and some natural fibres. As for steel fibres, wire and metal clips were used first in l9l0s to improve the properties of concrete. Extensive research on steel fibres began in the 1960's [1, 2]. Since then a substantial amount of research, development, application and commercialization have occurred [3-7].

Typically, the fibre volume fraction in Steel Fibre Reinforced Concrete (SFRC) is in the range of 0.5% to 1.5%. At the practical volume fraction used in SFRC (<1%), the increase in compressive, tensile, or flexural strength is small because the matrix cracks essentially at the same stress and strain as in plain concrete [8-12]. The real advantage of adding fibres is that, after matrix cracking, fibres bridge these cracks and restrain them. In order to further deflect the beam, additional forces and energy are required to pull out or fracture the fibres. This process, apart from preserving the integrity of concrete, improves the load-carrying capacity beyond cracking. This improvement creates a long post-peak descending portion in the load deflection curve.

Since fibres do not significantly improve the properties of concrete or strength prior to the peak (concrete cracks) as they do on the post peak response, it would be more practical to evaluate the performance of FRC based on the energy absorption (area under the load deflection curve). The area under the load deflection curve is usually referred to as the toughness obtained from a static test of a beam specimen up to a specified deformation.

The two most common methods to determine flexural toughness are based on ASTM C1018 and JSCE SF-4. In ASTM C1018, toughness is specified in terms of toughness indices (I_5 I_{10} and I_{20}), which refer to the area under the load-deflection curve calculated based on three different specified deflections. While, in the case of JSCE SF-4 the area under the load deflection curve up to a specified deflection (L/150) is measured and referred to as the toughness.

In this study, both ASTM and JSCE standards are used to determine the toughness of plain concrete as well as Polypropylene reinforced concrete beams. Results from both methods are then compared and discussed.

2. MATERIALS

The description of the materials used is given below.
Cement: Ordinary Portland Pozzolona cement 53 grade with a specific gravity of 3.15 as per IS1489-1976 [13].

Coarse Aggregate: Crushed blue granite passing through 20mm and retained on 10mm. It meets gradation requirements of IS 2386- Part III, 1963 [14]. The apparent specific gravity is 2.95 and fineness modulus is 7.1.

Fine Aggregate: Natural river sand with a fineness modulus of 2.64. Its gradation meets zone II of IS383-1970 requirements. Specific gravity is 2.63.

Fibre: Fibre mesh brand of (Fibrillated Polypropylene) fibres 24mm in length manufactured by a private firm in the USA and marketed by a private firm in India (Figure 1).

Water: Potable water is used.

The physical properties of cement and fibre used for the investigation are given in Table 1 and Table 2 respectively.

Fig. 1 Photograph of Polypropylene fibres

Table 1 Physical Properties of Cement

No	Particulars	53 Grade PPC
1	Normal Consistency (%)	30.0
2	Fineness (m^2/g)	285.5
3	Soundness (mm)	1.0
4	**Setting time (min)**	
	Initial setting time	80
	Final setting time	630
5	**Compressive strength (MPa)**	
	3-day	30.0
	7- day	37.0
	28- day	55.0

Table 2 Properties of Fibres

No	Properties	Particulars
1	Fibre type	Graded fibrillated Polypropylene fibres
2	Length, mm	12 to 24
3	Specific gravity, g/cc	0.9
4	Tensile strength, MPa	550-760
5	Youngs modulus, GPa	3.5
6	Density, kg/m^3	910
7	Thermal conductivity	Low
8	Electrical conductivity	Low
9	Acid and Salt resistance	High
10	Absorption	Nil

3. EXPERIMENTAL PROCEDURE

3.1 Prepartion of Beams

Nine beams of 100 x 100 x 500 mm were cast (three beams for each mixture corresponding to each fibre fraction). During the test, specimens were placed on a simple support with a clear span of 450 mm, and then

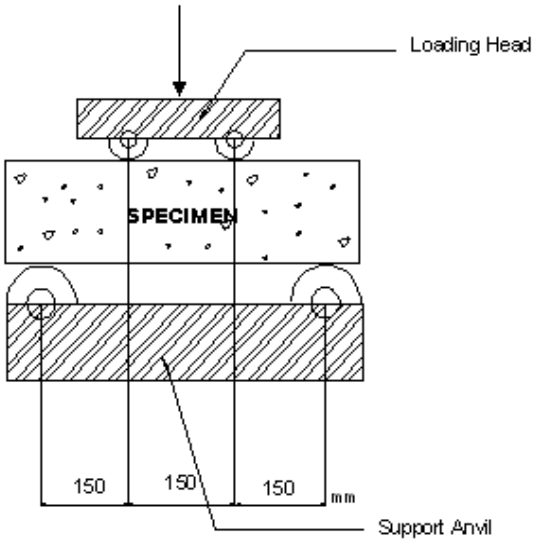

Fig. 2 Test setup

Table 3 Mix Proportioning Details of PFRC for 1m^3 of Concrete

Mix	Cement (kg)	Fine aggregate (kg)	Coarse Aggregate (kg)	Water (kg)	Ratio
M I	383.16	571.85	1161.64	191.58	1:1.49:3.03:0.50
M II	430.52	540.423	1153.54	191.58	1:1.26:2.63:0.45
M III	497.61	503.15	1135.99	191.58	1:1.01:2.28:0.39

subjected to a third-point loading at the rate of 0.05 in/min (two point-loads at 150mm of the clear span, Figure 2). The details of mix proportions for various mixes used in the present study are given in Table 3.

3.2 Determination of Flexural Toughness

Two methods are used for determining the flexural toughness namely: ASTM C1018 and JSCE SF-4.

3.2.1 ASTM C1O18

In ASTM C1018, toughness (or energy absorption defined as the area under the load deflection curve) is calculated at 4 specified deflections, δ, 3δ, 5.5δ and 10.5δ (Figure 3). The toughness is calculated at the deflection δ which is considered the elastic or pre-peak toughness (first-crack toughness), while the other three at 3δ, 5.5δ and 10.5δ are considered the post-peak toughness, as given below:

Area OAB = Toughness corresponding to a deflection of δ, (T_δ)

Area OACD = Toughness corresponding to a deflection of 3δ, ($T_{3\delta}$)

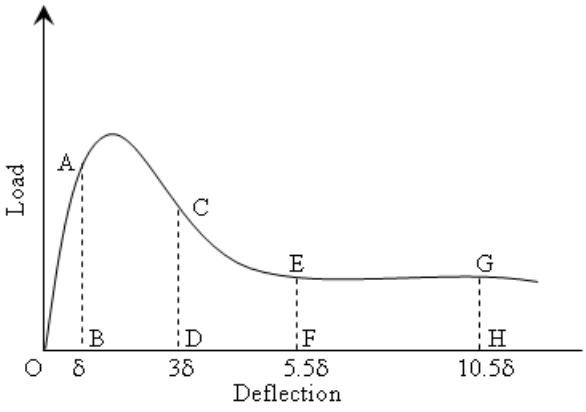

Fig. 3 Fracture toughness indices

Area OAEF = Toughness corresponding to a deflection of 5.5δ ($T_{5.5\delta}$)

Area OAGH = Toughness corresponding to a deflection of 10.5δ ($T_{10.5\delta}$)
where

δ = The deflection at the linear elastic limit .

In addition, the terms of toughness indices (I_5, I_{10} and I_{20}) are also calculated. Each index is the ratio between the post-peak toughness and the pre-peak (elastic) toughness (Figure 3).

I_5 = Area OACD/Area OAB
I_{10} = Area OAEF/Area OAB
I_{20} = Area OAGH/Area OAB

The residual strength represented by the average post-cracking load that the specimen may carry over a specific deflection interval, are usually determined as follows:

$R_{5,10} = 20 (I_{10} – I_5)$
$R_{10,20} = 10(I_{20} – I_{10})$

3.2.2 JSCE SF-4 Method

Unlike the ASTM Cl0l8, JSCE SF-4 provides just a single value of toughness. For a given load-deflection curve, toughness is the area under the load deflection curve measured up to a specified deflection, δtb = L/150, as referred to Area OABC in Figure 4.
The toughness factor (equivalent to the average residual strength) can also be determined as:

$$\text{Toughness Factor} = \text{Toughness} * \frac{L}{(B H^2 \delta_{tb})}$$

where

L = Span length
B = Width of the specimen
H = Height of the specimen
δtb = Deflection at L/150

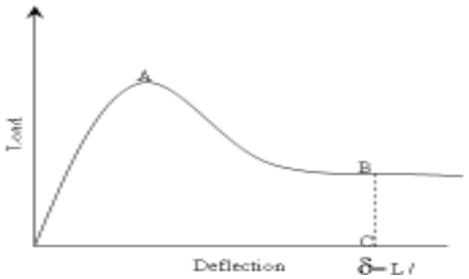

Fig. 4 Fracture toughness

4. RESULTS AND DISCUSSION

4.1 Load-Deflection Response (ASTM C1018 Method)

Typical load-deflection responses of plain concrete, and PFRC beams are given in Figures 5a to 5c.

On comparing plain concrete and FRC, it was the post-peak response that really differentiated the plain concrete from the FRC. For plain concrete, the behaviour was more in a brittle manner. Once the strain energy was high enough to cause the crack to self-propagate, fracture occurred almost instantaneously once the peak

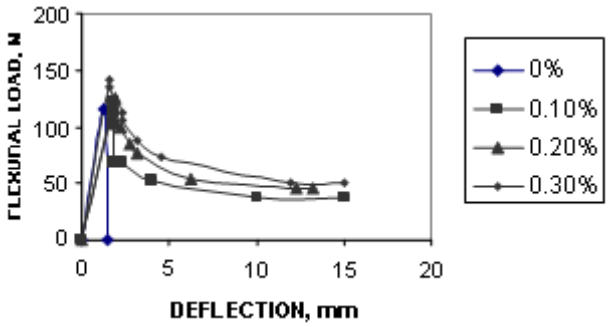

Fig. 5a Load-deflection responses of plain and PFRC concrete - Mix I

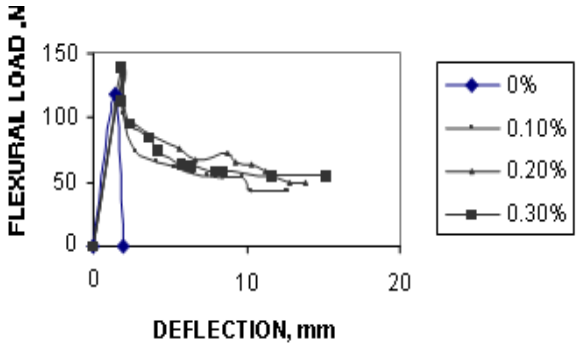

Fig. 5b Load-Deflection responses of plain and PFRC concrete - Mix II

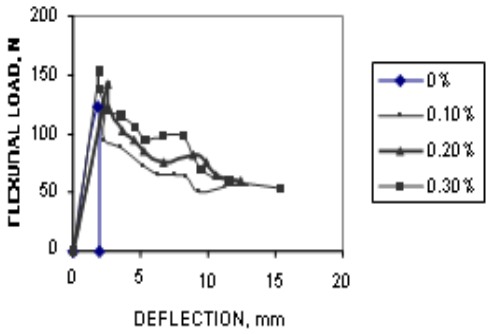

Fig. 5c Load-Deflection responses of plain and PFRC concrete - Mix III

load was reached, due to the tremendous amount of energy being released. For FRC, the fibre bridging effect helped to control the rate of energy release. Thus FRC maintained its ability to carry load after the peak. FRC was able to maintain the load carrying ability even after the concrete had cracked as shown in the descending long post peak response.

In the present work, toughness for FRC is measured according to the ASTM C1O18 and JSCE methods described before and the results are tabulated (Table 4 and Table 5). According to ASTM method, the toughness is measured at four different deflections: one prior to

Table 4 Toughness (According to ASTM C1018)

Sl. No.	Concrete Type	Flexural load (N)	Toughness (N-m)				Toughness Indices		
			δ	3δ	$5.5\,\delta$	$10.5\,\delta$	I_5	I_{10}	I_{20}
Mix I									
1	0%	116.20	0.075	-	-	-	1.00	1.00	1.00
2	0.1%	121.55	0.109	0.361	0.676	1.197	2.28	2.92	5.49
3	0.2%	125.50	0.120	0.293	0.510	0.944	2.43	4.23	7.83
4	0.3%	141.10	0.102	0.247	0.429	0.689	2.40	4.17	6.69
Mix II									
1	0%	118.80	0.089	-	-	-	1.00	1.00	1.00
2	0.1%	133.10	0.133	0.300	0.513	0.935	2.27	3.85	7.03
3	0.2%	136.00	0.136	0.335	0.585	1.080	2.47	4.30	7.98
4	0.3%	138.60	0.124	0.215	0.609	1.024	1.72	4.88	8.20
Mix III									
1	0%	123.50	0.111	-	-	-	1.00	1.00	1.00
2	0.1%	126.60	0.145	0.250	0.564	1.190	1.73	3.89	8.21
3	0.2%	142.20	0.177	0.452	0.796	1.484	2.54	4.48	8.34
4	0.3%	152.00	0.144	0.347	0.602	1.111	2.41	4.18	7.71

the peak (T_δ) and three after the peak ($T_{3\delta}$, $T_{5.5\delta}$ and $T_{10.5\delta}$). These are used to determine the toughness indices given in Table 4. For elastic–perfectly brittle material (i.e., if the beam collapses right after the first crack), the toughness values for all three would be 1.0.

If plain concrete beams are tested under load control, the beam would break in two pieces right after first crack, thus indicating a toughness of 1.0. However, the beams were shown to have reproducible descending curves if servo control systems are used to reduce the load right after first crack. In such case, even the plain concrete beam has a toughness value greater than 1. Since the load - carrying capacities decrease much faster (steeper descending branch) for plain concrete beams, the ratios I_{10}/I_5 and I_{20}/I_{10} tend to be 1.0.

Consider the pre-peak (or elastic) toughness (T_δ). In the case of the polypropylene fibre, the pre-peak toughness (T_δ) of PFRC was found to be similar to that of plain concrete and remained constant even with the increasing fibre content from 0. l% to 0.3%. The reason for this performance was partly due to the material properties of the polypropylene fibre itself.

Table 5 Toughness (According to JSCE-4)

Sl. No.	Concrete Type	Toughness (N-m)	Toughness factor
Mix I			
1	0%	0.075	0.011
2	0.1%	0.204	0.030
3	0.2%	0.218	0.033
4	0.3%	0.245	0.022
Mix II			
5	0%	0.118	0.017
6	0.1%	0.220	0.033
7	0.2%	0.229	0.034
8	0.3%	0.240	0.036
Mix III			
9	0%	0.111	0.017
10	0.1%	0.209	0.031
11	0.2%	0.227	0.034
12	0.3%	0.257	0.038

With low strength and elastic modulus, after the first concrete crack, polypropylene did not take action immediately and this resulted in a large drop of strength in the load-deflection curve. Thus the first peak response prior to the low recovery of PFRC got no action from the fibre and was, in fact, the response of the plain concrete. At low fibre content (0.1%), a small drop of load was found, and then followed by a quick recovery of load almost immediately. With the volume fraction of 0.2%, larger (twice) numbers of fibres were intercepted at the crack surface. This allowed fibres to pick up the load as soon as the concrete cracked, achieving no sign of strength drop.

Consider the post-peak toughness (3_δ, 5.5_δ and 10.5_δ) by looking at the toughness indices, at small deflection (3_δ and 5.5_δ), Mix III (0.2%) seemed to be tougher than Mix I and Mix II as indicated by the larger values of I_5 and I_{10}. This is because in the case of Mix I and Mix II with a large drop of load immediately after the peak, the area under the curve (toughness) of the PFRC became smaller than that of Mix III. However, at large deflection (10.5_δ), once the Polypropylene fibres in the PFRC came into play, the load started to recover and the toughness of the PFRC was found to be significantly increased, especially at 0.2% volume fraction. By looking at the toughness value, it is found that the Mix III (0.2%) corresponding to 10.5ü shows higher value.

4.2 Load-Deflection Response (JSCE SF-4 Method)

The toughness values and factor according to JSCE SF-4 of PFRC for various mixes are given in Table 5 and Figures 6a to 6c.

Based on this method, for a given load deflection curve, a value of toughness measured up to a deflection of L/l50 (3 mm) is calculated and then used to determine the toughness factor. The obtained results indicate that the performance of Mix III at 0.3% is higher than Mix I and Mix II.

Mix I

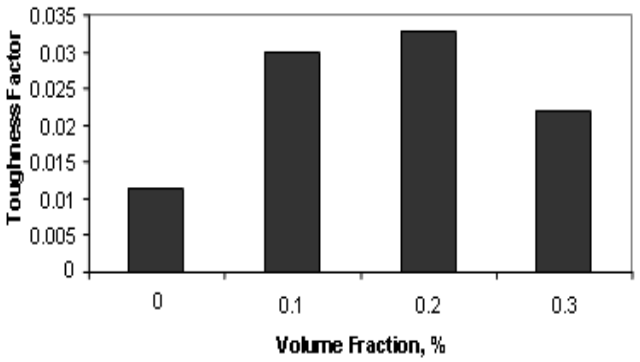

Fig. 6a Toughness according to JSCESF-4 for Mix I

Mix II

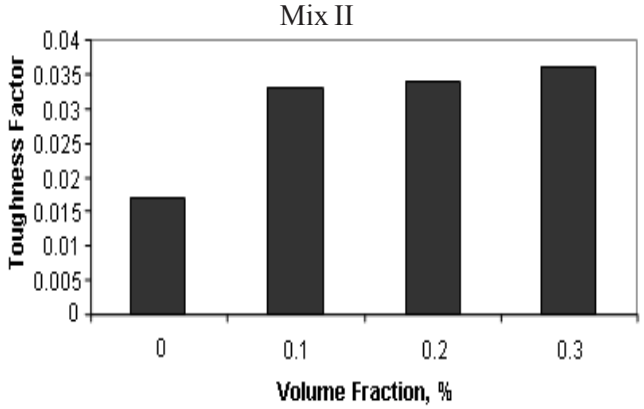

Fig. 6b. Toughness according to JSCESF-4 for Mix II

Mix III

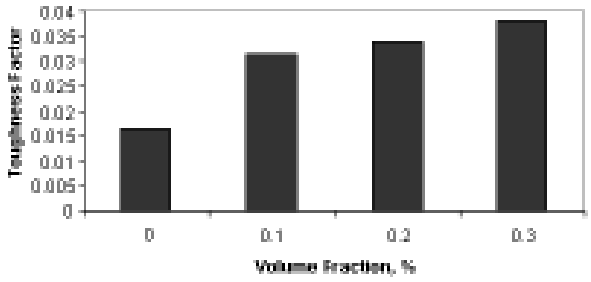

Fig. 6c Toughness according to JSCESF-4 for Mix III

4.3 COMPARISON BETWEEN ASTM C1018 and JSCE SF-4 Methods

On comparing these two methods, it is inferred that single value toughness measured using the JSCE method did not have any difficulty in reflecting the toughness property of the PFRC. However, in the case of PFRC, JSCE did not seem to be sufficient to reflect the true toughness property. For instance, if the toughness value alone provided by JSCE is considered without looking at the load-deflection curve, it will lead to the conclusion that the performance of PFRC was much poorer than that of SFRC which is not correct. It is true that the toughness of PFRC at small deflection was poorer than that of SFRC, but, at large deflection, the performance of PFRC was increased to almost the same as that of SFRC.

On the other hand, the toughness provided by ASTM at different deflections seems to work out well in term of capturing and reflecting the true toughness property. By considering the toughness indices alone without looking at the load-deflection curve, rough descriptions of the behaviour of PFRC could be achieved. For example, the small value of I_5 of the PFRC indicated that the PFRC did not perform well at small deflection. However, the increased value of I_{20} of the PFRC indicate that the performance of the PFRC was quite well at larger deformation.

5.CONCLUSIONS

From this study, the following conclusions can be drawn :

- Due to the properties of the fibres, the ehaviour of PFRC was clearly a double-peak response
- According to the ASTM method, with toughness measured at 4 different deflections, the obtained information seemed to capture and reflect the true toughness properties PFRC quite well.
- On the other hand, the JSCE method, with a single value toughness, was not quite sufficient in reflecting the real toughness properties of the PFRC.

REFERENCES

[1] J. P. Romualdi and G. B .Batson, "Mechanics of Crack Arrest in Concrete", Proceedings, ASCE Journal of Structural Engineering, Vol.89, 1963, pp. 147-168.

[2] J. P .Romualdi and J. A .Mandel, "Tensile Strength of Concrete Affected by Uniformly Distributed Closely Spaced Short Lengths of Wire Reinforcement", ACI Journal, Vol. 61, No.6, 1964, pp. 657 -61.

[3] S. Shah, "Concrete and Fibers Reinforced Concrete Subjected to Impact Loading Cement-Based Composites: Strain Rate Effects on Fracture", Materials Research Society Symposia Proceedings, Vol. 64, 1986.

[4] B.Cotteral, "Fracture Toughness and The Charpy V Notch Impact Tests", British Welding Journal, Vol. 9, No.2, 1962, pp. 83-90.

[5] G. E..Manfore, " A Review of Fiber Reinforcement of Portland Cement Paste, Mortar, and Concrete", PCA Research and Development Laboratories Journal, Vol.10, No.3, 1968, pp. 36-42.

[6] S. P Shah and B. V. Rangan, "Fiber Reinforced Concrete Properties", ACI Journal, Proceedings, Vol.68, No.2, 1971, pp. 126-l35.

[7] S. P Shah and B. V .Rangan, "Ductility of Concrete Reinforced with Stimrps, Fibers and Compression Reinforcement", ASCE Journal, Structural Division, Vol. 96, No.5-6, 1970, pp. l167-1 185.

[8] S .Mindess, J. F.Young, and D .Darwin, "Concrete 2nd Edition. Prentice Hall. 2002.

[9] C. D. Johnston, "Steel Fibre Reinforced Mortar and Concrete-A Review of Mechanical Properties", Fiber Reinforced Concrete, SP-44, American Concrete Institute, Detroit, 1914, pp. 124-142.

[10] G. R., Williamson, "The Effect of Steel Fibers on the Compressive Strength of Concrete", ACI Special Publication, SP-44: Fiber Reinforced Concrete, American Concrete Institute, Detroit, 1974, pp. 195-207,

[11] C. D .Johnston, and R. J.Gray, " Uniaxial Tension Testing of Steel Fibre Reinforced Cementitious Composites", Proceedings, International Symposium on Testing and Test Methods of Fibre-Cement Composites, ZULEM, Sheffield, 1978, pp.451- 461.

[12] S .Mindess, " Fibre Reinforced Concrete: Challenge and Prospects", Fiber Reinforced Concrete: Modem Development, 1995, pp. 1-12.

[13] Indian Standard Specification for Portland Pozzolana Cement, ISI 1489-1976, Bureau of Indian Standard, New Delhi.

[14] Indian Standard Methods of Test for Aggregates for Concrete, IS 2386 Part III, Bureau of Indian Standards, New Delhi , 1963.

EFFECT OF WATER-POWDER RATIO ON MECHANICAL PROPERTIES OF SELF-COMPACTING CONCRETE

V. Subramania Bharathi[1], J.V. Ramasamy[2], N. Arunachalam[3] and S. Sankaran[4]
[1,3&4]Department of Civil Engineering, Bannari Amman Institue of Technology,
Sathyamangalam - 638 401, Tamil Nadu
[2]Department of Civil Engineering , PSG College of Technology, Coimbatore - 641 004, Tamil Nadu
E mail: er_vs_bharathi@yahoo.co.in
(Received on 22 May 2007 and accepted on 13 August 2007)

Abstract

Well-proportioned and larger contents of paste and mortar portions give high deformability to fresh self-compacting concrete mix, which has also high resistance to segregation. Self-compacting concrete can flow under its own weight to completely fill the formwork without segregation and self consolidate without any means of mechanical vibration,and eventually high quality concrete is obtained. In mix design, EFNARC specification is followed. About 20% of cement is replaced with pulverized fuel-ash and by varying water-powder ratio, its role in high performance of concrete is put into limelight in concrete research. Workability tests satisfied the requirements of self-compacting concrete. The results of compressive strengths and split tensile strengths are logically encouraging.

Keywords: *Compressive Strength, Self-Compacting Concrete, Split Tensile Strength, Superplasticizer, Water-Powder Ratio, Workability.*

1. INTRODUCTION

1.1 Definition

A concrete which is capable of flowing under its own weight and completely fill the formwork, even in the presence of dense reinforcement, without the need of internal or external vibration while maintaining homogeneity is known as self-compacting concrete (SCC) [1].

1.2 Theoretical Background

A SCC does not have a specific concrete mix design; rather it is a continuum of mixes exhibiting similar flow characteristics. By altering the mix design and use of admixtures, the rheological properties are improved. A high range water reducing admixture, i.e., super plasticizer (SP) is used to provide high flowability, which is high slump concrete. The size and shape of coarse aggregate is important for successful production of SCC. Rounded aggregates are preferred over angular aggregates, as the latter have a tendency to lock together [2].

The SCC is viscous and is obtained by the following way.

- Fines content may be cement, fly ash, limestone screenings, finely ground glass and granulated ground blast furnace slag.
- When a viscosity modifying agent (VMA) is used, less fines content is preferred; low fines content with VMA is similar to high fines content without VMA [3].

The SCC has following merits:

- SCC can produce considerable savings in labour and turn-around time of form work.
- SCC reduces noise pollution and hence it is eco friendly.
- Using fly ash contributes to long term durability and strength as it imparts a continuous hydrating system to the concrete.
- SCC is poured in the same way as ordinary concrete, but vibration is avoided.
- SCC is very fluid and can pass around obstructions and fill all the corners.
- There is no entrapped air.

- This concrete mixture does not need compaction and it saves labour, energy and time. The surface finish produced by SCC is exceptionally good and patching is not required [4].

The SCC has following drawbacks:

- It utilizes many mineral and chemical admixtures.
- It is costlier than conventional vibrated concrete

2. MATERIALS AND METHODS

The main objective is to study the effect of water-powder ratio on mechanical properties of self-compacting concrete. In the present investigation, about 20% of the cementicious material has been replaced by grade I flyash.

The following materials are used in the present study.

2.1 Cement

A 53 grade cement has been used in this investigation. The properties of cement as per BIS are given below.

Table 1 Properties of Cement

Sl.No.	Particulars	Results
1	Specific gravity	2.88
2	Soundness (Le Chatlier apparatus)	2 mm
3	Initial setting time	75 min
4	Final setting time	230 min

2.2 Fine Aggregate

Clean river sand passing through 4.75mm sieve was used for the investigation. The properties of fine aggregate are fineness modulus = 2.6; specific gravity = 2.2.

The particle size distribution curve, drawn in semi log scale, showed that this sample fell in zone III as per BIS 383-1970.

2.3 Coarse Aggregate

The size of crushed granite angular aggregate used in our investigation was between 4.75mm and 20mm with specific gravity of 2.85.

2.4 Water

Water used in our investigation was taken from Bhavani river near Sathyamangalam.The same water was used for both concreting and curing purposes. The properties of water are pH = 7.6, Total Disolved Solids = 583ppm.

2.5 Fly Ash

It is specified that fractions of SiO_2+Al_2O_3+Fe_2O_3 should be greater than 70% for grade I and 50% for grade II as per Indian Standards.

ASTM C 618 specifies two categories of fly ash, Class C and Class F, depending on the type of coal and resultant chemical analysis. Class C fly ash normally produced from the combustion of lignite coal which contains CaO higher than 10% and possesses cementitious properties in addition to pozzolanic properties. Class F fly ash, normally produced from the combustion of bituminous coal contains CaO below 10% and possess pozzolanic properties. Fly ash used in this investigation falls under the category of Class F as per ASTM Standards and grade I as per the Indian Standards. The fineness modulus of fly ash = 1.

2.6 Superplasticizer

The chemical admixture used in the investigation is CONPLAST SP430. The properties include specific gravity = 1.22 to 1.225 at 30^0 C, air entrainment is 1.0%, and chloride content is nil.

Conplast SP430 complies with IS: 9103:1979 and BS: 5075 as part 3 and ASTM-C-494 Type 'F' as a high range water reducing admixture.

3. MIX DESIGN AND MIX PROPORTION

The mix design has been carried out following European Federation of National trade Association Representing producers and applicators of specialist building products (EFNARC) specifications [5].

To achieve the required combination of properties in fresh SCC mixes, the fluidity and viscosity of the paste is adjusted and balanced by careful selection and proportioning of the cement and additions, by limiting the

water/powder ratio (WPR) and then by adding a superplasticiser and (optionally) a viscosity modifying admixture. Correct controlling of these components of SCC, their compatibility and interaction are the key to achieving good filling ability, passing ability and resistance to segregation.

In order to control temperature rise and thermal shrinkage cracking as well as strength, the fine powder content may contain a significant proportion of type l or ll additions to keep the cement content at an acceptable level. The paste is the vehicle for the transport of the aggregate; therefore the volume of the paste must be greater than the void volume in the aggregate so that all individual aggregate particles are fully coated and lubricated by a layer of paste. This increases fluidity and reduces aggregate friction.

The coarse to fine aggregate ratio in the mix is reduced so that individual coarse aggregate particles are fully surrounded by a layer of mortar. This reduces aggregate interlock and bridging. The concrete should be such that it passes through narrow openings or gaps between reinforcement and increases the passing ability of the SCC.

These mix design principles result in concrete that, compared to traditional vibrated concrete, normally contains:

- lower coarse aggregate content
- increased paste content
- low water/powder ratio
- increased superplasticiser
- sometimes a viscosity modifying admixture [6].

Five sets of specimens each consisting of six cubes and three cylinders were cast. Three cubes were tested for 7 days compressive strength. Three cubes and three cylinders were tested for 28 days compressive and split tensile strengths respectively. The slump (Fig.1) were determined for each set before filling the concrete in to the moulds. The workability in terms of slump flow was observed as follows (Tables 2&3).

Three numbers of cube specimens of size 150mm x150mmx150mm were prepared for testing compressive strength after 7 days curing and three numbers of cube specimens of size 150mmx150mmx150mm were prepared for testing compressive strength after 28 days curing for each category of the investigation. Three numbers of cylindrical specimens of size 150 mm diameter and 300 mm height were prepared for split tensile strength testing after 28 days of curing (Fig.2).

Fig. 1 Slump flow

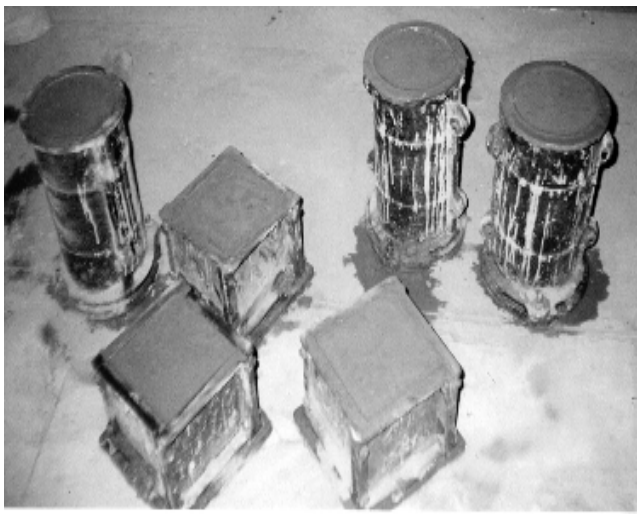

Fig. 2 Self - compacting concrete specimens

Table 2 Workability Values for Various Water-Powder Ratios (WPR)

Specimen	WPR	Cement (kg)	Fly Ash (kg)	Fine Aggregate (kg)	Coarse Aggregate (kg)	Water (kg)	SP (ml)
1	0.36	13.465	3.36	33.64	34	6.00	275
2	0.38	13.465	3.36	33.64	34	6.40	275
3	0.40	13.465	3.36	33.64	34	6.70	275
4	0.42	13.465	3.36	33.64	34	7.06	275
5	0.44	13.465	3.36	33.64	34	7.40	275

Table 3 Mix Proportion

WPR	Slump flow (mm)
0.36	655
0.38	660
0.40	660
0.42	670
0.44	675

4. RESULTS AND DISCUSSION

S.No	Specimen Designation	WPR	7days Compressive Strength, MPa	28days Compressive Strength, MPa	28days Split Tensile Strength, MPa
1	1S7,1S28	0.36	13.07	19.2	1.471
2	2S7,2S28	0.38	17.56	29.65	2.626
3	3S7,3S28	0.40	15.46	18.48	1.734
4	4S7,4S28	0.42	12.41	13.51	1.54
5	5S7,5S28	0.44	11.24	12.2	1.358

Initially, experiments were conducted using water which was not potable. This could not give adequate slump flow. Then it was decided to make use of potable water both for concreting as well as curing. Similarly, concreting had been done using 43 grade cement, which was not successful with workability testing. Then 53 grade cement has been used for the entire investigation.

Subsequently a part of the cement is replaced with Fly Ash in the production of SCC. Even 50% of the cement has been replaced in SCC in Canada Centre for Energy and Mineral Technology as high volume Fly ash SCC. However, in the present investigation only 20% of cement has been replaced with Fly Ash. Even then, the results are not satisfactory for high strength concrete.

Water-powder ratio is the main parameter which has been studied in this investigation. There is significant increase in the compressive strength as well as the tensile strength (Figure 3-5) of the specimens made with water-powder ratios of 0.36 to 0.38 (Table 4). At higher ratios up to 0.44, strength starts to diminish. Hence the water-powder ratio of 0.38 is to be concluded as optimum water-powder ratio for SCC with 20% replacement of cement with fly ash.

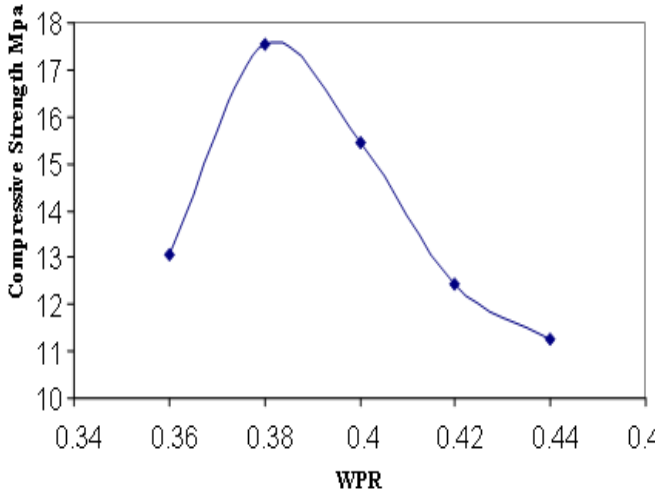

Fig.3 The 7 days compressive strength

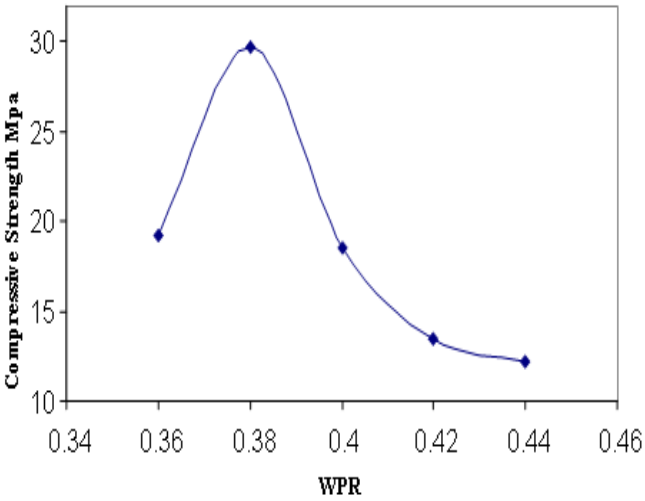

Fig.4 The 28 days compressive strength

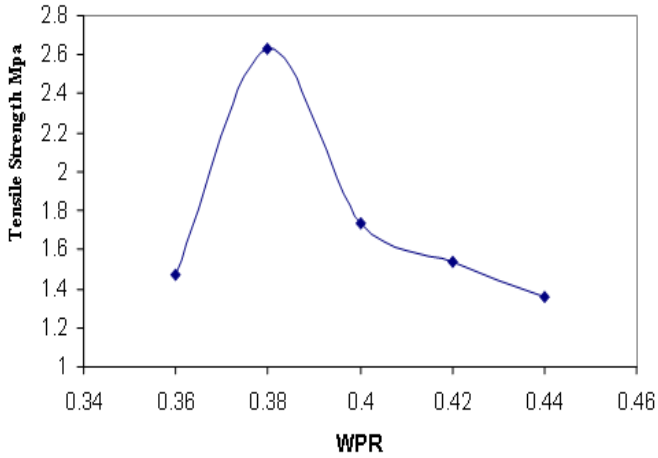

Fig.5 The 28 days tensil strength

5. CONCLUSIONS

Following conclusions could be drawn based on this investigation:

- In the mix proportion of SCC for 20% replacement of cement with fly ash the optimum WPR is 0.38.
- For the production of SCC, 53 grade cement is preferable and 43 grade cement is not recommended.
- When cement is replaced by flyash in high percentage, the strength is considerably reduced.

REFERENCES

[1] H.Okamura and M. Ouchi, "Self-Compacting Concrete", Journal of Advanced Concrete Technology, Vol.1, April 2003, pp. 5-15.

[2] A.R.Santhakumar , "Concrete Technology", Oxford University Press, First Edition, 2007, pp. 687- 693.

[3] P.L.Domone, "Self-Compacting Concrete: An Analysis of 11 Years of Case Studies", Cement & Concrete Composites , Vol.28 , 2006, pp. 197-208.

[4] V. Subramania Bharathi, "Introduction and Literature Survey on Self-Compacting Concrete", Proceedings of National Workshop on Research Methodology at Bannari Amman Institute Technology, Sathyamangalam, 2005, pp. 62-70.

[5] EFNARC, "The European Guidelines for Self-Compacting Concrete Specification, Production and Use", May 2005.

WATER RESOURCES OF HOSKOTE TALUK, BANGALORE RURAL DISTRICT – A CASE STUDY

M.T. Maruthesha Reddy[1], B.S.Shankar[2], D.S.S.Murthy[3] and B.C.Prabhakar[4]
[1]Depatment of Geology, M.V.J. College of Engineering, Bangalore - 560 067, Karnataka
[2]Department of Civil Engineering , East Point College of Engineering and Technology, Bangalore - 560 049, Karnataka
[3]Former Director, Central Groundwater Board, Bangalore - 560 011, Karnataka
[4]Department of Geology, Bangalore University, Bangalore - 560 056, Karnataka
E-Mail: madupurmaruthi@yahoo.co.in
(Received on 09 January 2007; revised received and accepted on 13 March 2007)

Abstract

The Hoskote Taluk of Bangalore Rural District in Karnanataka State, as such is devoid of any major stream and forms the upper catchment of Palar Ponnaiyar rivers. Streams are ephemeral in nature. The total number of tanks is 212, with a live capacity of 90 Million Cubic Metre (MCM). There is over exploitation of ground water resources in Hoskote Taluk. Actually, ground water mining is going on unabated, which needs to be regulated, so that the area should not face severe water shortage conditions in the near future. Hence, some strategies and measures have been suggested in this paper to improve the situation in the local planning area.

Keywords: *Jatropha, Local Planning Area, Strategies*

1. INTRODUCTION

Hoskote forms a part of Bangalore Rural District and the northern part of the district is lying between north latitude 12^0 51' to 13^o 15' and east longitudes 77^o 41' to 77^o 58'. The extent of the taluk is 582 sq.km and is bound by Kolar District to northeast, towards east by Mulbagal Taluk, by Devanahalli Taluk towards north, and by Bangalore Urban District to west and Tamilnadu state to South. The taluk is devoid of any major river, and forms the upper catchment of Ponnaiyar and Palar basins, hence most of the streams are ephemeral in nature. But a number of tanks exist, which harvest the surface flows and facilitate recharge to ground water, which is the main source of sustenance and meets the water requirements of the area.

2. AN OVERVIEW OF WATER RESOURCES

2.1 Surface Water

Most of the first and second order streams have been harnessed with small and medium tanks which when overflow, contribute to the stream flows. They are ephemeral in nature. Thus there are no major irrigation projects in the taluk. All the minor irrigation tanks in the taluk get filled only during monsoon months hence provide water for irrigation since their live storage capacity is reduced because of silting. Due to vagaries of the monsoon and low rainfall during earlier years, most of the tanks are dry. In addition to the above, the natural stream courses have been altered due to encroachment on the natural courses, and the channel width has got reduced. This has also contributed to the non-filling of the tanks, which needs to be revived. However, this has benefited to some extent in the sense that it has facilitated the recharging of ground water. As per the information available there are about 121 tanks under minor irrigation department and about 77 under the departments, and another 14 tanks in the Bangalore East. The total number of tanks is bout 212 with a live capacity of 90 MCM.

2.2 Ground Water Resources

Since peninsular gneisses predominantly underlie the area, a hard rock is devoid of any primary porosity. But due to weathering, chemical action and the tectonic activities the area has undergone, the rock mass has developed secondary porosity like joints, fractures and

weathering, and ground water occurs in these formation in cracks, crevices, fractures, lineaments and in the weathered rock. It occurs under phreatic conditions in the weathered rock and under semiconfined condition in the fractures down below. The thickness of weathering varies from less than a metre to more than 40m in the valleys, low-lying areas and tanks in ayacuts. This zone forms the buffer zone for holding water and which transmits water further down to the fractures in depth. Dug wells or open wells tap the weathered zone for meeting irrigation and other requirements, where as borewells are sufficiently deep and tap the water in the fractures at depth.

The general yield of the wells range from 30 m^3 / day to around 90 m^3 / day for a pumping period of 2 to 6 hours daily. Extremely good wells located in the valleys yield better, around 150 m^3 /day. However of late, due to failure of the monsoon frequently, water levels have gone down and in order to meet the demand, farmers have resorted to drilling of borewells. Hence the number of borewells has gone up from 736 in 1982-83 to more than 7400 by 2003-04. The borewell yields, which were quite high initially, have also come down.

The present average yield is around 1.5 to 2 litres per second (LPS) and the borewells located in the depressions, valleys, closer to stream courses and fracture zones yield slightly better, around 4 to 5 lps and sustain pumping for a long time. Due to intense cultivation and borewell irrigation, the top phreatic zone seems to have been dewatered and the borewells now tap fractures occuring in depth often as deep as 170 m or even beyond that depth. Prior to 1983, the main irrigation in the taluk used to be by dug wells and tanks. However, from the last few years, the area irrigated by tanks has dwindled since most of the tanks have little water due to erratic monsoon.

Simultaneously, there has been a tremendous increase in the number of bore wells, as farmers resorted to drilling of borewells to meet the water demand, as well as demand for water for drinking, domestic and industrial needs were also met from borewells. This has resulted in the lowering of the water table. The water table, which was around 5-10 m below ground level in1982-83, has now reached more than 25-29 m at present, which is a decline of almost a meter/year for the last two decades. Farmers are now going deeper and deeper, in order to meet the water demand. Borewells are being drilling up to 200 m and even beyond, with the hope of encountering fractures to improve the well yields.

2.2.1 *Ground Water Resources Availability*

The main source of recharge to ground water [1] in the area is from rainfall and as well as seepage from minor irrigation tanks, which are in good number in the taluk. Considering all the aspects of recharge draft and the balance available for development, The Central Ground Water Board (CGWB) south western region and the Department of Mines and Geology (DMG) of government of Karnataka have calculated the dynamic ground water resources in Karnataka as on March 2004. As per the report [2] the local planning area (LPA) is over exploited. The details are given below in Table 1.

Sl.No.	Particulars	Value
1	Total Annual Groundwater available	6081.62 ha.m
2	Net Annual Groundwater availability	5777.54 ha.m
3	Existing Gross Groundwater Draft for irrigation	12521.32 ha.m
4	Existing Gross Groundwater Draft for Domestic and Industries	390.98 ha.m
5	Existing Gross Groundwater Draft for all uses	12912.31 ha.m
6	Allocation for Domestic and Industrial use for next 25 years	554.16 ha.m
7	Net Ground Water Availability for future use	0
8	Category	Over exploited (225%)

From the above, it is clear that there is over exploitation of ground water resources in Hoskote. Actually, ground water mining is going on relentlessly, which needs to be regulated, so that the area should not face severe water shortage conditions in the near future.

2.3 Present Water Supply Scenario

Presently water supply is effected through rural water supply (RWS) schemes in the villages through drilling of bore wells and fitting hand pumps, and also through mini water supply (MWS) schemes and piped water supply (PWS) schemes. For urban areas like Hoskote, there are schemes to meet the water demand. Hoskote town area has a population of 36,323 (2001) and the demand at 80 litre per person per day (LPPD) has been worked out at 29,05,840 litres per day. There are 43 energized bore wells and 46 hand pumps. At present the town is getting 15,75,000 litres per day. That is almost 50% of the demand. There is a large gap, which needs to be bridged with additional resources or cut the demand by efficient management of the available resources. The projected population by 2021 is 80,000 with a projected demand of 64,00,000 Liter per day (LPD). The present rural population of Hoskote LPA is 1,95533 and the demand at 55 LPPD works out 107,54,315 LPD or 10.75 MLD. The projected rural population by 2021 of the LPA is 2,80,866 and the projected demand is 1,54,47,630 LPD or 15.44 MLD. It is impossible to meet this demand, as there are no surface sources in the area and to meet the demand, groundwater is the only source. Since the groundwater is already over exploited, the other alternative is to adopt the water conservation techniques, to carry out rainwater harvesting to harness any surface flows and store them properly in tanks and other surface features for use.

3. STRATEGIES TO BE ADOPTED TO IMPROVE THE WATER RESOURCES AVAILABILITY OF THE LPA

Several strategies are available to improve the water resource availability in the LPA . Since ground water is already over developed, there is a need to reduce the dependability on ground water and simultaneously adopt certain techniques to improve the situation. Some of the methods or techniques available are discussed here.

3.1 Rain Water Harvesting

Rain water harvesting [3] can be taken up on a large scale so that, drinking and domestic needs can be met at the village level / individual level by harnessing the roof water, sorting it in PVC or other tanks, filtering it and using it whenever required by the villager. At the urban or town level, it can be used apart from domestic for flushing, washing toilets in the offices, schools and other establishments.

3.2 Construction of Nalabunds

Nalabunds, Check dams or Weirs can be constructed across stream courses in the rural areas, in times of storms, the surface runoff is harvested, which will also arrest soil erosion, as well as create minor storage ponds (percolation ponds) which will facilitate as a source of drinking water for cattle, and as well a means of recharging groundwater. However before it is taken up on a large scale, investigation needs to be carried out as to the location of suitable sites, for construction, catchment and local soil and other geological conditions.

3.3 Desilting of Tanks

Most of the irrigation tanks are old and are silted up and do not have the original live storage capacity. These tanks need to be revived and desilting of these tanks need to be taken up in phases. The priority, the extent and the volume of desilting to be taken up along with the cost has to be worked out in detail. In periods of heavy rainfall, these tanks once desilted will have enough space to store the excess water, which will meet the irrigation and other demands and also once desilted, it will facilitate deep percolation and recharge ground water in the Ayacut which might help revive open wells down stream.

3.4 Construction of Farm Ponds

Farm Ponds construction, especially in the sandy soil helps retain water in the agricultural farm of the farmer and help retain moisture for a long time as well as facilitate recharge groundwater locally. Farm Ponds constructed over a large area might aid in retaining moisture over larger period and may help in dry land cultivation. In course of time it will also help in recharging groundwater.

3.5 Agro Forestry

Agro forestry and tree plantation in dry barren land might help to arrest runoff and facilitate retain moisture. However cultivation of Eucalyptus plantations need to be discouraged as it is a water intensive tree and instead, casuarinas or Jatropha plantation, can be encouraged, which will be remunerative to the farmers.

3.6 Recharging of Ground Water

Recharging of ground water in the LPA is very much needed since the area is over exploited. Recharge wells at suitable locations, trenching across the hill slopes and construction of percolation ponds, recharge weirs, and watershed development will have to be taken up to augment the resources and arrest decline of water levels.

3.7 Conservation of Water

Conservation of water is the need of the day. Farmers and general public need to be educated about the usage and conservation of water, and wherever possible,wastage needs to be avoided. In order to educate them, mass awareness such as 'Jala Jagriti' programmes, seminars can be arranged through audio and video, which will help generate interest among the public. As far as farmers concerned, they have to be made aware how to cultivate only dry crops and not water intensive crops like paddy, sugar cane, etc.

3.8 Wastewater Treatment and Recycling

With the awareness created among rural public about health consciousness and in view of more number of industries coming up and urbanization, the generation of wastewater is going up. Recycling of wastewater can be taken up by setting up waste treatment plant at Hoskote town, and the recycled water can be utilized for meeting, domestic, gardening and even industrial needs. The industries, hospital complex can be encouraged to go in for such plants, which will meet their water requirement partially.

3.9 Regulation of Groundwater Development

Though the area is over exploited, there is no control yet, on ground water development and farmers and ground water consumers are drilling bore wells and going deeper in search of water every year. This needs to be regulated [4]. Barring drilling for meeting the domestic and drinking water needs, a control needs to be exercised either by State Ground Water Authority or by Central Ground Water Authority (CGWA), permission need to be obtained from the Authority for drilling of bore wells where there is large scale construction, like apartments, small scale industries, educational establishments, like institutional complex, etc.

These are some of the strategies and measures which can be thought about to improve the situation in the Local Planning Area.

4. CONCLUSIONS

There are nearly 212 tanks in the area with a live storage capacity of 90.45 MCM. All these tanks are silted up. Hence considering 50% of the capacity, the total water availability from the tanks will be around 45.0 MCM. This quantity can be utilised for meeting the water demand for domestic means and can meet the demand to the extent of 100%. Balance water available, can be utilised to meet the demand for industries and irrigation. Hence a strategy and action plan need to be adopted so that water needs are met, development won't suffer and also there is no further stress on ground water resources of the area.

REFERENCES

[1] Pradeep K. Nayak, K.Arun, and K. Awasthi, "Groundwater Resources Development in the Koyna River Basin, Maharashtra - Strategy For The Western Ghats Region", Journal of Indian Water Resources Society, Vol.25 No.3, 2005, pp. 25- 32.

[2] Central Groundwater Board, "Detailed Guidelines for Implementing the Groundwater Estimation Methodology 1997", Central Groundwater Board, Central Region, Nagpur, 1998, pp. 219.

[3] R.C.Srivastava, R.B. Sighandhupe, R.K. Mohanty, and H.N.Verma, " Water Resources Development Through Rain Water Harvesting and its Management by Multiple Use of Water", WTCER, Bhubaneswar, 2001, pp. 212-234.

[4] K.R. Karanth, "Groundwater Assessment Development and Management", Tata McGraw Hill, New Delhi, 1987, pp. 217-247.

FLEXURAL BEHAVIOUR OF BEAMS WITH PARTIAL REPLACEMENT OF COARSE AGGREGATE UNDER CYCLIC LOADING

E.K.Mohanraj [1] and S. Kandasamy [2]

[1]Department of Civil Engineering, Kongu Engineering College, Perundurai - 638 052, Tamil Nadu

[2]Department of Civil Engineering, Government College of Engineeirng, Salem - 636 011, Tamil Nadu

E-mail: mohan8899@yahoo.co.in

(Received on 15 March 2007 and accepted on 10 June 2007)

Abstract

Rapid increase in the construction activities leads to acute shortage of conventional construction materials. Attempts have been made to replace coarse aggregate by various locally available waste materials to reduce the cost of concrete. It is reported that around 2 to 5 percent of buildings and other structures are demolished in the major cities due to various reasons. In order to use these waste materials effectively in the construction industry, an experimental study is carried out to investigate the strength and behaviour of concrete under cyclic compressive loading. Tests on beams containing partial replacement of coarse aggregate by waste granite, rubber and construction & demolition (C&D) debris in different proportions by weight of concrete have been conducted to establish the load-deflection curve. The range of compressive strengths obtained shows that partial replacement of waste materials can be used for both plain and reinforced cement concrete construction.

Keywords: *C&D Debris, Cyclic Loading, Rubber*

1. INTRODUCTION

The idea of recycling concrete waste as coarse aggregates for new concrete construction is gaining importance on the international scale. Although the mechanical properties of recycled aggregate concrete are well known, the study on durability performances of recycled aggregate concrete appears to be very limited. This study was an attempt to investigate and compare the strength and behaviour of the conventional and partial replacement of coarse aggregate by waste materials. Recycling of concrete waste as an aggregate for new concrete construction not only saves huge disposal cost, but also conserves natural resources and in some cases provides economic benefits.

In olden days, slabs, beams, and columns were constructed with concrete and steel. Conventionally concrete is a mix of cement, sand and aggregate. Continuous research efforts have established concrete as a versatile material; concrete required for intensive construction activity can always be made available, since all the ingredients of concrete are of geological origin. Although these materials are usually available, at some places it is economical to substitute these materials by locally suitable ones. At the same time, increasing quantity of rubber and granite waste and C&D debris is available as waste. The disposal of this waste is a serious environmental problem. If it is possible to use this waste in making concrete and mortar by partial / full replacement of natural river sand, then this will not only save the cost of construction but at the same time it will solve the problem of disposal of this waste.

With the ongoing research to develop appropriate technology and field trails to monitor the performance and assessment of economic feasibility, the use of this alternative material will become more viable. There has been inadequate utilization of large quantities of granite stone as alternative material left out after crushing of granite to obtain granite flooring. Wang *et al.* [1] studied the reinforced concrete with recycled rubbers. Several studies performed recently showed application of the recycled tyre rubber might improve the weak characteristics of concrete. More than 250 million scrap tyres weighing more than 3 million tonnes are generated each year in the United States. This is considered as one of the major environmental challenges facing municipalities around the world, because waste rubber is not easily biodegradable even after a long period of

landfill treatment. One of the solutions suggested is the use of tire rubber particles as additives in cement-based materials. Although concrete is the most popular construction material, it has some limitations, like properties: low tensile strength, low ductility, low energy absorption, shrinkage and cracking associated with hardening and curing.

Many experiments were done to find out appropriate methods of rubber application [2]. Commonly, fully replacing coarse aggregate (gravel) or fine aggregate (sand) with rubber is not appropriate because the loss of strength is too severe. However, with small portion of aggregates replaced, the loss in compressive strength was not significant. Experiments under the laboratory environments commonly presented that the use of rubber in the cement concrete mix reduced drying shrinkage, brittleness, and elastic modulus, which might improve the overall durability and serviceability of cement concrete.

The United State Environmental Protection Agency Municipal and Industrial Solid Waste Division [2] say that the C&D debris is waste material that is produced in the process of construction, renovation, or demolition of structures. Land clearing debris such as stumps, rocks, and dirt are also included in some state definitions of C&D debris. In this work, the land clearing debris is not considered.

Granite is a common and widely-occurring type of intrusive, folic, igneous rock. Granite is nearly always massive, hard and tough, and it is for this reason it has gained widespread use as a construction stone. The average density of granite is 2.75 g/cm^3 with a range of 1.74 g/cm^3 to 2.80 g/cm^3.

The purpose of this study was to examine the effects of granite and rubber waste and C&D debris concrete on the strength and behaviour of concrete. The studies carried out by the authors in the last two years on the influence of waste materials are used as a partial / full replacement of coarse aggregate.

The manufacture of granite by crushing rock ballast produces large amount of crushed stone as waste material. In rubber industry also many tyres are there after used as waste material. This poses a serious disposal problem. In many regions of India, acres of land have become barren due to disposal of crushed granite stone, rubber and C&D debris on it. This study is mainly directed towards exploring the possibility of making effective use of the discarded granite stone in concrete.

2. EXPERIMENTAL PROCEDURE

2.1 Materials

The cement used for the investigation was 53 grade ordinary portland cement. The initial and final setting times were 45 and 300 minutes respectively; the 3-day and 7-day compressive strengths were 20.2 N/mm2 and 28.0 N/mm^2. Crushed granite aggregate having nominal size of 20 mm was used as coarse aggregate for conventional concrete. Sand collected from nearby river was used without any refinement. Crushed granite, rubber and C&D debris from concrete was used as a partial replacement of coarse aggregate. The basic concrete mix of 1: 1.68: 3.00; w/c = 0.5 is chosen. The mix of proportion were obtained using IS method of mix design [3] to achieve M^{20} grade concrete, with coarse aggregate and river sand.

2.2 Preparation of Specimens

The exact amount of cement, sand, granite and C&D debris were weighed. Rubber is measured by volume basis and then placed in a laboratory concrete mixer machine. The water was added in required amount and workability of fresh concrete was measured by compacting factor method immediately after mixing. The test specimens were cast in steel mould and compacted in vibrating table. They are de-moulded a day after casting. The specimens were cured in water until the test date.

2.3 Tests

For M^{20} batch of concrete three 150 mm cubes were tested to determine the compressive strength, three 100 mm x 100 mm x 500 mm size prisms were tested under two point loading to determine modulus of rupture and three 150 mm x 300 mm cylinders were tested for split tensile strength at the age of 28 days.

2.4 Mixing and Casting

Sand and cement were mixed dry and kept separately. Then coarse aggregates, dry mix of cement and sand were kept in three layers and approximate amount of

water was sprinkled on each layer and mixed thoroughly. Mixing procedure was felt to be extremely tedious due to formation of small lumps.

The cube (150 x 150 x 150 mm), prism (100 x 100 x 500 mm), cylinder (150 x 300 mm) and beam (100 x 150 x 1200 mm) of both conventional concrete and other mixes were casted. Specimens were cured for 28 days in fresh water after 24 hours of their casting and till 48 hours before testing.

3. TESTING AND RESULTS

The specimens are tested to determine the basic mechanical properties. The cube specimen was placed over the compression testing machine and the load was gradually applied till the failure of the specimen. The ultimate load was noted down as collapse load and compressive strength was calculated.

The prism is placed on electronic universal testing machine to find out the flexural strength. The split tensile test was carried out with concrete cylinders using compression testing machine.

The beam specimens were tested on electronic universal testing machine with two point load. The loading was done at a distance of L/3 from support as shown in Fig.1. A 25 mm deflectometer (0.01 mm) was setup at the midsection of beam and cyclic loading was done up to 80% of ultimate load. By doing 10 cycles, central deflection, first crack load, ultimate load values of various types of beams are measured and the same are shown in Figures 2-7.

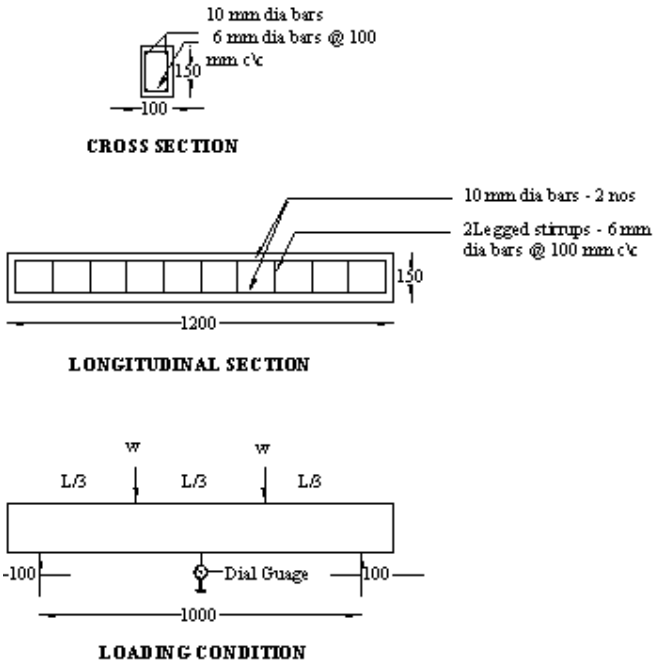

Fig. 1 Loading condition

4. CONCLUSIONS

Upon analysing the results, conclusions are drawn:

- C&D debris concrete provides greater stiffness. It allows beams to deflect more and it also arrests the crack that develops in the concrete.
- By using waste materials, environmental pollution can also be minimized.
- Using rubber will minimize the deflection and it satisfies the Hooke's Law.
- Using granite provides greater energy absorption capacity which had a vital role in earth quake loads.

REFERENCES

[1] Y. Wang, H.C. Wu and V.C. Li, "Concrete Reinforcement with Recycled Rubbers", Emerging Construction Technologies (Construction Engineering and Management, CEM), 2000.

[2] R. Ahmed, Klundert, Arnold Van de, and I. Lardinois, "Rubber Waste, Options for Resource Recovery and Waste", A Book Aimed at Small Scale Rubber Reuse in Concrete, 1996.

[3] IS 10262 – 1982 Recommended Guidelines for Concrete Mix Design.

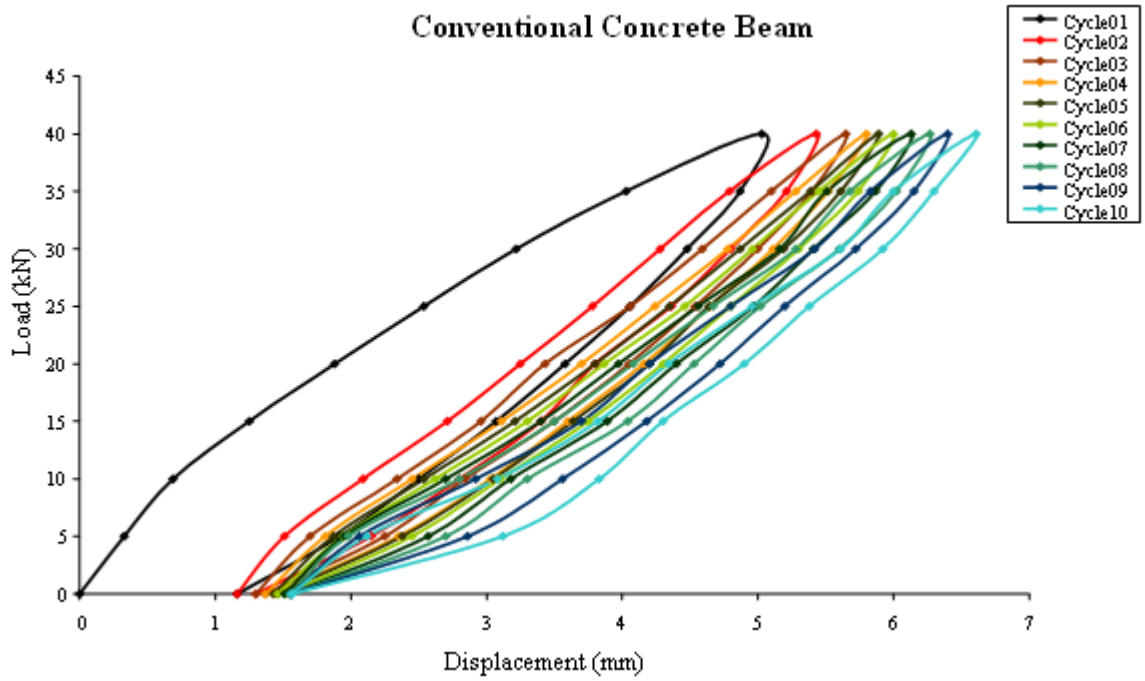

Fig. 2 Load vs displacement curve for various cycles

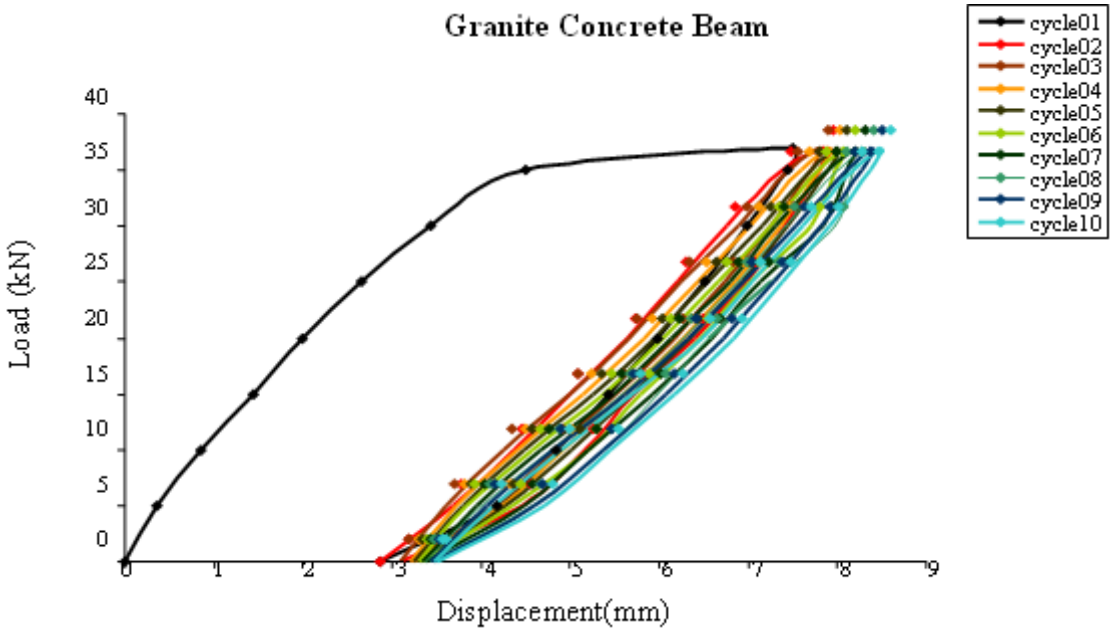

Fig. 3 Load vs displacement curve for various cycles

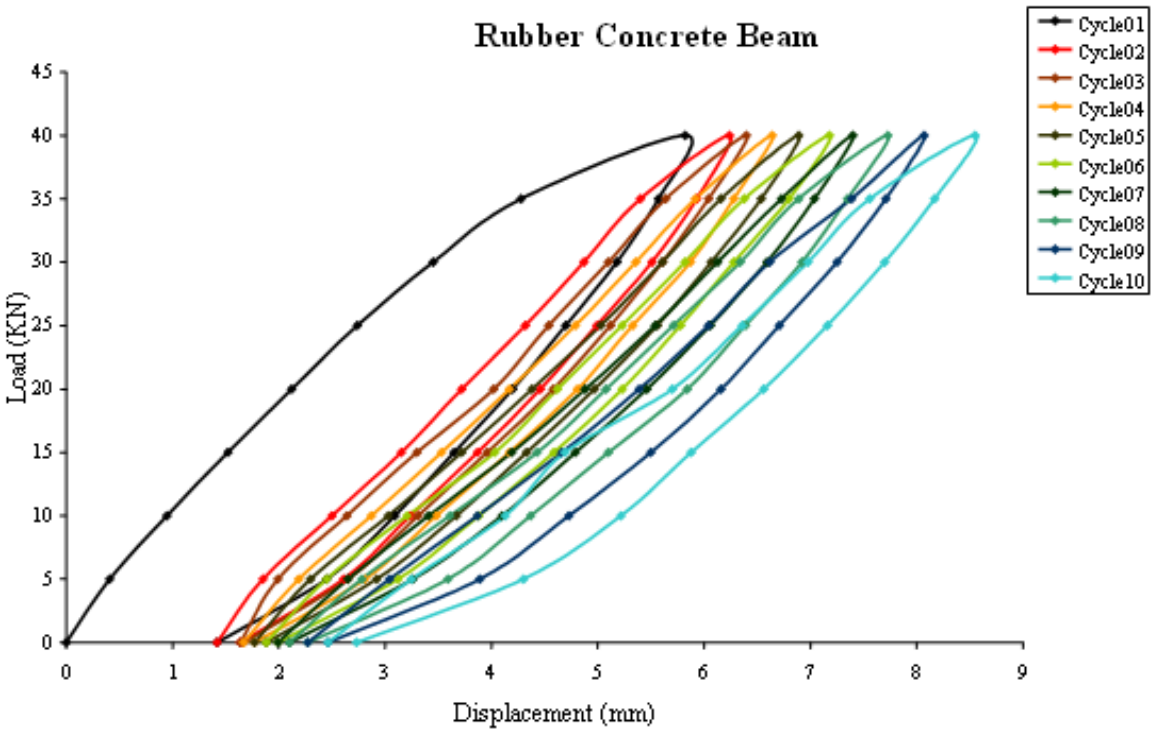

Fig. 4 Load vs displacement curve for various cycles

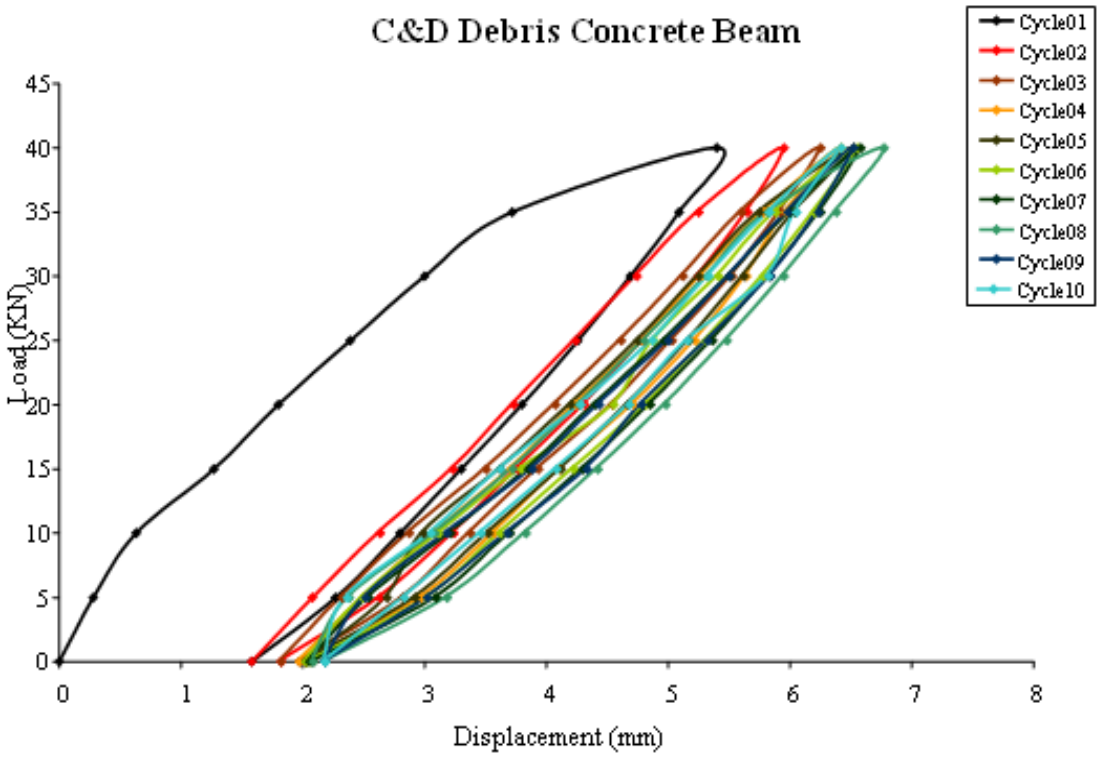

Fig. 5 Load vs displacement curve for various cycles

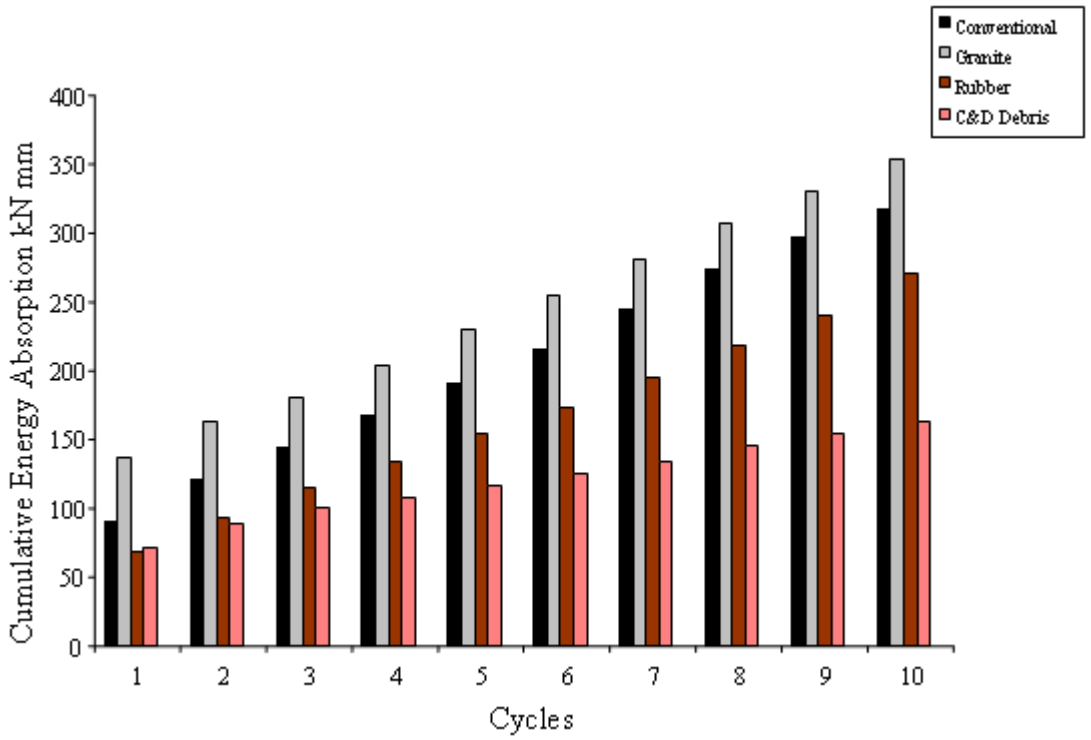

Fig. 6 Energy absorption capacities of various types of beams

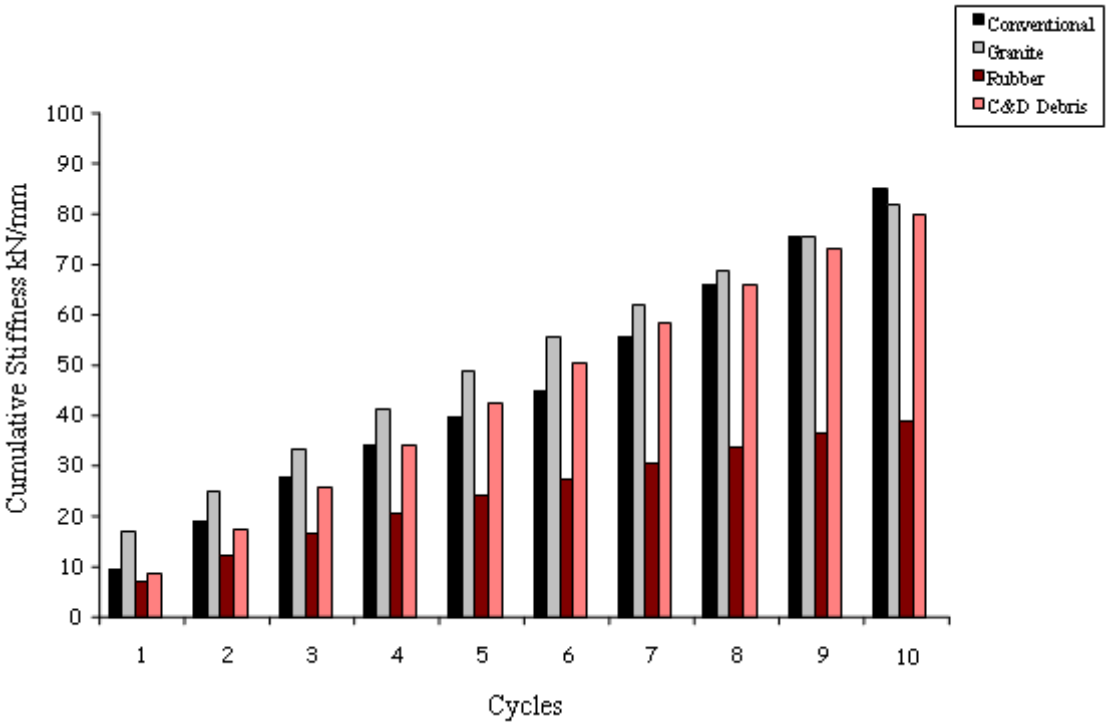

Fig. 7 Stiffness factors of various types of beams

FUZZY CONTROLLER FOR TEST PATTERN ANALYSIS

C. Thiyagarajan[1] and P.T. Vanathi[2]
[1]Department of Electronics & Communication Engineering , Kumaraguru College of Technology, Coimbatore - 641006, Tamil Nadu
[2]Department of Electronics & Communication Engineering , PSG College of Technology, Coimbatore - 641004, Tamil Nadu
E-mail: ptvani@yahoo.com; gctprocessor@yahoo.co.in
(Received on 05 May 2007 and accepted on 12 July 2007)

Abstract

Testing computer hardware is a complex and tedious process. The existing testing methods use dozens of techniques to improve the performance of the testers. Test time, test data size, response pattern length, fault coverage, test data traffic, multiple fault detection and ability to detect the fault when signature sample space is damaged, influence the quality of tests and performance of testers. This paper presents a method to generate and use differential transient response patterns (DTRP) to reduce test data length, thereby, the test data traffic in bus and memory sub system, number of test responses for fault detection, and to increase fault coverage. Two sub systems, DTRP generator and Fuzzy Inference Engine are used. The former is build into system under test; the later is with automatic test equipment (ATE). This paper focuses on the later. The generated DTRPs are analysed using fuzzy logic to detect traditional faults modeled by struck-at models, and other non-functional faults such as oxide faults (OF1), real faults with low resistance (RF1), real faults with large resistance (RF2), and soft fault due to changes in load capacitance (SF1).

Keywords: *Differential Transient Response Patterns, Fuzzy Logic, Non-functional Faults, Transient Signals*

1. INTRODUCTION

Testing is an integral part of integrated circuits manufacturing process. With the increasing complexity and quality requirements for integrated circuits, efficient testing techniques remain critical. For instance, CMOS fabrication of digital integrated circuits includes defects that cannot be represented using conventional idealistic stuck-at or bridging fault models. Unfortunately, such defects represent a significant fraction of faults in complex digital circuits [1]. Testing based on this stuck-at fault model does not fully cover bridging and open faults caused by physical defects such as spot defects and gate oxide shorts, called non-functional faults. To include more faults, a more realistic fault model is needed to replace and supplement the traditional stuck-at-fault model. As transistor size shrinks, such resistive defects influence the fault detection even more and thus it is vital to investigate their presence, effects, and detectability. A fault occurs when two nodes are accidentally connected together. We call these faults (e.g. stuck-at or bridge) with zero resistance ideal faults. In design scenario, parasitic resistance (R), capacitance (C), and inductance (L) are always associated with the defects in the VLSI chips [2]. The faults with their associated resistances are called real faults. It changes switching (transient) characteristics (TC) of circuit under test (CUT), also its voltage transfer characteristics (VTC). TC based testing needs more samples. This paper uses fuzzy logic to analyze differential transient responses for fault detection.

2. TESTER DESIGN APPROACH

Test can be done externally, which employs Automatic Test Equipment (ATE), and internally, such as Built-In Self-Test (BIST). A problem commonly associated with BIST is the quality of its test patterns. The randomly generated vectors cannot detect many faults. External testing by ATE has the advantage of generating and utilizing deterministic fault-oriented patterns by which all detectable faults can be found. As ATE vectors have good test quality and slow application time, it is possible to find a point where BIST speed can be combined with ATE quality to achieve a high coverage in a short test time [3]. The focus of this paper is a facility for combining both ATE and BIST with less modifications to cover more faults. Thereby the fault coverage is increased in a short test time. To achieve this goal, BIST is used to obtain

differential transient response patterns (DTRP) as shown in Figure 1. DTRP generator is also a digital circuit, which converts incoming test signatures from circuit under test. Using differential voltage sensors, which are made of p&n sub networks like a logic gate.

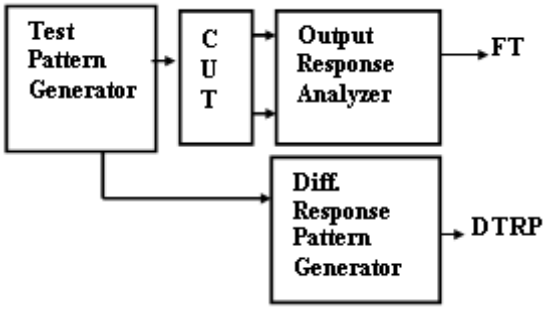

Fig. 1 Modified BIST structure

The ATE is enhanced with fuzzy controller (FC) [4] to analyse DTRP. The FC only uses differential transient patterns to detect the non-functional faults. It adjusts the membership function shape to detect faults.

Transient Signal Analysis (TSA) is a parametric approach for testing circuits. TSA is based on a measurement of the changes in transient response of CUT. The variations produced by defects in the form of voltage and current transients of defective devices. TSA is able to distinguish between these two types of variations by additionally measuring voltage transients at a set of test points, called differential transients patterns (DTP) [5]. Use of DTP considerably magnifies the variations in transition region of transient response and VTC. Also the changes from original transition are either positive or negative, and takes linear, ramp, triangular, 's' or 'z' shaped, sometimes semi-sinusoidal, and often irregular.

3. FUZZY PATTERN ANALYSIS

Fuzzy controller (FC) is part of ATE for analysing DTP to detect non-functional faults. A fuzzy logic fault inference system comprises of four principal components: a fuzzificator, a knowledge base, decision making logic or inference engine, and a defuzzificator as shown in Fig.2. The fuzzificator acquires and measures the values of input DTRPs and converts them into corresponding linguistic values. The proposed system uses two types of inputs, they are: single DTRP and double DTRP inputs. The knowledge base comprises of rules for detecting faults [6]. The decision-making logic uses these rules for fault predictation. The defuzzificator converts the range of DTRP linguistic values of output variables into numerical value (0 to 1) to say about faultiness of CUT.

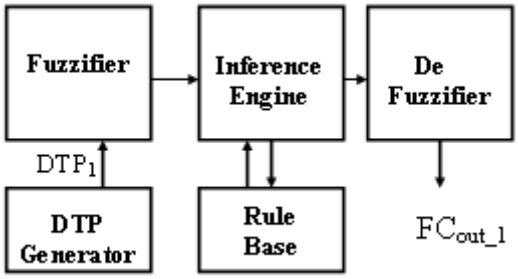

Fig. 2 Model of a Fuzzy Controller

3.1 Pattern Representation

The role of fuzzifier is to map DTRP samples to fuzzy sets defined by their membership functions (MF). The quality of fuzzy approximation depends on the quality of rules, which in turn depends on the nature of the membership functions described by their shapes, spread, and position on DTP sample space. The input DTRP pattern is identified and given with meaningful linguistic states. Each state covers a specific range of the DTRP. Representing these states by membership function that is symmetric and equally spread over each range. This is a type of quantization, called fuzzy fault quantization [6]. Two types of quantization are used. They are using single DTRP and two DTRPs. The DTRPs are partitioned into zones, for monitoring the changes because of faults. Changes in TC are measured in voltage w.r.t. time. But it is converted into variations in MF values and their attributes as shown in Fig. 3.

3.2 FC Design for DTRP Diagnosis

Since the transition region in DTRP reflects the non-functional fault characteristics, crisp samples from this region are used to find out changes in the slope as positive large (PL), positive medium (PM), positive small (PS), approximated to zero (Z), negative small (NS), negative medium (NM), and negative large (NL) as shown in the Fig. 3.

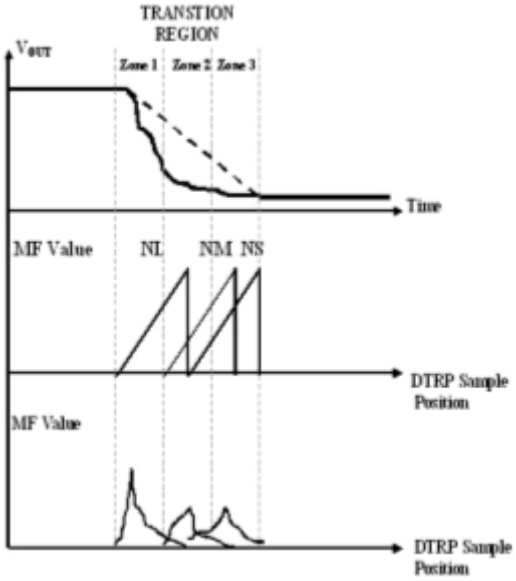

Fig. 3 A Typical Representation of Dr Patterns using Possible Fuzzy Quantization

This paper uses narrow membership functions to cover more quantization points. Thus, more linguistic terms in the rule base provide more adjustment can be made to the piecewise characteristics of fuzzy systems to increase accuracy of FC output on faultiness. We have used MF with straight lines offer a simplified notation. Also, it considerably boosts the speed of FC. We have used triangular MFs to fuzzy zones as in Fig. 3. The correlation of DTRP and zonal MFs are also plotted in bottom side curves of Fig. 3. These curves characterize a fault in fuzzy domain.

3.3 Fuzzy Rule Base for Fault Detection

In our proposed FC, a DTR is generated. From one differential voltage sensor correlates input test vector and CUT output data. DRP is converted into seven linguistic states; the total number of possible non-conflicting fuzzy rules is 71 = 7. Firstly, FC uses 7 rules to evaluate entire transition region. Secondly, we have divided the region into 3 zones. Each region is scanned by 7 rules. Thus, totally, 21 states are used to cover transition region. They can be conveniently represented in matrix form called Fuzzy Associative Memory (FAM), is a transformation [7]. FAM for all non-functional faults has been shown in Fig. 4a. A fault is identified by combining more states shown as shaded states. The output is encoded with three linguistic states. They are good (G), partial (P), and bad (B) for all faults.

For OF1 faults, these three output states are encoded using MF values as given shown thro' FAM in Fig. 4b. we commonly found a fact that the MF value for a fault in each states is combined and they are defined with an interval whose end points are tabulated as ì1& ì2.

	Min Max	PL	PM	PS	Z	NS	NM	NL
OF1	µ1	0.1	0.3	0.1	0.2	0.4	0.7	0.6
	µ2	0.2	0.4	0.0	0.3	0.3	0.2	0.3
RF1	µ1	0.1	0.1	0.4	0.0	0.1	0.2	0.6
	µ2	0.2	0.2	0.1	0.1	0.7	0.3	0.3
RF2	µ1	0.0	0.0	0.0	0.5	0.9	0.4	0.6
	µ2	0.1	0.2	0.6	0.3	0.7	0.3	0.8
SF1	µ1	0.0	0.7	0.3	0.5	0.1	0.1	0.6
	µ2	0.3	0.2	0.6	0.3	0.7	0.3	0.2

Fig. 4a Fuzzy Associative Memory FAM-1 for Non-functional Faults

	Min Max	PL	PM	PS	Z	NS	NM	NL
G	µ1	0.1	0.3	0.0	0.0	0.0	0.0	0.0
	µ2	0.0	0.1	0.1	0.0	0.0	0.0	0.0
P	µ1	0.6	0.3	0.0	0.0	0.8	0.5	0.5
	µ2	0.2	0.6	0.1	0.0	0.0	0.1	0.0
B	µ1	0.1	0.3	0.1	0.2	0.4	0.7	0.6
	µ2	0.2	0.4	0.0	0.3	0.3	0.2	0.3

Fig. 4b Fuzzy Associative Memory FAM for of 1 Faults

3.4 Fuzzy Inference

The previous two methods yield less accuracy. To enhance the accuracy of FC, two DTRPs are generated and fed onto FC. The DTRP1 has been divided into 6 linguistic states and DTRP2 is with 5 states, corresponding FAM is given in Fig. 5. The diagnosis schema used for detecting RF1 type fault is:

Rule 1a: if DRP1 Slope is <PM> AND DRP2 Slope is <NL>, THEN Fault Detected IS RF1.
Rule 1b: if DRP1 Slope is <PS> AND DRP2 Slope is <NL>, THEN Fault Detected IS RF1.
Rule 1c: if DRP1 Slope is <Z> AND DRP2 Slope is <NL>, THEN Fault Detected IS RF1.
Rule 1d: if DRP1 Slope is <NS> AND DRP2 Slope is <NL>, THEN Fault Detected IS RF1.
Rule 1e: if DRP1 Slope is <PS> AND DRP2 Slope is <NS>, THEN Fault Detected IS RF1.
Rule 1f: if DRP1 Slope is <Z> AND DRP2 Slope is <NS>, THEN Fault Detected IS RF1.
Rule 1g: if DRP1 Slope is <NS> AND DRP2 Slope is <NS>, THEN Fault Detected IS RF1.

FAM	DTRP1						
		PM	PS	Z	NS	NM	NL
DTRP2	NL	RF1 RF2	RF1 RF2	RF1 RF2	RF1		
	NM	RF2	RF1 RF2	RF1 OF1 RF2	RF1 OF1 RF2	OF1	OF1
	NS		SF1 OF1	RF1 OF1 SF1	OF1 SF1 RF2	OF1 SF1 RF2	OF1 RF2
	Z	SF1	SF1	SF1	SF1	SF1	RF2
	PS	SF1	SF1	SF1	SF1		RF2

Fig. 5 FAM-2 with two DTRPS

Similarly Rule 2, Rule 3 & Rule 4 are derived from FAM-2 for Faults OF1, RF2, and SF1.

4. SIMULATION

The DTRPs obtained by simulation using Tina Pro and HSPICE. These are analysed using Matlab software with fuzzy toolbox support. Figures 6.a and 6.b. show simulated DTRPs for RF1 and RF2 type faults. The faults produce linear changes in transition as shown in Fig. 7.

Because linear increase in the resistance causes increase in Vo drop in TC. DTRP1 and DTRP2 are generated from CUT's input versus output, and output versus ground respectively. The linear changes in Fig. 7 are from zone-2 after splitting DTRP2 into 5 zones. The FC uses Gaussian, triangular functions to ensample the two DTRPs. Output variable uses 'z' function for decision making purpose.

Evaluation of DTRP1&DTRP2 by their MF is shown in Fig. 8. Where a fault introduces changes in zone-2. It is identified as RF1 type after inference using the rules shown in Fig. 5. The FC generates output for a cycle in TC as depicted in Fig. 9, where the effect of fault is clearly identified. Similarly for other non-functional faults we obtained set of responses from the proposed FC system.

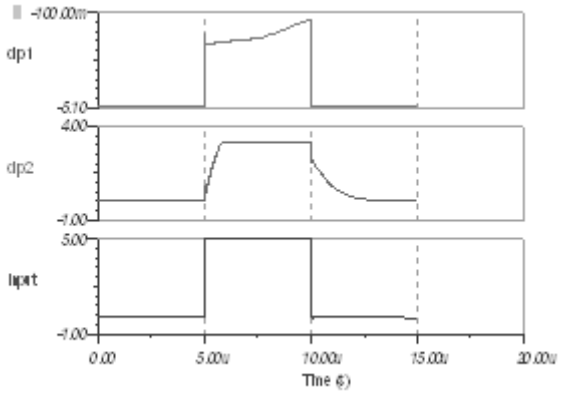

Fig. 6a DTR Patterns for RF1 faults

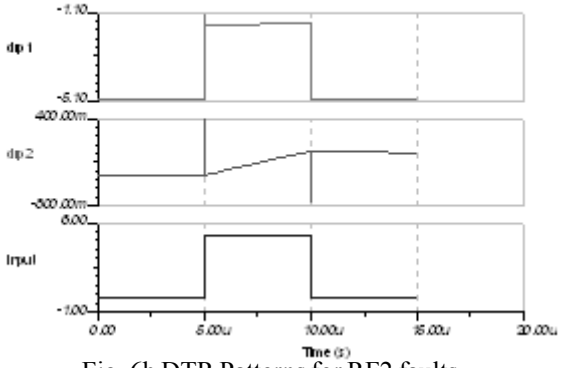

Fig. 6b DTR Patterns for RF2 faults

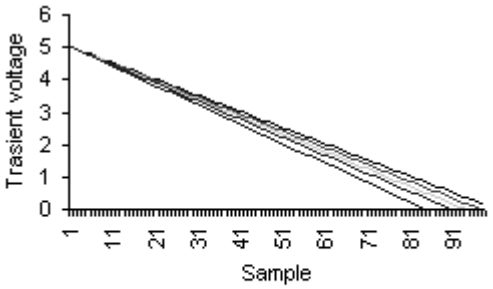

Fig. 7 Changes in Transition due to faults

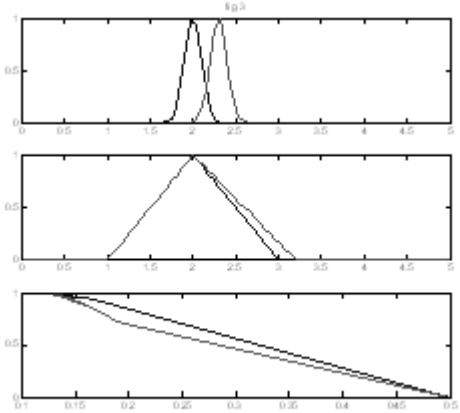

Fig. 8 Changes in FC inputs and output variables due to RF1 fault

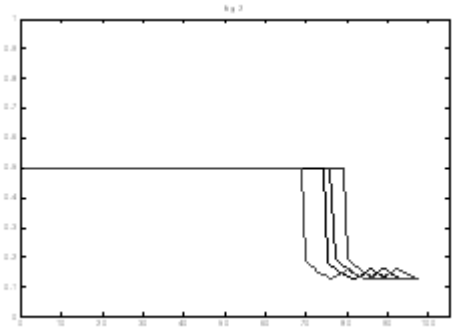

Fig. 9 Changes in FC output due to transition

5. RESULTS AND DISCUSSION

Based on the Fuzzy analysis on the DTRPs, if a set of membership functions has been selected and deployed, more features can be obtained like increased fault detectability Table 1, reduced test vector and response length, there by indirectly, less memory requirements, as shown in Table 2. Table 1 undoubtedly outlines the better fault detectability of DTRP method over two of its basic methods: function testing and TSA method. Table 2 briefs about the minimum test response length required to improve detectability. Windowing can be used for further test response data compaction in TSA and DTRP analysis.

Fault coverage (fC) [8] is an important parameter, here, can be more flexibly controlled either reducing test vector size or that of DTRP size. The relationship between these two parameters with fault coverage is carefully simulated, tested, and plotted in Figures 10.a. & 10.b. respectively for three testing methods. Fig. 10.a. clearly reveals a fact that the DTRP method has good fault coverage for medium test lengths. On the hand, from Fig. 10.b, DTRP yields good fC if its medium size response pattern length is selected. If the method is implemented in practice, it is must to set memory bound, data bandwidth, and bus speed as per AT2 model [9] for estimating test architecture performance. These are evaluated using test data traffic [10].

For that, traffic is monitored and shown in Fig.11, the traffic of DTRP method pose saturated data traffic pattern for selected fC range and in turn, that of FT is linearly increasing. The decision-making in fC is understood from cut-set and interval analysis [11] on the outputs for RF faults as given in Table 3. When RF1 type fault affected on four DTRPs, the changes in TC is analysed, the cut set analysis helps to study sub zonal properties. Similarly, x1 and x2 are boundaries of cut sets; observe MF's base length changes.

Table 1 Fault Coverage

Tests	Faults Detectable	
	Analog CUT	Digital CUT
Function Test	3	4
Transient Test	5	7
DTRP Analysis	11	9

Table 2 Required Test Vector and Response Lengths for Maximum Fault Detectability

Tests	Test Length		
	Test Vector (Bytes)	Test Response (Bytes)	Window support
FT	24	24	No
TSA	12	32	Yes
DTRP	12	12	Yes

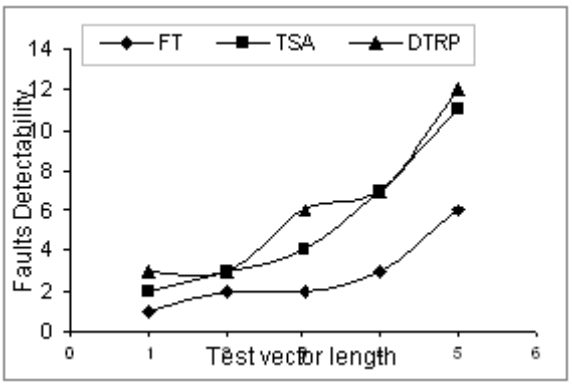

Fig. 10a Fault coverage w.r.t Test vector size

The linear changes in interval in Table 3 shows the effect of RF1.

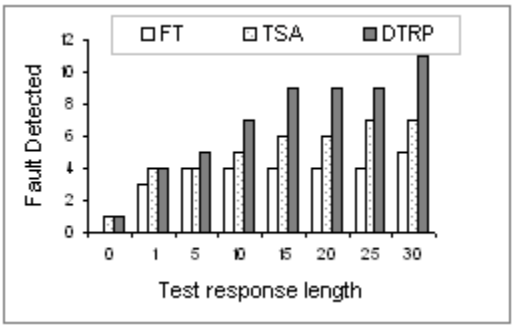

Fig. 10b Fault coverage w.r.t Test response pattern size

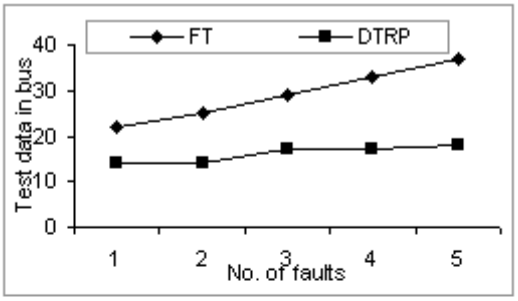

Fig. 11 Test data traffic in test bus

Table 3 Fuzzy Cut Set and Interval Analysis on FC Output

Patterns	Fuzzy Controller Output			
	α -cut	x_1	x_2	Interval
w1, w2	0.5	2.0	2.2	0.2
w2, w3	0.65	2.0	2.65	0.65
w3, w4	0.72	1.8	2.5	0.7
w4, w5	0.72	1.8	2.5	0.7

6. CONCLUSION

The transient analysis results show that the proposed method using fuzzy logic can detect more faults from differential transient patterns. Also, it enhances tester performance using short test vectors, less test traffic, medium length and compressible signatures. More fault coverage, short test time results in good test cost efficiency and data traffic. Moreover, it can be used for building hybrid BIST and advanced ATE.

REFERENCES

[1] V. Panic and D. Milovanovic, "IDDQ Fault Model Generation", Proceedings of 21st International Conference on Microelectronics, Vol.2 No.1, September 1997, pp.14-17.

[2] Amir Attarha, "Modeling and Simulation of Real Defects Using Fuzzy Logic", Proceedings of ACM-DA Conference 2000, Los Angeles, California, 2000, pp.188-89.

[3] Ho Hashempour and etc, "Test Time Reduction by Combining BIST and ATE", Proceedings of the 17th IEEE International Conference on DFT in VLSI Systems, 2002, pp.1063.

[4] W.D. Tseng and K. Wang , "Fuzzy-Based CMOS Circuit Partitioning In BICT", IEEE VLSI Systems, Vol. 7, No.1, March 1999, pp.116-21.

[5] James F. Plusquellic, Chintan Patel and Ying Ouyang, "QSA for IC Diagnosis," Proceedings of IEEE ITC, 2000, pp.143.

[6] D.Driankov, "An Introduction to Fuzzy Control", Sringer-Verlag, 2001.

[7] S.Kumar, "Fuzzy Controller for Mobile Phones", Journal of CSI,Vol.32, No.1, March 2002, pp.34-39.

[8] N. Burgess and others, "Physical Faults in MOS Circuits", IEE Proceedings, Vol. 13, January 1988, pp. 1-5.

[9] H.Kawang, "AdvancedComputer Architecture", McGrew Hill Inc., 2001.

[10] R.Kumar, M.Mishra and A.K.Sarje, "A Rewiw of QoS Route Provisioning in MAHN", Journal of DIM, Vol.5, No.1, February 2007.

[11] T.J.Rose,"Fuzzy Logic With Engineering Applications", McGrew Hill Inc., 1997.

DEVELOPMENT OF TERNARY BLEND CONCRETE

P. Murthi[1] and V. Sivakumar[2]

[1]Department of Civil Engineering, Kongu Engineering College, Perundurai, Erode – 638 052, Tamil Nadu

[2]Department of Chemical Engineering, Kongu Engineering College, Perundurai, Erode – 638 052, Tamil Nadu

E-Mail: murthihani@kongu.ac.in

(Received on 24 May 2007 and accepted on 16 August 2007)

Abstract

This study is intended to overcome the slower strength development of binary blend concrete by means of developing ternary blend concrete. The study consists of two stages of investigation. The development of binary blend concrete was considered in the first stage using ASTM Class F Fly Ash (FA) and Rice Husk Ash (RHA). The partial replacement of cement by FA and RHA at the rate of 5,10,15,20 and 25% by weight was considered to predict the optimum replacement level in the binary blend system. The second stage of this study was developing the ternary blend concrete using Silica Fume (SF). The replacement of cement in the binary system by the second mineral admixture was suggested as 4, 8 and 12% of total powder content by weight. The other parameters, like total cementitious material content, water binder ratio, fine and coarse aggregate content were maintained as constant. Properties of the fresh concrete such as slump, air content and bleeding were determined. The optimum replacement level of cement for developing the binary and ternary blend concrete was determined based on the compressive strength.

Keywords: *Binary Blend, Compressive Strength, Fly Ash, Rice Husk Ash, Silica Fume, Ternary Blend*

1. INTRODUCTION

The developments of ternary blend cements have been the subject of investigations for the past three decades [1]. Some of the developed countries are currently producing the ternary blend cement including a combination of Fly Ash and Silica Fume. In Canada, ternary blended cement incorporating silica fume and slag is currently marked as regular cement [2]. The development of construction industry in the global level needs more and more quantity of cement for sustainable growth. But the production of each tonne of cement clinker releases one tonne of carbon dioxide, which affects the earth's ecosystem [3]. Thus increasing world wide production of Ordinary Portland Cement (OPC) is aggravating the problems associated with its production and use. The addition of pozzolanic materials with OPC, a centurary old practice, is an alternative practice in the construction industry. The longevity of old monuments proves the efficiency of the lime blended material.

The fly ash, one of the factories made by product, was utilized as pozzolanic material in cement world wide. The replacement of cement by fly ash improves from minimum level to a maximum of 60 % for mass concrete construction. One of the greatest drawbacks while using fly ash as pozzolanic material in concrete is in the early age performance of concrete. The initial strength development of fly ash blended concrete shows poor performance than the ordinary concrete. The development of ternary blends by means of adding a superfine mineral admixture, like SF is an alternative possible way to overcome the drawback of binary blends with the fly ash. The SF in the ternary blend improves the early age performance of concrete and the fly ash continuously improving the properties of the hardened concretes [4]. According to several researchers, ternary blends are vastly superior to portland cement concrete in terms of durability of structures [5].

The objective of this research work is to develop the ternary blend concrete using Indian grade cement and ASTM class F fly ash, RHA, SF as mineral admixtures. The results will provide guidelines to determine the optimum replacement level (that is, replacement by mass of the Portland cement) of mineral admixtures both in binary and ternary blend concretes.

2. EXPERIMENTAL PROCEDURE

This study consists of two stages of investigations. The first one is the development of binary blend concrete and the second one is the development of ternary blend concrete. The following combinations were considered in both cases:

Binary blended concrete
- Cement + FA
- Cement + RHA

Ternary blended concrete
- Cement + FA + SF
- Cement + RHA + SF

The optimum replacement level of mineral admixtures in the binary system was determined based on the compressive strength of the concrete cube specimens. The ternary blend concrete was developed by replacing the cement content with SF from the binary blend system. The replacement of cement in the binary blend system by the second mineral admixture was suggested as 4%, 8% and 12% of total powder content by weight.

The results obtained were compared with the control concrete mix. In the meantime, other parameters, like total cementitious material content, water/binder ratio, fine and coarse aggregate content were maintained constant. Properties of the fresh concrete such as slump, air content and bleeding were determined. The concrete cubes were cast using 100mm size steel moulds and compacted with the help of table vibrator. Demoulding agent was applied on the inner surface of the mould before casting. The concrete was prepared using tilting type laboratory concrete mixer machine and more precautions were taken to ensure uniform mixing of ingredients. After 24 hours of casting, the specimens were demoulded and placed immediately in water tank for further curing.

2.1 Materials Used

The ordinary portland cement (43 grade as per IS: 8114-1978) was used in this investigation and other cementitious materials used in this experimental programme were low calcium fly ash (ASTM type F), silica fume and rice husk ash. The specific gravity of the cement and fly ash was 3.15 and 2.92 respectively. The specific gravity of the other mineral admixtures, RHA and SF was 2.67 and 2.28 respectively. The fineness of cement was determined as 2950 cm^2/g. The fineness FA and RHA was 2170 and 2550 cm^2/g respectively. The fineness of the other mineral admixture used to form the ternary blend system via Silica Fume was 21750 cm^2/g. The combinations of $SiO_2 + Al_2O_3 + Fe_2O_3$ and all the cementitious materials was mentioned in the Table 1.

Local river (Cauvery) sand was used as fine aggregate with the fineness modulus of 2.67, which belongs to the grade zone-II. The specific gravity of the sand was 2.71. Blue granite metal of 20mm size (maximum) was used as coarse aggregate. The fineness modulus and the specific gravity of the coarse aggregate were 2.78 and 7.19 respectively. Both the aggregate complied with the requirements of IS: 383-1970.

2.2 Mix Proportions

In this study, the concept of making the normal strength (M20 grade) ternary blend concrete was considered. The mix design for the normal concrete was followed by the BIS code procedure as per IS: 10262 - 1982. Water/binder ratio of the mix was considered as 0.55. Table 2 shows the summery of concrete mix proportion for control concrete used in this investigation. The various mix combinations of binary and ternary blend concrete are shown in the Tables 3 and 4.

2.3 Testing the Concrete Specimens

The workability of fresh concrete was determined by slump cone apparatus as per IS: 7320 - 1974 and the air content was determined with the help of pressure type air meter. A container of approximately 7 L capacity was filled with fresh concrete for determining the bleeding [4].

Water accumulated at the top of the concrete surface is drawn by means of pipette at 10 minutes interval for the first 40 minutes and at 30 minutes interval subsequently till the bleeding ceases. The compressive strength of concrete cubes was done using 2000kN electrically operated compression testing machine. All results mentioned in this paper were the average of three specimens under the laboratory environment.

Table 1 Chemical Composition of Cementitious Materials

S.No	Chemical Composition (%)	Cement	Fly Ash	Rice Husk Ash	Silica Fume
1	$SiO_2 + Al_2O_3 + Fe_2O_3$	26.18	85.90	91.89	87.10
2	CaO	61.60	0.62	0.78	0.9
3	LoI	1.70	1.09	3.49	2.50

Table 2 Mix Proportion for One Cubic Metre of Control Concrete

S.No.	Cement(kg)	Fine Aggregate(kg)	Coarse Aggregate (kg)	Water(Litre)
1	326	675	1109	179
2	1	2.07	3.40	0.55

Table 3 Mix Proportion for Binary Blend Concrete

S.No	Cement		Fly Ash		Rice Husk Ash	
	%	kg/m^3	%	kg/m^3	%	kg/m^3
1	100	326.0	-	-	-	-
2	95	309.7	5	16.3	-	-
3	90	293.4	10	32.6	-	-
4	85	277.1	15	48.9	-	-
5	80	260.8	20	65.2	-	-
6	75	244.5	25	81.5	-	-
7	95	309.7	-	-	5	16.3
8	90	293.4	-	-	10	32.6
9	85	277.1	-	-	15	48.9
10	80	260.8	-	-	20	65.2
11	75	244.5	-	-	25	81.5

Table 4 Mix Proportion for Ternary Blend Concrete

S.No	Mix Designation	Cement Content (%)		Mineral Admixture Content (%)					
				Fly Ash		Rice Husk Ash		Silica Fume	
		%	kg/m^3	%	kg/m^3	%	kg/m^3	%	kg/m^3
1	PCC	100	326.00	-	-	-	-	-	-
2	BFC-20	80	260.80	20	65.20	-	-	-	-
3	BRC-18	82	267.30	-	-	18	58.70	-	-
4	TFS-4	76	247.76	20	65.20	-	-	4	13.04
5	TFS-8	72	234.72	20	65.20	-	-	8	26.08
6	TFS-12	68	221.68	20	65.20	-	-	12	39.12
7	TRS-4	78	254.26	-	-	18	58.70	4	13.04
8	TRS-8	74	241.22	-	-	18	58.70	8	26.08
9	TRS-12	70	228.18	-	-	18	58.70	12	39.12

3. RESULTS AND DISCUSSION

3.1 Binary Blend Concrete

Normally, the strength at the age of 28 days was considered as the compressive strength of concrete. Based on the well known concept of pozzolanic materials reacts with calcium hydroxide, a byproduct of hydration process of cement, improves the strength of concrete beyond 28 days of curing period. Thus it is essential to determine the later age strength of the blended concrete.

The early age strength of concrete was also determined for identifying the strength development pattern. Therefore, the results show the strength at the age of 7, 28 and 90 days of curing. The compressive strength of control concrete at the age of 28 days was 32.60 MPa and the early age (7 days) and the later age (90 days) strength of the concrete were 20.36 and 35.47 MPa respectively. When fly ash was added from 5 to 25%, the compressive strength ranges from 18.17 MPa to 10.47 MPa for 7 days curing. The results were reduced from the control concrete in all the replacement levels at the age of 28 days. The reduction may be due to the slower pozzolanic reaction of the mineral admixtures at early ages. Similar kind of observations was made in the various research reports [2-4, 6].

The compressive strength of FA based binary blend concrete at the age of 90 days was increased up to 10% replacement level and then reduced. This shows the hydration process continued even after 28 days curing in the blend concrete. The same kind of observation was also noticed when the cement replaced by the RHA to develop the other form of binary blend concrete. The results of various cement replacement levels in both the cases were mentioned in the Figures 1&2. Based on the strength development pattern of concrete as shown in Figures 1&2 and the theoretical (as per IS: 10262 - 1982) required target mean strength (26.6 MPa) of the mix, the optimum replacement of cement for developing the binary blend concrete using FA and RHA was determined as 20 and 18% respectively.

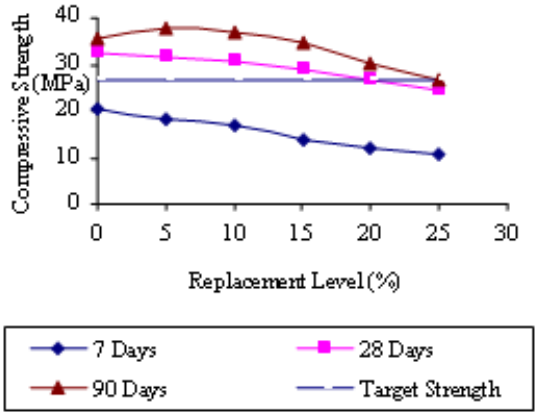

Fig.1 Compressive strength of binary blended concrete using fly ash

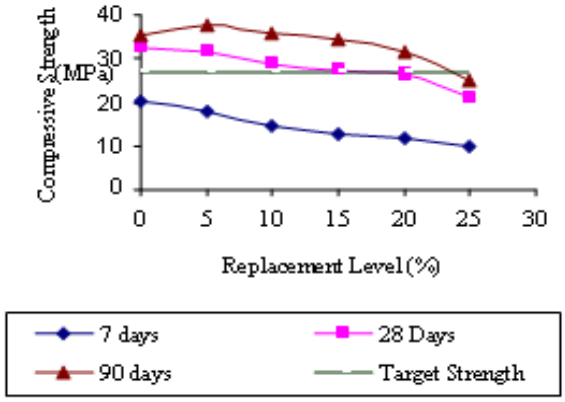

Fig. 2 Compressive strength of binary blended concrete using Rice Husk Ash

3.2 Ternary Blend Concrete

3.2.1 Slump Value of Concrete

The workability of fresh concrete was measured by slump test apparatus, in accordance with ASTM C 143 – 90(a) and IS: 7320 - 1974. Table 5 presents the fresh concrete properties of ternary blend concrete. The slump value of PCC was 20 mm. The use of FA (20%) in concrete also maintained the slump of 18 mm. The geometrical shape of the FA was spherical in nature which gives the ball bearing effect to the concrete and maintained the flow ability and also the workability. The addition of RHA (18%) in cement concrete reduces the slump value but not much difference with control concrete. The addition of the second mineral admixture causes the reduction of slump value. This is due to the super fine nature of SF in concrete. The fineness value of SF is nearly 10 times more than that of the cement. The SF particles have more contact surfaces with water and therefore require more water demand. But due to the presence of superplasticiser, the slump values not reduced to the lower level when compared to the control concrete. The replacement of cement in the ternary blend system by SF was restricted up to 12%, because the 12% SF in concrete illustrates around 50% lesser value of slump than the control mix.

3.2.2 Bleeding

The results of investigation on bleeding were mentioned in the Table 4. The bleeding of PCC ranged from 0.0311 to 0.053 ml/cm^2. The average value of six

samples was 0.0392 ml/cm^2. The bleeding of FA based binary blended concrete was increased slightly more than the value of PCC. The average values of bleeding of FA and RHA concrete were 0.0414 and 0.0408ml/cm^2 respectively. This is due to the pore filling effect of mineral admixtures in concrete. The excess water available in the pores between cement grains were squeezed out due to the filling effect of FA and RHA. The ternary blend concrete incorporating 4% SF shows the negative response to bleeding. The concrete containing 8% and 12% SF did not show any significant bleeding due to the more water demand for superfine mineral admixture. Similar results were observed by Nabil Bouzoubaa and others [3].

3.2.3 Air Content

The air content of PCC was measured as 2.4 %. FA and RHA based binary blend concretes show 2.8%. The addition of 4% SF in FA and RHA based binary blend concrete reduces the air content from 2.8% to 2.0 and 2.2% respectively. In the meantime the air content increases with increasing the second mineral admixture portion in the ternary mix concrete. The addition of 12% SF shows the maximum air content in FA and RHA based ternary blend concrete and the values are 2.8 and 2.9% respectively. Similar results were observed by Nabil Bouzoubaa and others [3].

Table 5 Properties of Ternary Blend Concrete

S. No.	Mix Designation	Slump Value (mm)	Air content (%)	Bleeding (mL/cm^2)	Compressive Strength (MPa)		
					7 Days	28 Days	90 Days
1	PCC	20	2.4	0.0392	19.37	30.60	32.07
2	BFA-20	18	2.8	0.0414	12.13	23.67	28.03
3	BRA-18	15	2.8	0.0408	12.00	22.63	27.70
4	TFS-4	16	2.0	0.0117	19.07	30.97	34.67
5	TFS-8	13	2.3	0.0109	18.10	27.17	31.93
6	TFS-12	10	2.8	0.0107	15.93	24.90	27.03
7	TRS-4	15	2.2	0.0143	18.77	28.93	32.37
8	TRS-8	12	2.6	0.0141	17.03	25.73	29.10
9	TRS-12	9	2.9	0.0129	15.20	24.00	25.87

3.2.4 Compressive Strength

The strength development of FA and SF based ternary blend concrete is shown in Figure 3 and that of RHA and SF based ternary blend concretes is shown in Figure 4. There is a reasonable improvement (57.21%) in the early age (7 days) strength of ternary blend concrete when compared to the FA based binary blend concrete.

The strength at the age of 7 days for 4% silica fume based ternary blend concrete was almost similar to the control concrete. The compressive strength of FA based ternary blend concrete using 8% and 12% SF was lesser than the control concrete via 18.1 and 15.93 MPa and in the RHA based ternary system, the compressive strength values were also lesser than the control concrete. But the results show better than the binary system. However, the 28 days strength of ternary blend concrete shows marginal variations.

The variations between the ternary blend system and binary blend concrete using FA and SF were identified as 5.2 (12% SF) to 30.8% (4% SF). Similar trend was observed in RHA and SF based ternary blend system. Relative strength of all the mixes with reference to 28 days strength of control concrete is shown in Figure 5.

Due to the presence of FA and RHA in the binary blend concrete reduces the cement content in the total ingredient of concrete. Hence it reduces the hydration process during the initial stage. But the mineral admixtures react with the calcium hydroxide developed during hydration of cement causes the second hydration process in the later stage.

The drawback of reduction in hydration of cement and also reduction in the rate of strength development in the binary blend system during the early ages was overcome with the ternary blend system.

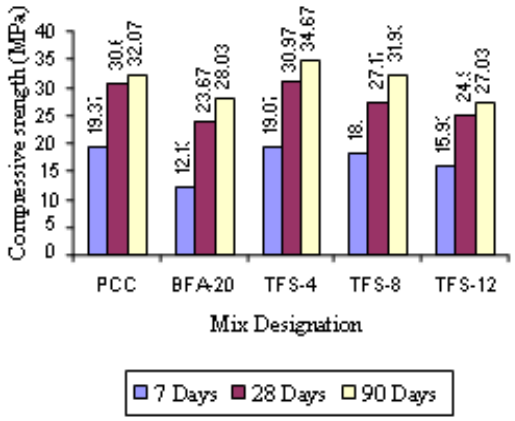

Fig.3 Comparison of compressive strength of FA and SF based ternary blend concrete with plain cement concrete

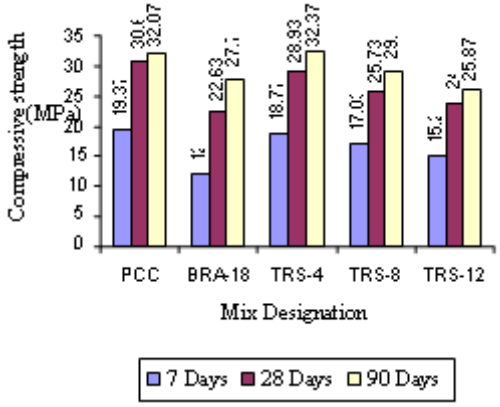

Fig.4 Comparison of compressive strength of RHA and SF based ternary blend concrete with plain cement concrete

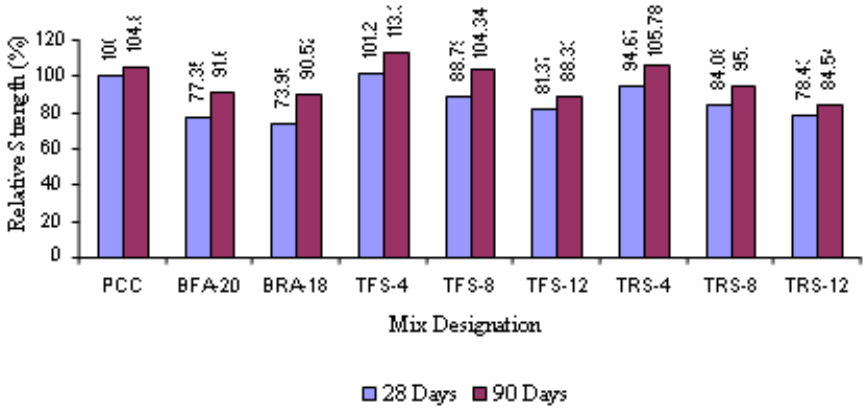

Fig.5 Relative strength with reference to 28 days strength of control concrete

This is due to the micro-filler effect and mitigates voids in the concrete. When the SF is added in the binary blend, it fills the voids present between the cement as well as the FA particles [7, 8]. Similar trend in the strength development was observed in the RHA based blended concrete [9, 10] and increases the strength [11, 12]. In the mean time SF reacts with saturated solution of calcium hydroxide with in few minutes [13] leading to overcome drawbacks in the binary blend concrete during the early ages. The optimum replacement levels of cement in the ternary blend normal strength concrete was identified from the Figures 6&7 and the values are 8 and 6% respectively with SF and RHA based binary blend concrete. The experimental investigation predicts the combinations to develop ternary blend high performance normal strength concrete as 72% cement + 20% FA + 8% SF and 76% cement + 18% RHA + 6% SF.

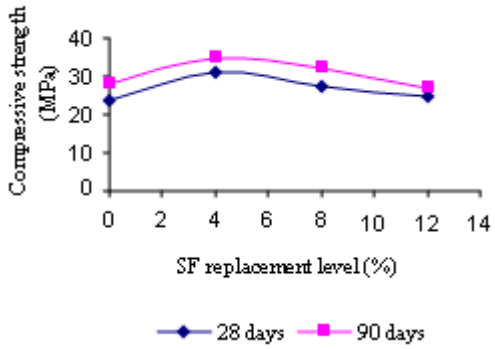

Fig. 6 Strength development of ternary blend concrete using FA (20%) and SF

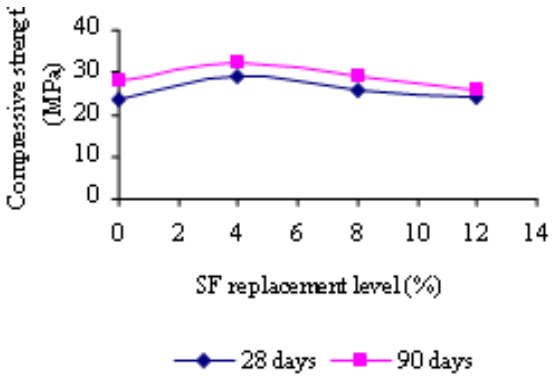

Fig.7 Strength development of ternary blend concrete using RHA (18%) and SF

4. CONCLUSIONS

From this investigation, following conclusions are drawn:

- The optimum replacement of cement for developing the binary blend concrete using FA and RHA was determined as 20 and 18% respectively.
- The replacement of cement in the ternary blend system by SF was restricted up to 12%, because the 12% SF in concrete illustrates 20% lesser value of slump than the control mix.
- The average value of bleeding in control concrete was 0.0392 ml/cm^2. The average value of bleeding of FA and RHA concrete were 0.0414 and 0.0408ml/cm^2 respectively. The concrete containing 8% and 12% SF did not show any significant bleeding due to more water demand for SF.
- During the early age (7 days), the compressive strength of ternary blend concrete using 4% SF and 20% FA was similar to that of control concrete and more than 57% of binary blend concrete.
- The compressive strength of ternary blend concrete with 8% SF in FA based binary blend concrete and 6% SF in RHA based binary blend concrete shows the same value of control concrete at 28 days.
- Due to high early strength and good workability, the optimum replacement levels of cement by SF in the ternary blend concrete were 8% and 6% respectively with FA and RHA based binary blend concrete.
- The experimental investigation predicts the following combinations to develop the ternary blend concrete:
  72% Cement + 20% FA + 8% SF
  76% Cement + 18% RHA + 6% SF

REFERENCES

[1] E.E. Berry, "Strength Development of Some Blended Cement Mortars", Cement and Concrete Research, Vol.10, No.1, 1980, pp. 1-11.

[2] M.Nehdi, "Ternary and Quaternary Cements for Sustainable Development", Concrete International, Vol.23, No.4, April 2004, pp. 34-42.

[3] D.S.R.Murty *et al*, "Conservation of Concrete Making Materials", Journal of Structural Engineering, Vol.33, No.3, Aug-Sep 2006, pp. 237-241.

[4] Nabil Bouzoubaa *et al*, "Development of Ternary Blends for High Performance Concrete", ACI Material Journal, Vol.101, No.1, Jan-Feb 2004, pp. 19-29.

[5] A.K.Mullick, "Performance of Concrete with Binary and Ternary Cement Blends", The Indian Concrete Journal, January 2007, pp. 15-22.

[6] S.Gopalakrishnan *et al*, "Effect of Partial Replacement of Cement with Fly Ash on The Strength and Durability of Hpc", The Indian Concrete Journal, May 2001, pp. 335-341.

[7] N.Ganesan and T.Sekar, "Effect of Micro-silica and Steel Fibres on the strength of High Performance Concrete Composites", Journal of Structural Engineering, Vol.33, No.3, Aug-Sep 2006, pp. 225-229.

[8] Omar Saeed Baghabra Al-Amoudi *et al*, "Prediction of Long-term Corrosion Rersistance of Plain and Blended Cement Concrete", ACI Material Journal, Vol. 90, No.6, Nov-Dec 1993, pp. 564-570.

[9] Salim Ahmed Barbhuiya *et al*, "Use of Classified Rice Husk Ash for High Strength Concrete", The Indian Concrete Journal, May 2006, pp. 11-16.

[10] N.P. Rajamane and D.Sabitha, "Effect of Fly Ash and Silica Fume on Alkalinity of Cement Mortar", The Indian Concrete Journal, March 2005, pp. 43-48.

[11] Suwimol Asavapisit and Nittaya Ruengrit, "The Role of Rha – Blended Cement in Stabilizing Metal – Containing Wastes", Cement and Concrete Composites, Vol.27, 2005, pp. 782-787.

[12] D.D.Bui *et al*, "Particle Size Effect on Strength of Rice Husk Ash Blended Gap-graded Portland Cement Concrete", Cement and Concrete Composites, Vol.27, 2005, pp. 357-366.

[13] S.C.Ahluwalia, "Materials used for High Performance Concrete", NBM&CW, September 2004, pp. 38-44.

Indian Journal of Engineering, Science, and Technology (IJEST)

(ISSN: 0973-6255)
(A half-yearly refereed research journal)

Information for Authors

1. All papers should be addressed to The Editor-in-Chief, Indian Journal of Engineering, Science, and Technology (IJEST), Bannari Amman Institute of Technology, Sathyamangalam - 638 401, Erode District, Tamil Nadu, India.
2. Two copies of manuscript along with soft copy are to be sent.
3. A CD-ROM containing the text, figures and tables should separately be sent along with the hard copies.
4. Submission of a manuscript implies that : (i) The work described has not been published before; (ii) It is not under consideration for publication elsewhere.
5. Manuscript will be reviewed by experts in the corresponding research area, and their recommendations will be communicated to the authors.

Guidelines for submission

Manuscript Formats

The manuscript should be about 8 pages in length, typed in double space with Times New Roman font, size 12, Double column on A4 size paper with one inch margin on all sides and should include 75-200 words abstract, 5-10 relevant key words, and a short (50-100 words) biography statement. The pages should be consecutively numbered, starting with the title page and through the text, references, tables, figure and legends. The title should be brief, specific and amenable to indexing. The article should include an abstract, introduction, body of paper containing headings, sub-headings, illustrations and conclusions.

References

A numbered list of references must be provided at the end of the paper. The list should be arranged in the order of citation in text, not in alphabetical order. List only one reference per reference number. Each reference number should be enclosed by square brackets.

In text, citations of references may be given simply as "[1]". Similarly, it is not necessary to mention the authors of a reference unless the mention is relevant to the text.

Example

[1] M.Demic, "Optimization of Characteristics of the Elasto-Damping Elements of Cars from the Aspect of Comfort and Handling", International Journal of Vehicle Design, 13(1), 1992, pp. 29-46.

[2] S.A.Austin, "The Vibration Damping Effect of an Electro-Rheological Fluid", ASME Journal of Vibration and Acoustics, 115(1), 1993, pp. 136-140.

SUBSCRIPTION

The annual subscription for IJEST is Rs.600/- which includes postal charges. To subscribe for IJEST a Demand Draft may be sent in favour of IJEST, payable at Sathyamangalam and addressed to IJEST. Subscription order form can be downloaded from the following link http:// www.bitsathy.ac.in./ ijest.html.

For subscription / further details please contact:

IJEST
Bannari Amman Institute of Technology
Sathyamangalam - 638 401, Erode District, Tamil Nadu Ph: 04295 - 221289
Fax: 04295 - 223775 E-mail: ijest@bitsathy.ac.in Web:www.bitsathy.ac.in/ijest.html

Published by

BANNARI AMMAN INSTITUTE OF TECHNOLOGY
Sathyamangalam - 638 401 Erode District Tamil Nadu India
Ph: 04295-221289 Fax: 04295-223775
www.bitsathy.ac.in E-mail: ijest@bitsathy.ac.in